Title
Autoantigen discovery across monogenic and acquired human autoimmunity by proteome-wide PhIP-seq

Author
Vazquez, Sara Elisabeth

Publication Date
2021

Peer reviewed|Thesis/dissertation

Autoantigen discovery across monogenic and acquired human autoimmunity by proteome-wide PhIP-Seq

by
Sara Elisabeth Vazquez

DISSERTATION
Submitted in partial satisfaction of the requirements for degree of
DOCTOR OF PHILOSOPHY

in

Biochemistry and Molecular Biology

in the

GRADUATE DIVISION
of the
UNIVERSITY OF CALIFORNIA, SAN FRANCISCO

Approved:

DocuSigned by:
Alexander Marson
7F25CDCE383C4A8...

Alexander Marson
Chair

DocuSigned by:
Jason Cyster
[illegible]40D...

Jason Cyster

DocuSigned by:
Joseph DeRisi
[illegible]423...

Joseph DeRisi

DocuSigned by:
Mark Anderson
657D61B3C699406...

Mark Anderson

Committee Members

Dedication and Acknowledgments

I thank my PIs Joseph DeRisi and Mark Anderson, who have been wonderful mentors over the past 4.5 years, as well as my thesis committee members Jason Cyster and Alexander Marson. I am grateful to members of the DeRisi and Anderson lab for support, encouragement, and advice - both scientific and personal. I'd also like to thank the dozens of collaborators I've had the opportunity to work with during my PhD, who have each taught me specific and important aspects of technical, biological or clinical aspects of autoimmunity and autoantigen discovery. My family and friends across the world – from Zurich to Boston to San Francisco – thank you for your continual love and support, even across increasingly inconvenient time zones. Finally, thanks to my (soon-to-be) husband Joseph – being able to hear your (admittedly pretty loud) voice from a bay and a half away was really what kept me going.

Contributions

Chapter 1 *is reprinted largely as it appears in:*

Vazquez, S.E., Ferré, E.M., Scheel, D.W., Sunshine, S., Miao, B., Mandel-Brehm, C., Quandt, Z., Chan, A.Y., Cheng, M., German, M., Lionakis, M. S., DeRisi, J. L. and Anderson, M.S, 2020. Identification of novel, clinically correlated autoantigens in the monogenic autoimmune syndrome APS1 by proteome-wide PhIP-Seq. Elife, 9, p.e55053.

Chapter 2 *includes contributions from:*

Sabrina A Mann, Aaron Bodansky, Andrew F Kung, Zoe Quandt, Nils Landegren, Daniel Eriksson, Paul Bastard, Shen-Ying Zhang, Jamin Liu, Anthea Mitchell, Brenda Miao, Gavin Sowa, Kelsey Zorn, Chisato Shimizu, Adriana Tremoulet, Kara Lynch, Jean-Laurent Casanova, Luigi D. Notarangelo, Jane Burns, Michael Wilson, Michael S. Lionakis, Olle Kampe, Troy Torgerson, Mark S Anderson, Joseph L DeRisi

Abstract

Autoantigen discovery across monogenic and acquired human autoimmunity by proteome-wide PhIP-Seq

Sara Elisabeth Vazquez

The identification of autoantigens remains a critical challenge for understanding and treating autoimmune diseases. Phage Immunoprecipitation-Sequencing (PhIP-Seq) allows for unbiased, proteome-wide autoantigen discovery across a variety of disease settings, with identification of disease-specific autoantigens providing new insight into previously poorly understood forms of immune dysregulation with autoimmunity.

The first chapter of this thesis explores autoantigen discovery in the disease Autoimmune polyendocrine syndrome type 1 (APS1), a rare monogenic form of autoimmunity that presents as widespread autoimmunity with T and B cell responses to multiple organs. Importantly, autoantibody discovery in APS1 can illuminate fundamental disease pathogenesis, and many of the antigens found in APS1 extend to common autoimmune diseases. Here, I applied PhIP-Seq to sera from an APS1 cohort and discovered multiple common antibody targets. These novel autoantigens exhibit tissue-restricted expression, including expression in enteroendocrine cells and dental enamel. Using detailed clinical phenotyping, novel associations between autoantibodies and organ-restricted autoimmunity are described, including between anti-KHDC3L autoantibodies and premature ovarian insufficiency, and between anti-RFX6 autoantibodies and diarrheal-type intestinal dysfunction. These data highlight the utility of PhIP-Seq for interrogating antigenic repertoires in human autoimmunity and the importance of antigen discovery for improved understanding of disease mechanisms.

In the second chapter, I discuss and address how despite several successful implementations of PhIP-Seq for autoantigen discovery, current protocols are inherently difficult to scale to accommodate large cohorts of cases and importantly, healthy controls. I develop and validate a high throughput extension of PhIP-seq in the context of monogenic and acquired autoimmune disease, including APS1, IPEX, patients with RAG1/2 deficiency, Kawasaki Disease, multisystem inflammatory syndrome in children, and finally, mild and severe forms of COVID19. These scaled datasets enable machine-learning approaches that result in robust prediction of disease status, as well as the ability to detect both known and novel, autoantigens, such as PDYN in APS1 patients, and intestinally expressed proteins BEST4 and BTNL8 in IPEX patients. Remarkably, BEST4 antibodies were also found in 2 patients with a RAG1/2 deficiency, one of which had very early onset IBD. Scaled PhIP-Seq examination of both MIS-C and KD demonstrated rare, overlapping antigens, including CGNL1, as well as several strongly enriched putative pneumonia-associated antigens in severe COVID19, including the endosomal protein EEA1. Together, scaled PhIP-Seq provides a valuable tool for broadly assessing both rare and common autoantigen overlap between autoimmune diseases of varying origins and etiologies.

Table of Contents

List of Figures

List of Tables

INTRODUCTION

The scope of this thesis work encompasses the discovery of multiple novel autoantigens, as well as the exploration of principles of autoantigen discovery using proteome-wide Phage Immunoprecipitation Sequencing (PhIP-Seq). This work is divided into 2 chapters, each of which contains distinct results, figures, and discussion of the results. Extended introductory material, which goes beyond the brief overview presented here, is presented at the beginning of each chapter.

In *Chapter 1*, I present the rationale behind autoantigen discovery specifically in the disease Autoimmune Polyglandular Syndrome Type 1 (APS1), a rare disease that is well-suited to PhIP-Seq-based autoantigen discovery. Furthermore, I demonstrate a number of novel autoantigens which I validate extensively, each of which have correlations with specific diseases. These novel antibody-disease associations highlight new concepts in the field of human autoimmunity, including the presence and characterization of cell-type specific immune responses including towards the intestinal enteroendocrine cell in and the female oocyte.

Chapter 2 builds on the work in *Chapter 1*, demonstrating the need for scaled protocols and further technical studies in order to apply PhIP-Seq-based antigen discovery to larger and more diverse disease cohorts. From a technical standpoint, this chapter provides a scaled platform with which to perform parallel PhIP-Seq on 600-800 patient samples; data from these technical studies particularly highlight the need for well-controlled experiments in current and future PhIP-Seq studies to avoid non-specific candidate autoantigen selection. From a biological and clinical standpoint, *Chapter 2* presents multiple datasets across human immune-mediated diseases including APS1, Immune Dysregulation, Polyendocrinopathy, Enteropathy, X-linked (IPEX), RAG deficiency, Kawasaki disease, as well as COVID-related phenotypes including severe acute COVID19 pneumonia and Multisystem Inflammatory Syndrome in Children (MIS-C). In each disease context, we describe the presence of both previously described and novel

autoantigens, some of which correlate with specific diseases and therefore carry importance for subsequent follow-up biological studies as well as evaluation of clinical predictive or diagnostic utility.

The text, figures and tables in this thesis have been adapted with minor changes from work that is published (*Chapter 1; Vazquez et al, Elife 2020*) and in preparation for publication (*Chapter 2*).

CHAPTER 1

BACKGROUND

Autoimmune Polyglandular syndrome type 1 (APS1) or Autoimmune Polyglandular-Candidiasis-Ectodermal Dystrophy (APECED; OMIM #240300) is an autoimmune syndrome caused by monogenic mutations in the *AIRE* gene that result in defects in AIRE-dependent T cell education in the thymus (Aaltonen et al., 1997; Anderson, 2002; Conteduca et al., 2018; Malchow et al., 2016; Nagamine et al., 1997). As a result, people with APS1 develop autoimmunity to multiple organs, including endocrine organs, skin, gut, and lung (Ahonen et al., 1990; Ferré et al., 2016; Söderbergh et al., 2004). Although the majority of APS1 autoimmune manifestations are thought to be primarily driven by autoreactive T cells, people with APS1 also possess autoreactive B cells and corresponding high-affinity autoantibody responses (DeVoss et al., 2008; Gavanescu et al., 2008; Meyer et al., 2016; Sng et al., 2019). These autoantibodies likely derive from germinal center reactions driven by self-reactive T cells, resulting in mirroring of autoantigen identities between the T and B cell compartments (Lanzavecchia, 1985; Meyer et al., 2016).

Identification of the specificity of autoantibodies in autoimmune diseases is important for understanding underlying disease pathogenesis and for identifying those at risk for disease (Rosen & Casciola-Rosen, 2014). However, despite the long-known association of autoantibodies with specific diseases in both monogenic and sporadic autoimmunity, many autoantibody specificities remain undiscovered. Challenges in antigen identification include the weak affinity of some autoantibodies for their target antigen, as well as rare or low expression of the target antigen. One approach to overcome some of these challenges is to interrogate autoimmune patient samples with particularly high affinity autoantibodies. Indeed, such an approach identified GAD65 as a major autoantigen in type 1 diabetes by using sera from people with Stiff Person Syndrome (OMIM #184850), who harbor high affinity autoantibodies (Baekkeskov et al., 1990).

We reasoned that PhIP-Seq interrogation of APS1, a defined monogenic autoimmune syndrome with a broad spectrum of high affinity autoantibodies, would likely yield clinically meaningful targets – consistent with previously described APS1 autoantibody specificities that exhibit strong, clinically useful associations with their respective organ-specific diseases (Alimohammadi et al., 2008, 2009; Ferré et al., 2019; Landegren et al., 2015; Popler et al., 2012; Puel et al., 2010; Shum et al., 2013; Söderbergh et al., 2004; Winqvist et al., 1993).

The identification of key B cell autoantigens in APS1 has occurred most commonly through candidate-based approaches and by whole-protein microarrays. For example, lung antigen BPIFB1 autoantibodies, which are used to assess people with APS1 for risk of interstitial lung disease, were discovered first in *Aire*-deficient mice using a combination of targeted immunoblotting, tissue microscopy, and mass spectrometry (Shum et al., 2013, 2009). Recently, there have been rapid advances in large platform approaches for antibody screening; these platforms can overcome problems of antigen abundance by simultaneously screening the majority of proteins from the human genome in an unbiased fashion (Jeong et al., 2012; Larman et al., 2011; Sharon & Snyder, 2014; Zhu et al., 2001). In particular, a higher-throughput antibody target profiling approach utilizing a fixed protein microarray technology (ProtoArray) has enabled detection of a wider range of proteins targeted by autoantibodies directly from human serum (Fishman et al., 2017; Landegren et al., 2016; Meyer et al., 2016). Despite initial success of this technology in uncovering shared antigens across APS1 cohorts, it is likely that many shared antigens remain to be discovered, given that these arrays do not encompass the full coding potential of the proteome.

Here, we took an alternate approach to APS1 antigen discovery by employing Phage Immunoprecipitation-Sequencing (PhIP-Seq) based on an established proteome-wide tiled library (Larman et al., 2011; O'Donovan et al., 2018). This approach possesses many potential advantages over previous candidate-based and whole-protein fixed array approaches, including (1) expanded, proteome-wide coverage (including alternative splice forms) with 49 amino acid

(AA) peptide length and 24AA resolution tiling, (2) reduced volume requirement for human serum, and (3) high-throughput, sequencing based output (Larman et al., 2011; O'Donovan et al., 2018). Of note, the PhIP-Seq investigation of autoimmune diseases of the central nervous system, including paraneoplastic disease, has yielded novel and specific biomarkers of disease (Larman et al., 2011; Mandel-Brehm et al., 2019; O'Donovan et al., 2018).

Using a PhIP-Seq autoantibody survey, we identify a collection of novel APS1 autoantigens as well as numerous known, literature-reported APS1 autoantigens. We orthogonally validate seven novel autoantigens including RFX6, KHDC3L, and ACP4, all of which exhibit tissue-restricted expression (Jeong et al., 2012; Larman et al., 2011; Sharon & Snyder, 2014; H. Zhu et al., 2001). Importantly, these novel autoantigens may carry important implications for poorly understood clinical manifestations such as intestinal dysfunction, ovarian insufficiency, and tooth enamel hypoplasia, where underlying cell-type specific antigens have remained elusive. Together, our results demonstrate the applicability of PhIP-Seq to antigen discovery, substantially expand the spectrum of known antibody targets and clinical associations in APS1, and point towards novel specificities that can be targeted in autoimmunity.

RESULTS

Investigation of APS1 serum autoantibodies by PhIP-Seq

Individuals with APS1 develop autoantibodies to many known protein targets, some of which exhibit tissue-restricted expression and have been shown to correlate with specific autoimmune disease manifestations. However, the target proteins for many of the APS1 tissue-specific manifestations remain enigmatic. To this end, we employed a high-throughput, proteome-wide programmable phage display approach (PhIP-Seq) to query the antibody target identities within serum of people with APS1 (Larman et al., 2011; O'Donovan et al., 2018). The PhIP-Seq technique leverages large scale oligo production and efficient phage packaging and expression to present a tiled-peptide representation of the proteome displayed on T7 phage. Here, we utilize a phage library that we previously designed and deployed for investigating paraneoplastic autoimmune encephalitis (Mandel-Brehm et al., 2019; O'Donovan et al., 2018). The library itself contains approximately 700,000 unique phage, each displaying a 49 amino acid proteome segment. As previously described, phage were immunoprecipitated using human antibodies bound to protein A/G beads. In order to increase sensitivity and specificity for target proteins, eluted phage were used for a further round of amplification and immunoprecipitation. DNA was then extracted from the final phage elution, amplified and barcoded, and subjected to Next-Generation Sequencing **(Figure 1.1A)**. Finally, sequencing counts were normalized across samples to correct for variability in sequencing depth, and the fold-change of each gene was calculated (comprised of multiple unique tiling phage) as compared to mock IPs in the absence of human serum (further details of the protocol can be found in the methods section).

From a cohort of 67 APS1 serum samples, a total of 39 samples were subjected to PhIP-Seq investigation, while the remaining 28 samples were obtained at a later time point and reserved for downstream validation experiments (for clinical data, refer to **Supplementary Table S1.1**). In addition, 28 non-APS1 anonymous blood donor serum samples were subjected to PhIP-

Seq, and an additional group of 61 non-APS1 plasma samples were used for downstream validation experiments.

Detection of literature-reported APS1 autoantigens

PhIP-Seq results were first cross-referenced with previously reported APS1 autoantibody targets (Alimohammadi et al., 2008, 2009; Clemente et al., 1997; Fishman et al., 2017; Hedstrand et al., 2001; Husebye et al., 1997; Kluger et al., 2015; Kuroda et al., 2005; Landegren et al., 2016, 2015; Leonard et al., 2017; Meager et al., 2006; Meyer et al., 2016; Oftedal et al., 2015; Pöntynen et al., 2006; Sansom et al., 2014; Shum et al., 2013, 2009; Söderbergh et al., 2004). To avoid false positives, a conservative set of criteria were used as follows. We required a minimum of 2/39 APS1 samples and 0/28 non-APS1 control samples to exhibit normalized gene counts in the immunoprecipitation (IP) with greater than 10-fold enrichment as compared to the control set of 18 mock-IP (beads, no serum) samples. This simple, yet stringent criteria enabled detection of a total of 23 known autoantibody specificities **(Figure 1.1B)**. Importantly, many of the well-validated APS1 antigens, including specific members of the cytochrome P450 family (CYP1A2, CYP21A1, CYP11A1, CYP17A1), lung disease-associated antigen KCRNG, as well as IL17A, IL17F, and IL22, among others were well represented **(Figure 1.1B)**. In contrast, the diabetes-associated antigens GAD65 and INS did not meet these stringent detection criteria and only weak signal was detected to many of the known interferon autoantibody targets known to be present in many people with APS1, perhaps due to the conformational nature of these autoantigens **(Figure 1.1B & Supplementary Figure S1.1)** (Björk et al., 1994; Meager et al., 2006; Meyer et al., 2016; Wolff et al., 2013; Ziegler et al., 1996).

Three known autoantigens that were prevalent within our cohort were selected to determine how PhIP-Seq performed against an orthogonal whole protein-based antibody detection assay. A radioligand binding assay (RLBA) was performed by immunoprecipitating *in vitro* transcribed and translated S35-labeled proteins CYP11A1, SOX10, and NLRP5 with APS1

serum (Alimohammadi et al., 2008; Berson et al., 1956; Hedstrand et al., 2001; Winqvist et al., 1993). Importantly, and in contrast to PhIP-Seq, this assay tests for antibody binding to full-length protein **(Figure 1.1C)**. By RLBA, these three antigens were present in and specific to both the initial discovery APS1 cohort (n=39) as well as the expanded validation cohort (n = 28), but not the non-APS1 control cohort (n = 61). Together, these results demonstrate that PhIP-Seq detects known APS1 autoantigens and that PhIP-Seq results validate well in orthogonal whole protein-based assays.

To determine whether the PhIP-Seq APS1 dataset could yield higher resolution information on antigenic peptide sequences with respect to previously reported targets, the normalized enrichments of all peptides belonging to known disease-associated antigens CYP11A1 and SOX10 were mapped across the full length of their respective proteins **(Supplementary Figure S1.2)**. The antigenic regions within these proteins were observed to be similar across all samples positive for anti-CYP11A1 and anti-SOX10 antibodies, respectively **(Supplementary Figure S1.2)** suggesting peptide-level commonalities and convergence among the autoreactive antibody repertoires across individuals. These data suggest that people with APS1 often target similar, but not identical protein regions.

Identification of novel APS1 autoantigens

Having confirmed that PhIP-Seq analysis of APS1 sera detected known antigens, the same data were then investigated for the presence of novel, previously uncharacterized APS1 autoantigens. We applied the same positive hit criteria as described for known antigens, and additionally increased the required number of positive APS1 samples to 3/39 to impose a stricter limit on the number of novel candidate autoantigens. This yielded a list of 82 genes, which included 10 known antigens and 72 putative novel antigens **(Figure 1.2)**.

The most commonly held hypotheses regarding the nature and identity of proteins targeted by the aberrant immune response in APS1 are that targeted proteins (1) tend to exhibit

AIRE-dependent thymic expression and (2) have restricted expression to one or few peripheral organs and tend not to be widely or ubiquitously expressed. We investigated whether our novel antigens were also preferentially tissue-restricted. In order to systematically address this question, tissue-specific RNA expression was assessed using a consensus expression dataset across 74 cell types and tissues (Uhlen et al., 2015). For each gene, the ratio of expression in the highest tissue as compared to the sum of expression across all tissues was calculated, resulting in higher ratios for those mRNAs with greater degrees of tissue-restriction. Using this approach, the mean tissue-specificity ratio of the 82 PhIP-Seq positive antigens was increased by approximately 1.5-fold ($p=0.0017$) as compared to the means from iterative sampling of 82 genes (**Supplementary Figure S1.3**).

Identification of novel antigens common to many individuals

Identified autoantigens were ranked by frequency within the cohort. Five antigens were positive in ten or more APS1 samples, including two novel antigens. In addition, the majority of antigens found in 4 or more APS1 sera were novel (**Figure 1.3A**). Five of the most frequent novel antigens were selected for subsequent validation and follow-up. These included RFX6, a transcription factor implicated in pancreatic and intestinal pathology (Patel et al., 2017; S. B. Smith et al., 2010); ACP4, an enzyme implicated in dental enamel hypoplasia (Choi et al., 2016; Seymen et al., 2016; C. E. Smith et al., 2017); KHDC3L, a protein with oocyte-restricted expression (Li et al., 2008; Zhang et al., 2018; K. Zhu et al., 2015); NKX6-3, a gastrointestinal transcription factor (Alanentalo et al., 2006); and GIP, a gastrointestinal peptide involved in intestinal motility and energy homeostasis (Adriaenssens et al., 2019; Moody et al., 1984; Pederson & McIntosh, 2016). Several less frequent (but still shared) novel antigens were also chosen for validation, including ASMT, a pineal gland enzyme involved in melatonin synthesis (Ackermann et al., 2006; Rath et al., 2016); and PDX1, an intestinal and pancreatic transcription factor (Holland et al., 2002; Stoffers et al., 1997) (**Figure 1.3A**). Of note, this group of seven novel antigens all exhibited either

tissue enriched, tissue enhanced, or group enhanced expression according to the Human Protein Atlas database (Uhlen et al., 2015) **(Supplementary Table S1.2).** Using a whole-protein radiolabeled binding assay (RLBA) for validation, all seven proteins were immunoprecipitated by antibodies in both the PhIP-Seq APS1 discovery cohort (n=39), as well as in the validation cohort of APS1 sera that had not been interrogated by PhIP-Seq (n=28). Whereas an expanded set of non-APS1 controls (n=61) produced little to no immunoprecipitation signal by RLBA as compared to positive control antibodies (low antibody index), APS1 samples yielded significant immunoprecipitation signal enrichment for each whole protein assay (high antibody index) (**Figure 1.3B & Supplementary Table S1.3**).

The comparison of PhIP-Seq data to the results from the RLBAs (n=39, discovery cohort only) yielded positive correlations between the two datasets (r = 0.62-0.95; **Supplementary Figure S1.4**). Notably, for some antigens, such as NLRP5, and particularly for ASMT, the RLBA results revealed additional autoantibody-positive samples not detected by PhIP-Seq **(Figure 1.3B & Supplementary Figure S1.4 & Supplementary Figure S1.2)**.

Autoantibody-disease associations for both known and novel antigens

Because the individuals in this APS1 cohort have been extensively phenotyped for 24 clinical manifestations, the PhIP-Seq APS1 data was queried for phenotypic associations. Several autoantibody specificities, both known and novel, were found to possess highly significant associations with several clinical phenotypes **(Figure 1.4 & Supplementary Figure S1.5)**. Among these were the associations of KHDC3L with ovarian insufficiency, RFX6 with diarrheal-type intestinal dysfunction, CYP11A1 (also known as cholesterol side chain cleavage enzyme) with adrenal insufficiency (AI), and SOX10 with vitiligo (**Figure 1.4**). Strikingly, anti-CYP11A1 antibodies are present in AI and are known to predict disease development (Betterle et al., 2002; Obermayer-Straub et al., 2000; Winqvist et al., 1993). Similarly, antibodies to SOX10, a

transcription factor involved in melanocyte differentiation and maintenance, have been previously shown to correlate with the presence of autoimmune vitiligo (Hedstrand et al., 2001).

Anti-KHDC3L antibodies in APS1-associated ovarian insufficiency

Primary ovarian insufficiency is a highly penetrant phenotype, with an estimated 60% of females with APS1 progressing to an early, menopause-like state (Ahonen et al., 1990; Ferré et al., 2016). Interestingly, a set of 5 proteins (KHDC3L, SRSF8, PNO1, RASIP1, and MORC2) exhibited a significant association with ovarian insufficiency in this cohort (**Figure 1.4**). A publicly available RNA-sequencing dataset from human oocytes and supporting granulosa cells of the ovary confirmed that of these 5 genes, only *KHDC3L* exhibited expression levels in female oocytes comparable to the expression levels seen for the known oocyte markers *NLRP5* and *DDX4* (Zhang et al., 2018) (**Supplementary Figure S1.6**). We therefore chose to further investigate the relationship between anti-KHDC3L antibodies and ovarian insufficiency in our cohort (**Figure 1.5**).

KHDC3L is a well-studied molecular binding partner of NLRP5 within the ovary (Li et al., 2008; K. Zhu et al., 2015). Together, NLRP5 and KHDC3L form part of a critical oocyte-specific molecular complex, termed the subcortical maternal complex (SCMC) (Bebbere et al., 2016; Brozzetti et al., 2015; Li et al., 2008; Liu et al., 2016; K. Zhu et al., 2015). Furthermore, knockout of the *NLRP5* and *KHDC3L* in female mice results in fertility defects, and human genetic mutations in these genes of the SCMC have been linked to infertility and molar pregnancies (Li et al., 2008; Y. Zhang et al., 2018; K. Zhu et al., 2015). Interestingly, previous work established NLRP5 as a parathyroid-specific antigen in APS1, with potential for additional correlation with ovarian insufficiency (Alimohammadi et al., 2008). However, anti-NLRP5 antibodies lack sensitivity for ovarian insufficiency. Importantly, unlike NLRP5, KHDC3L is expressed primarily in the ovary, and thus potentially represents a more oocyte-specific autoantigen (Liu et al., 2016; Virant-Klun et al., 2016; Y. Zhang et al., 2018). Using the dataset from Zhang et. al, we confirmed that

KHDC3L, as well as NLRP5 and the known oocyte marker DDX4, are highly expressed within the oocyte population, but not in the supporting granulosa cell types (Y. Zhang et al., 2018) **(Figure 1.5A).** Interestingly, the majority (64%) of APS1 sera had a concordant status for antibodies to KHDC3L and NLRP5 **(Figure 1.5B)**. Although previous reports did not find a strong gender prevalence within samples positive for anti-NLRP5 antibodies, the mean anti-NLRP5 and anti-KHDC3L antibody signals were increased in females in this cohort **(by 1.6- and 2.1-fold, respectively; Figure 1.5C)**. Finally, all 10 females in the expanded APS1 cohort with diagnosed ovarian insufficiency were also positive for anti-KHDC3L antibodies **(Figure 1.5D)**.

High prevalence of anti-ACP4 antibodies

Similar to known antigens CYP11A1, SOX10, and LCN1, the novel antigen ACP4 was found to occur at high frequencies in this cohort (**Figure 1.3A**). ACP4 (acid phosphatase 4) is highly expressed in dental enamel, and familial mutations in the *ACP4* gene result in dental enamel hypoplasia similar to the enamel hypoplasia seen in ~90% of this APS1 cohort (Seymen et al., 2016; C. E. Smith et al., 2017). Strikingly, 50% of samples were positive for anti-ACP4 antibodies by RLBA, with excellent correlation between RLBA and PhIP-Seq data (**Figure 1.3B & Supplementary Figure S1.4**). Consistently, samples from individuals with enamel hypoplasia exhibited a trend towards higher anti-ACP4 antibody signal by RLBA (**Supplementary Figure S1.4, p = 0.064**).

High prevalence of anti-RFX6 antibodies

In this cohort, 82% (55/67) of APS1 sera exhibited an RFX6 signal that was at least 3 standard deviations above the mean of non-APS1 control signal due to the extremely low RFX6 signal across all non-APS1 controls by RLBA **(Figure 1.3B)**. Using a more stringent cutoff for RFX6 positivity by RLBA at 6 standard deviations above the mean, 65% of APS1 samples were positive for anti-RFX6 antibodies. RFX6 is expressed in both intestine and pancreas, and loss of

function RFX6 variants in humans lead to both intestinal and pancreatic pathology (Gehart et al., 2019; Patel et al., 2017; Piccand et al., 2019; S. B. Smith et al., 2010). Interestingly, across all samples with anti-RFX6 antibodies, the response targeted multiple sites within the protein, suggesting a polyclonal antibody response **(Supplementary Figure S1.7**).

Anti-enteroendocrine and anti-RFX6 response in APS1

The extent and frequency of intestinal dysfunction in people with APS1 has only recently been clinically uncovered and reported, and therefore still lacks unifying diagnostic markers as well as specific intestinal target antigen identities (Ferré et al., 2016). This investigation of APS1 sera revealed several antigens that are expressed in the intestine, including RFX6, GIP, PDX1, and NKX6-3. We chose to further study whether autoimmune response to RFX6+ cells in the intestine was involved in APS1-associated intestinal dysfunction. Using a publicly available murine single-cell RNA sequencing dataset of 16 different organs and over 120 different cell types, *RFX6* expression was confirmed to be present in and restricted to pancreatic islets and intestinal enteroendocrine cells (Schaum et al., 2018) **(Supplementary Figure S1.7)**. Serum from an individual with APS1-associated intestinal dysfunction and anti-RFX6 antibodies was next tested for reactivity against human intestinal enteroendocrine cells, revealing strong nuclear staining that colocalized with ChromograninA (ChgA), a well-characterized marker of intestinal enteroendocrine cells (Goldspink et al., 2018; O'Connor et al., 1983) (**Figure 1.6A, right panel and inset**). In contrast, enteroendocrine cell staining was not observed from APS1 samples that lacked anti-RFX6 antibodies or from non-APS1 control samples. **(Figure 1.6A, center & left panels)**. Furthermore, serum from samples with anti-RFX6 antibodies stained transfected tissue culture cells expressing RFX6 **(Figure 1.6B, Supplementary Figure S1.8)**. These data support the notion that there exists a specific antibody signature, typified by anti-RFX6 antibodies, associated with enteroendocrine cells in APS1.

Both mice and humans with biallelic mutation of the gene encoding RFX6 have enteroendocrine cell deficiency and intestinal malabsorption (Mitchell et al., 2004; Piccand et al., 2019; S. B. Smith et al., 2010), and humans with other forms of genetic or acquired enteroendocrine cell deficiency also suffer from chronic malabsorptive diarrhea (Akoury et al., 2015; Li et al., 2008; Reddy et al., 2012; X. Wang et al., 2018; W. Zhang et al., 2019). In this cohort, 54/67 (81%) of individuals have intestinal dysfunction defined as the presence of chronic diarrhea, chronic constipation or an alternating pattern of both, without meeting ROME III diagnostic criteria for irritable bowel syndrome, as previously described (Ferré et al., 2016). When the cohort was subsetted by presence or absence of intestinal dysfunction, the anti-RFX6 RLBA signal was significantly higher when intestinal dysfunction was present (**Figure 1.6C**). Further subsetting of the cohort by subtype of intestinal dysfunction revealed that individuals with anti-RFX6 antibodies belonged preferentially to the diarrheal-type (as opposed to constipation-type) group of intestinal dysfunction (**Figure 1.6D & Figure 6: Figure Supplement 3A**). Given that RFX6 is also expressed in the pancreas, we also examined the association of anti-RFX6 antibodies with APS1-associated type 1 diabetes. We observed that 6/7 APS1-associated type 1 diabetes samples had positive signal for anti-RFX6 antibodies by RLBA (**Supplementary Figure S1.9**). However, due to small sample size, an expanded cohort would be needed to determine the significance of this observation. Together, these data suggest that RFX6 is a common, shared autoantigen in APS1 that may be involved in the immune response to intestinal enteroendocrine cells as well as pancreatic islets. Future studies will help to determine whether testing for anti-RFX6 antibodies possesses clinical utility for prediction or diagnosis of specific APS1 autoimmune disease manifestations as well as for non-APS1 autoimmune disease.

DISCUSSION

Here, we have identified a new set of autoantigens that are associated with autoimmune features in APS1 by using the broad-based antigen screening platform of PhIP-Seq. Unlike fixed protein arrays, programmable phage display possesses the advantage of being able to comprehensively cover all annotated proteins and their isoforms. The PhIP-Seq library used here is composed of over 700,000 peptides, each 49 amino acids, and corresponding to approximately 20,000 proteins and their known splicing isoforms. This is highly complementary to recently published protein arrays that cover approximately 9,000 distinct proteins (Fishman et al., 2017; Landegren et al., 2016; Meyer et al., 2016). Recent protein array approaches with APS1 samples using strict cutoffs have been able to identify a number of new autoantigen targets that include PDILT and MAGEB2 (Landegren et al., 2016). Several new targets, including RFX6, KHDC3L, ACP4, NKX6-3, ASMT, and PDX1, were likely discovered here because these antigens were not present on previously published protein array platforms. Only a subset of the novel targets identified here were validated orthogonally. While none failed validation relative to non-APS1 controls, further validation work will be needed for the many additional novel targets identified by PhIP-Seq. It is also worth mentioning that the PhIP-Seq method leverages continuing declines in the cost of oligonucleotide synthesis and Next-Generation Sequencing. Both technologies benefit from economies of scale, and once constructed, a PhIP-Seq phage library may be propagated in large quantities at negligible cost. The primary disadvantage of PhIP-Seq is the fact that conformation specific antibodies are likely to be missed, unless short linear subsequences carry significant binding energy. For example, PhIP-Seq detected only limited signal towards some literature reported antigens, including GAD65 and interferon family proteins in this APS1 cohort. Given that these antigens have been reported to involve conformational epitopes, antibodies to these antigens would not be predicted to be easily detected by linear peptides (Björk et al., 1994; Meager et al., 2006; Meyer et al., 2016; Wolff et al., 2013; Ziegler et al., 1996). Nonetheless, the

ability to detect anti-interferon antibodies in a subset of APS1 samples highlights the utility of PhIP-Seq for antigen discovery despite decreased sensitivity for certain epitopes **(Supplementary Figure S1.1)**.

People with (Anderson, 2002; Cheng & Anderson, 2018; Husebye et al., 2018; Malchow et al., 2016)APS1 develop autoimmune manifestations over the course of many years, and it is thought that each manifestation may be explained by autoimmune response to one or few initial protein targets. In principle, these target proteins would most likely (1) exhibit thymic AIRE-dependency and (2) be restricted to the single or narrow range of tissues associated with the corresponding autoimmune disease. For example, adrenal insufficiency, which results from autoimmune response to cells of the adrenal gland, is thought to occur due to targeting of adrenally-expressed cytochrome p450 family members (Obermayer-Straub et al., 2000; Winqvist et al., 1993). However, a more complete understanding of the protein target spectrum paired with clinical phenotypic associations has been lacking. This, combined with the limited applicability of murine observations to the human disease, has left the question of which clinical characteristics best associate with APS1 autoantigens a heavily debated subject (Pöntynen et al., 2006).

Testing for defined autoantibody specificities provides substantial clinical benefit for prediction and diagnosis of autoimmune disease. A primary goal of this study was to identify autoantigens with potential clinical significance; consistently, our analyses focused primarily on antigens that appeared across multiple samples, rather than autoantigens that were restricted to individual samples. Using conservative inclusion criteria, we discovered 72 novel autoantigens that were shared across a minimum of 3 APS1 samples, of which 7/7 were successfully validated at the whole protein level. Overall, we have expanded the known repertoire of common APS1 antigens, confirming that the antibody target repertoire of common antigens in APS1 is larger than previously appreciated. Interestingly, our data also suggest that the size of the commonly autoantibody-targeted repertoire of proteins is dramatically lower than the number of genes (~4000) that exhibit AIRE-dependent thymic expression.

The spectrum of different autoimmune diseases that can be observed in APS1 is extensive and has continued to expand through investigation of larger cohorts (Ahonen et al., 1990; Bruserud et al., 2016; Ferré et al., 2016). In this study, clinical metadata encompassing disease status across 24 individual disease manifestations in a total of 67 people with APS1 was leveraged to uncover (among others) an association of anti-KHDC3L antibodies and ovarian insufficiency, a disease that affects over half of all women with APS1 and manifests as abnormal menstrual cycling, reduced fertility, and early menopause. While autoreactivity to the steroidogenic granulosa cells – the cells surrounding and supporting the oocytes – has been proposed as one etiology of the clinical ovarian insufficiency, it has also been suggested that there may exist an autoimmune response to the oocyte itself (Jasti et al., 2012; Maclaren et al., 2001; Obermayer-Straub et al., 2000; Otsuka et al., 2011; Welt, 2008). Our finding that females with APS1-associated ovarian insufficiency exhibit autoantibodies to KHDC3L, an oocyte specific protein, supports this hypothesis. As exemplified by autoantibody presence in other autoimmune conditions, anti-KHDC3L antibodies may also have predictive value. Specifically, in our cohort, we found anti-KHDC3L antibodies to be present in many young, pre-menstrual females; these observations will require additional studies in prospective, longitudinal cohorts for further evaluation of potential predictive value. Interestingly, primary ovarian insufficiency (POI) in the absence of AIRE-deficiency is increasingly common and affects an estimated 1 in 100 women; up to half of these cases have been proposed to have autoimmune etiology (Huhtaniemi et al., 2018; Jasti et al., 2012; Nelson, 2009; Silva et al., 2014).

We noted that the majority of samples with antibodies to KHDC3L also exhibited antibodies to NLRP5, and vice versa. Remarkably, both of these proteins are critical parts of a subcortical maternal complex (SCMC) in both human and murine oocytes (Li et al., 2008; K. Zhu et al., 2015). Indeed, “multi-pronged” targeting of the same pathway has been previously implicated in APS1, where antibodies to DDC and TPH1 – enzymes in the serotonin and melatonin synthesis pathways – have been described (Ekwall et al., 1998; Husebye et al., 1997;

Kluger et al., 2015). In addition to these targets, our data revealed an additional autoantibody-targeted enzyme ASMT in the same melatonin synthesis pathway. While the earlier TPH1- and DDC-catalyzed steps occur in both the intestine and pineal gland and precede the formation of serotonin, ASMT is predominantly expressed in the pineal gland and catalyzes the last, post-serotonin step in melatonin synthesis, suggesting that targeting of this pathway occurs at multiple distinct steps. To our knowledge, this is the first reported autoantigen in APS1 whose expression is restricted to the central nervous system.

In past and ongoing investigations, some individuals with APS1 have been reported to feature histologic loss of intestinal enteroendocrine cells on biopsy (Högenauer et al., 2001; Oliva-Hemker et al., 2006; Posovszky et al., 2012, Natarajan et al., manuscript in preparation). The association of anti-RFX6 antibodies with the diarrheal type of intestinal dysfunction is consistent with published studies in murine models of *Rfx6* (and enteroendocrine cell) ablation (Piccand et al., 2019; S. B. Smith et al., 2010). In addition, human enteroendocrine cell deficiency as well as mutations in enteroendocrine gene *NEUROG3* have been linked to chronic diarrhea and malabsorption, and recently, intestinal enteroendocrine cells have been suggested to play a role in mediating intestinal immune tolerance (Ohsie et al., 2009; Sifuentes-Dominguez et al., 2019; J. Wang et al., 2006). In sum, although APS1-associated intestinal dysfunction may have multiple etiologies, including autoimmune enteritis or dysfunction of exocrine pancreas, our findings of highly prevalent anti-RFX6 antibodies provide evidence of a common, shared autoantigen involved with this disease phenotype. In addition, patients with type 1 diabetes alone (not in association with APS1) frequently exhibit intestinal dysfunction related to multiple etiologies including Celiac disease, autonomic neuropathy, and exocrine pancreatic insufficiency (Du et al., 2018); future studies will be needed to determine whether anti-RFX6 antibodies may distinguish a subset of these patients with an autoimmune enteroendocrinopathy contributing to their symptoms.

While we report many novel antigens, we also acknowledge that the relationship between autoantibody status and disease is often complicated. This concept can be illustrated by examining the well-established autoantibody specificities in autoimmune diabetes (Taplin & Barker, 2009). First, islet autoantibodies (GAD65, ZNT8, etc.) can be found within non-autoimmune sera, where they are thought to represent an increased risk of developing disease as compared to the antibody-negative population. Second, not all patients with autoimmune diabetes are autoantibody positive. In sum, while autoantibodies can be extremely useful for risk assessment as well as for diagnosis, they often lack high sensitivity and specificity; both of these caveats can result in difficulties detecting strong clinical associations. For example, anti-ACP4 antibodies are highly prevalent in our cohort, but they exhibit only a trending association with dental enamel hypoplasia despite the strong biological evidence that ACP4 dysfunction leads to enamel hypoplasia (Seymen et al., 2016; C. E. Smith et al., 2017). Our data in humans is currently insufficient to determine whether immune responses to novel antigens such as ACP4 are pathogenic, indirectly linked to risk of disease, or instead simply represent a B-cell bystander effect. To better address these questions, we propose that future studies in mouse models could elucidate whether immune response to specific proteins, including ACP4, can result in the proposed phenotypes.

As the spectrum of diseases with potential autoimmune etiology continues to expand, the characteristic multiorgan autoimmunity in APS1 provides an ideal model system to more broadly approach the question of which proteins and cell types tend to be aberrantly targeted by the immune system. The data presented here have illuminated a collection of novel human APS1 autoimmune targets, as well as a novel antibody-disease association between RFX6 and diarrheal-type intestinal dysfunction, a highly prevalent disorder in APS1 that has until now lacked clinically applicable predictive or diagnostic markers. In sum, these data have significantly expanded the known autoantigen target profile in APS1 and highlighted several new directions for exploring the mechanics and clinical consequences of this complex syndrome.

MATERIALS AND METHODS

Data collection

All patient cohort data was collected and evaluated at the NIH, and all APECED/APS1 patients were enrolled in a research study protocols approved by the NIAID, NIH Clinical Center, and NCI Institutional Review Board Committee and provided with written informed consent for study participation. All NIH patients gave consent for passive use of their medical record for research purposes (protocol #11-I-0187). The majority of this cohort data was previously published by Ferré et al. 2016 and Ferré et al. 2019.

Phage Immunoprecipitation – Sequencing (PhIP-Seq)

For PhIP-Seq, we adapted a custom-designed phage library consisting of 731,724 49AA peptides tiling the full protein-coding human genome including all isoforms (as of 2016) with 25AA overlap as previously described (O'Donovan et al., 2018). 1 milliliter of phage library was incubated with 1 microliter of human serum overnight at 4C, and human antibody (bound to phage) was immunoprecipitated using 40ul of a 1:1 mix of protein A/G magnetic beads (Thermo Fisher, Waltham, MA, #10008D & #10009D). Beads were washed 4 times and antibody-bound phage were eluted into 1ml of E. Coli at OD of 0.5-0.7 (BLT5403, EMD Millipore, Burlington, MA) for selective amplification of eluted phage. This library was re-incubated with human serum and repeated, followed by phenol-chloroform extraction of DNA from the final phage library. DNA was barcoded and amplified (Phusion PCR, 30 rounds), gel purified, and subjected to Next-Generation Sequencing on an Illumina MiSeq Instrument (Illumina, San Diego, CA).

PhIP-Seq Analysis

Sequencing reads from fastq files were aligned to the reference oligonucleotide library and peptide counts were subsequently normalized by converting raw reads to percentage of total

reads per sample. Peptide and gene-level enrichments for both APS1 and non-APS1 sera were calculated by determining the fold-change of read percentage per peptide and gene in each sample over the mean read percentage per peptide and gene in a background of mock-IP (A/G bead only, n = 18). Individual samples were considered positive for genes where the enrichment value was 10-fold or greater as compared to mock-IP. For plotting of multiple genes in parallel (**Figures 1.1 & 1.2**), enrichment values were z-scored and hierarchically clustered using Pearson correlation.

Statistics

For comparison of distribution of PhIP-Seq gene enrichment between APS1 patients with and without specific disease manifestations, a (non-parametric) Kolmogorov-Smirnov test was used. For radioligand binding assays, antibody index for each sample was calculated as follows: (sample value – mean blank value) / (positive control antibody value – mean blank value). Comparison of antibody index values between non-APS1 control samples and APS1 samples was performed using a Mann-Whitney *U* test. Experimental samples that fell 3 standard deviations above of the mean of non-APS1 controls for each assay were considered positive, except in the case of RFX6, where a cutoff of 6 standard deviations above the mean of non-APS1 controls was used.

Assessing tissue-specific RNA expression

To determine tissue-specificity and tissue-restriction of *Rfx6* expression in mice, we used publicly available Tabula Muris data (tabula-muris.ds.czbiohub.org) (Schaum et al., 2018). For investigation of *KHDC3L* expression in human ovary, we downloaded publicly available normalized FPKM transcriptome data from human oocytes and granulosa cells (GSE107746_Folliculogenesis_FPKM.log2.txt) (Y. Zhang et al., 2018). With this data, we

performed principle component analysis, which clustered the two cell types correctly according to their corresponding sample label, and plotted log2(FPKM) by color for each sample.

293T overexpression assays

Human kidney embryo 293T (ATCC, Manassas, VA, #CRL-3216) cells were plated at 30% density in a standard 24-well glass bottom plate in complete DMEM media (Thermo Fisher, #119651198) with 10% Fetal Bovine Serum (Thermo Fisher, #10438026), 292ug/ml L-glutamine, 100ug/ml Streptomycin Sulfate, and 120Units/ml of Penicillin G Sodium (Thermo Fisher, #10378016). 18 hours later, cells were transiently transfected using a standard calcium chloride transfection protocol. For transfections, 0.1ug of sequence-verified pCMV-insert-MYC-FLAG overexpression vectors containing either no insert (Origene #PS100001; 'mock' transfection) or RFX6 insert (Origene #RC206174) were transfected into each well. 24 hours post-transfection, cells were washed in 1X PBS and fixed in 4% PFA for 10 minutes at room temperature.

293T indirect immunofluorescence

Fixed 293T cells were blocked for 1 hour at room temperature in 5% BSA in PBST. For primary antibody incubation, cells were incubated with human serum (1:1000) and rabbit anti-FLAG antibody (1:2000) in 5% BSA in PBST for 2 hours at room temperature (RT). Cells were washed 4X in PBST and subsequently incubated with secondary antibodies (goat anti-rabbit IgG 488, Invitrogen, Carlsbad, CA; #A-11034, 1:4000; & goat anti-human 647, Invitrogen #A-21445, 1:4000) for 1 hour at room temperature. Finally, cells were washed 4X in PBST, incubated with DAPI for 5 minutes at RT, and subsequently placed into PBS for immediate imaging. All images were acquired with a Nikon Ti inverted fluorescence microscope (Nikon Instruments, Melville, NY). All experiments were performed in biological duplicates.

Indirect dual immunofluorescence on human fetal intestine

Human fetal small bowels (21.2 days gestational age) were processed as previously described (Berger et al., 2015). Individual APS1 sera (1:4000 dilution) were used in combination with rabbit antibodies to human Chromogranin A (Abcam, Cambridge, MA; #ab15160, 1:5000 dilution). Immunofluorescence detection utilized secondary Alexa Fluor secondary antibodies (Life Technologies, Waltham, MA; 488 goat anti-human IgG, #A11013; & 546 goat anti-rabbit IgG, #A11010). Nuclear DNA was stained with Hoechst dye (Invitrogen, #33342). All images were acquired with a Leica SP5 White Light confocal laser microscope (Leica Microsystems, Buffalo Grove, IL).

35S-radiolabeled protein generation and binding assay

DNA plasmids containing full-length cDNA under the control of a T7 promoter for each of the validated antigens (**Supplementary Table S1.3**) were verified by Sanger sequencing and used as DNA templates in the T7 TNT in vitro transcription/translation kit (Promega, Madison, WI; #L1170) using [35S]-methionine (PerkinElmer, Waltham, MA; #NEG709A). Protein was column-purified on Nap-5 columns (GE healthcare, Chicago, IL; #17-0853-01) and immunoprecipitated on Sephadex protein A/G beads (Sigma Aldrich, St. Louis, MO; #GE17-5280-02 and #GE17-0618-05, 4:1 ratio) in duplicate with serum or control antibodies in 96-well polyvinylidene difluoride filtration plates (Corning, Corning, NY; #EK-680860). Each well contained 35'000 counts per minute (cpm) of radiolabeled protein and 2.5ul of serum or appropriately diluted control antibody **(Supplementary Table S1.3**). The cpms of immunoprecipitated protein was quantified using a 96-well Microbeta Trilux liquid scintillation plate reader (Perkin Elmer).

FIGURES

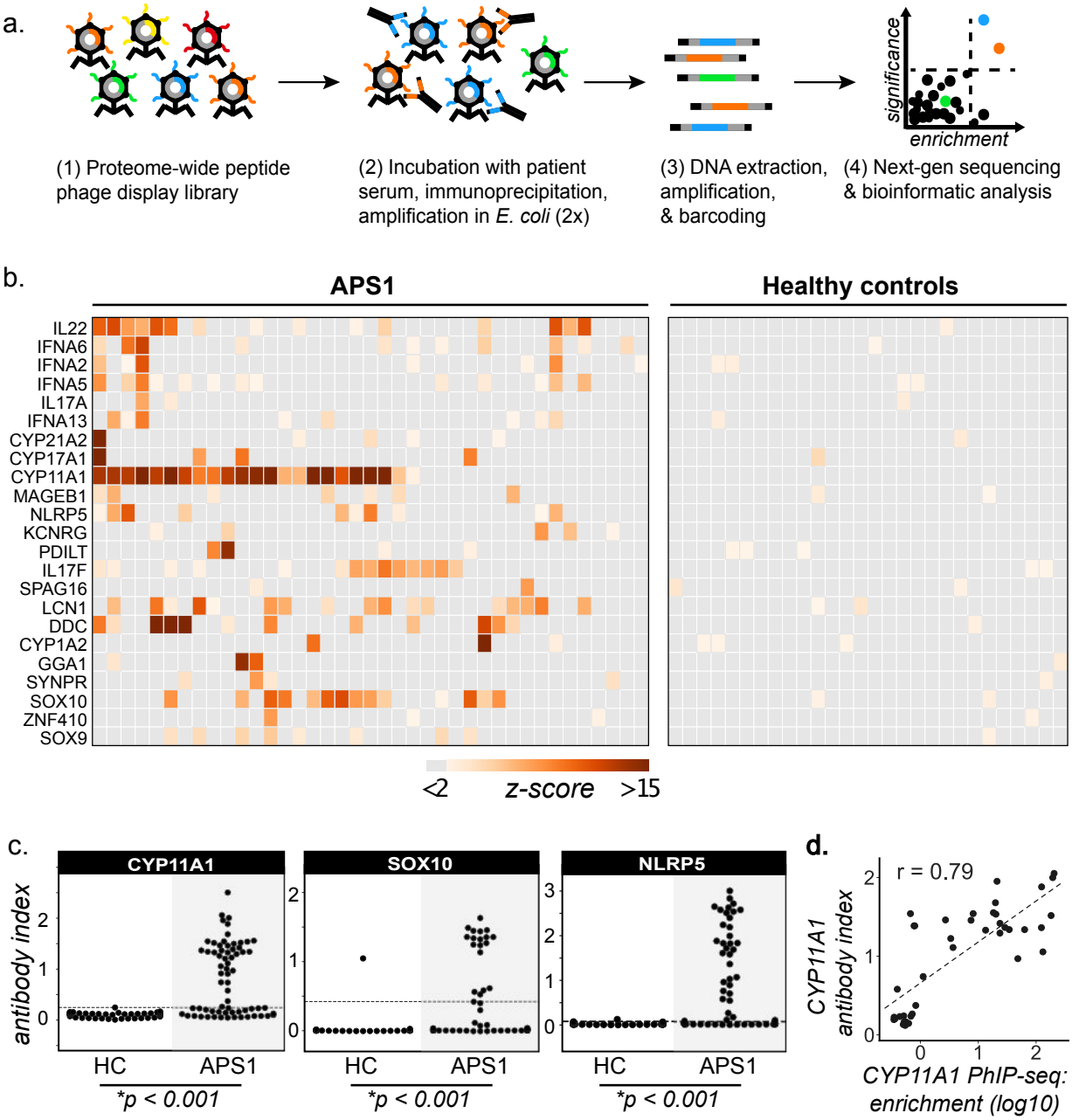

Figure 1.1. PhIP-Seq identifies literature-reported autoantigens in APS1 A. Overview of PhIP-Seq experimental workflow. **B.** PhIP-Seq identifies known autoantibody targets in APS1. Hierarchically clustered (Pearson) z-scored heatmap of literature reported autoantigens with 10-fold or greater signal over mock-IP in at least 2/39 APS1 sera and in 0/28 non-APS1 control sera. See also Figure 1: Figure Supplement 1. **C**. Radioligand binding assay (RLBA) orthogonal validation of literature-reported antigens CYP11A1, SOX10, and NLRP5 within the expanded cohort of APS1 (n = 67) and non-APS1 controls (n = 61); p-value was calculated across all samples using a Mann-Whitney U test. **D**. CYP11A1 RLBA antibody index and CYP11A1 PhIP-Seq enrichment are well correlated (r = 0.79); see also Figure 1: Figure Supplement 2.

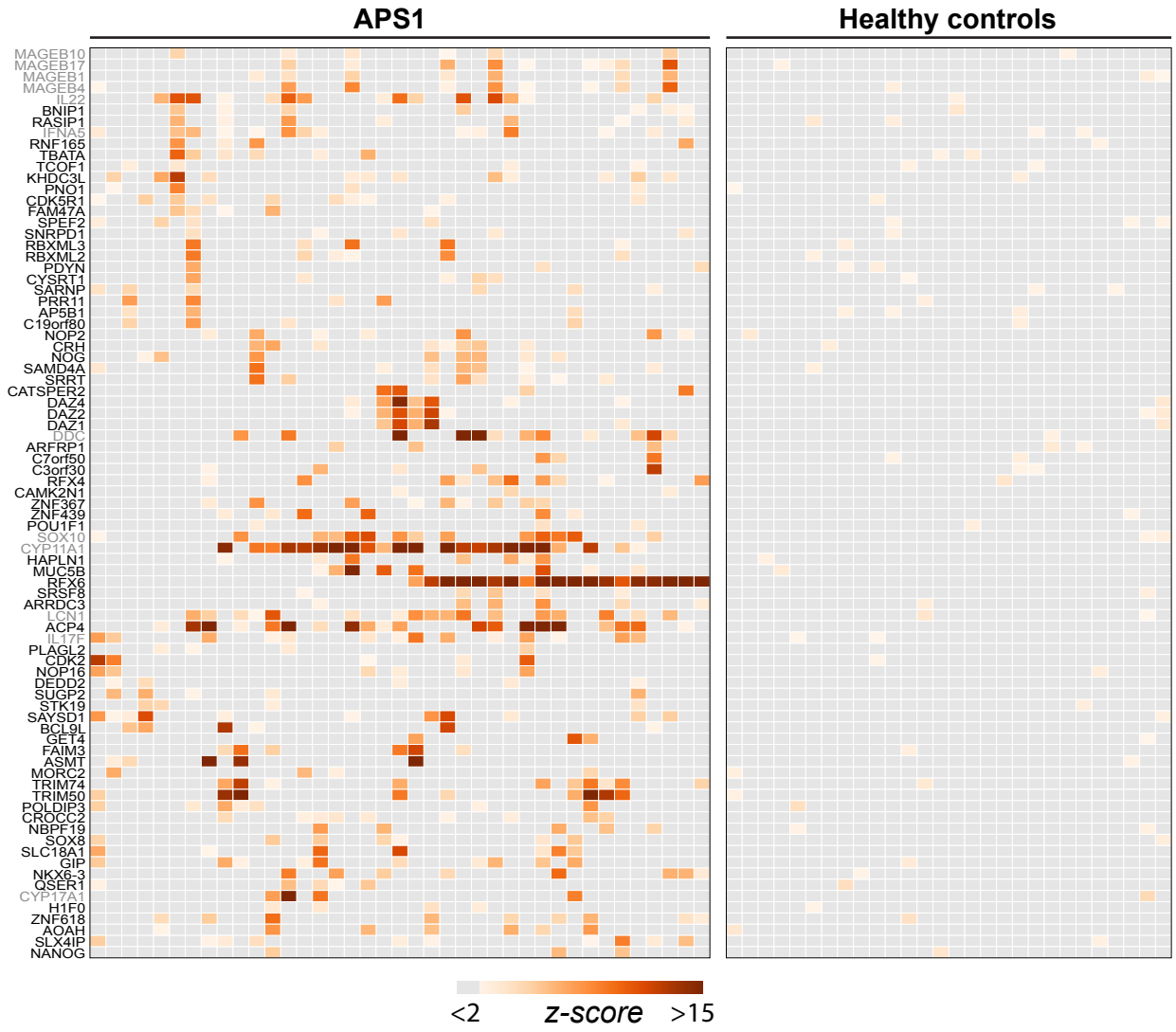

Figure 1.2. PhIP-Seq identifies novel antigens across multiple APS1 sera. A. Hierarchically clustered (Pearson) Z-scored heatmap of all genes with 10-fold or greater signal over mock-IP in at least 3/39 APS1 sera and in 0/28 non-APS1 sera. Black labeled antigens (n=69) are potentially novel and grey labeled antigens (n=12) are previously literature-reported antigens. See also Figure 2: Figure Supplement 1.

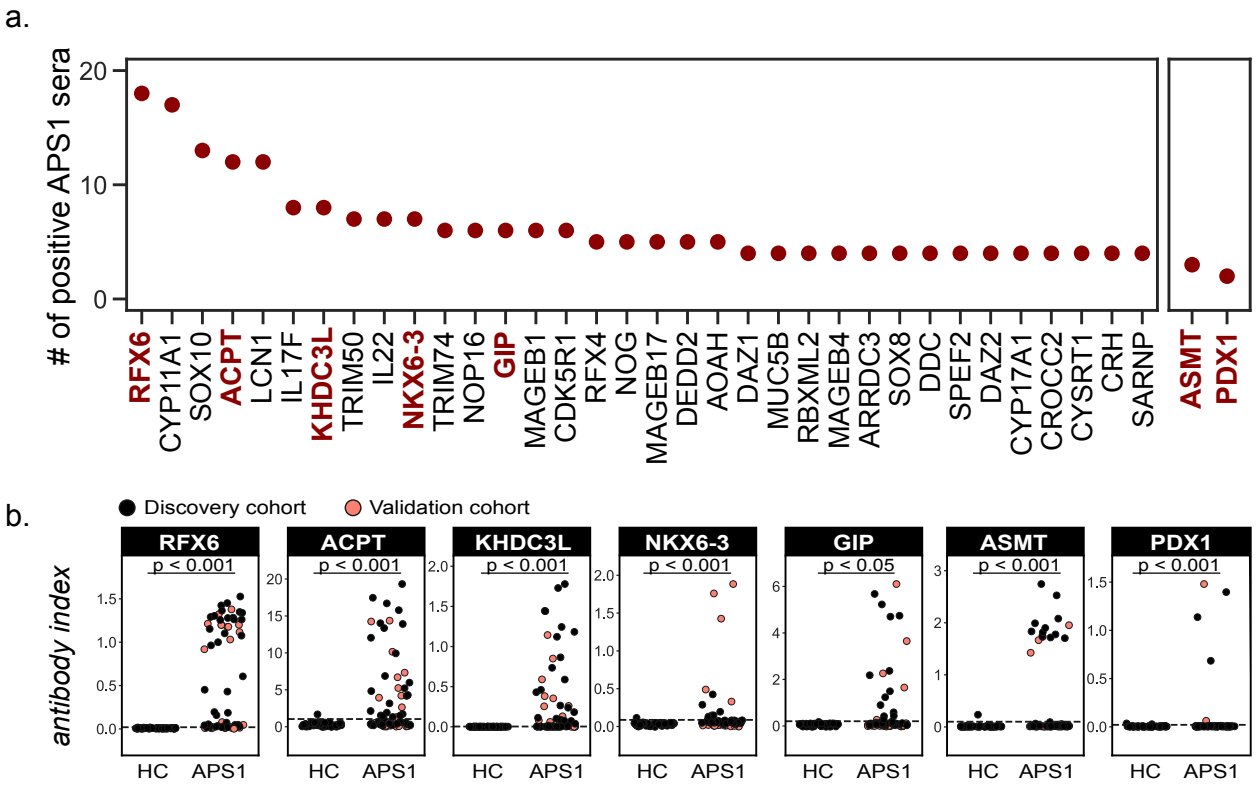

Figure 1.3. Novel PhIP-Seq autoantigens are shared across multiple APS1 samples. A. Graph of the PhIP-seq autoantigens from Figure 2 that were shared across the highest number of individual APS1 sera (left panel). ASMT and PDX1 were positive hits in 3 and 2 sera, respectively, but are known to be highly tissue specific (right panel). Genes in red were chosen for validation in whole protein binding assay. **B.** Validation of novel PhIP-Seq antigens by radiolabeled binding assay, with discovery cohort (black, n_{APS1} = 39), validation cohort (light red, n_{APS1} = 28) and non-APS1 control cohort (n_{HC} = 61). P-value was calculated across all samples using a Mann-Whitney U test. See also Figure 3: Figure Supplement 1.

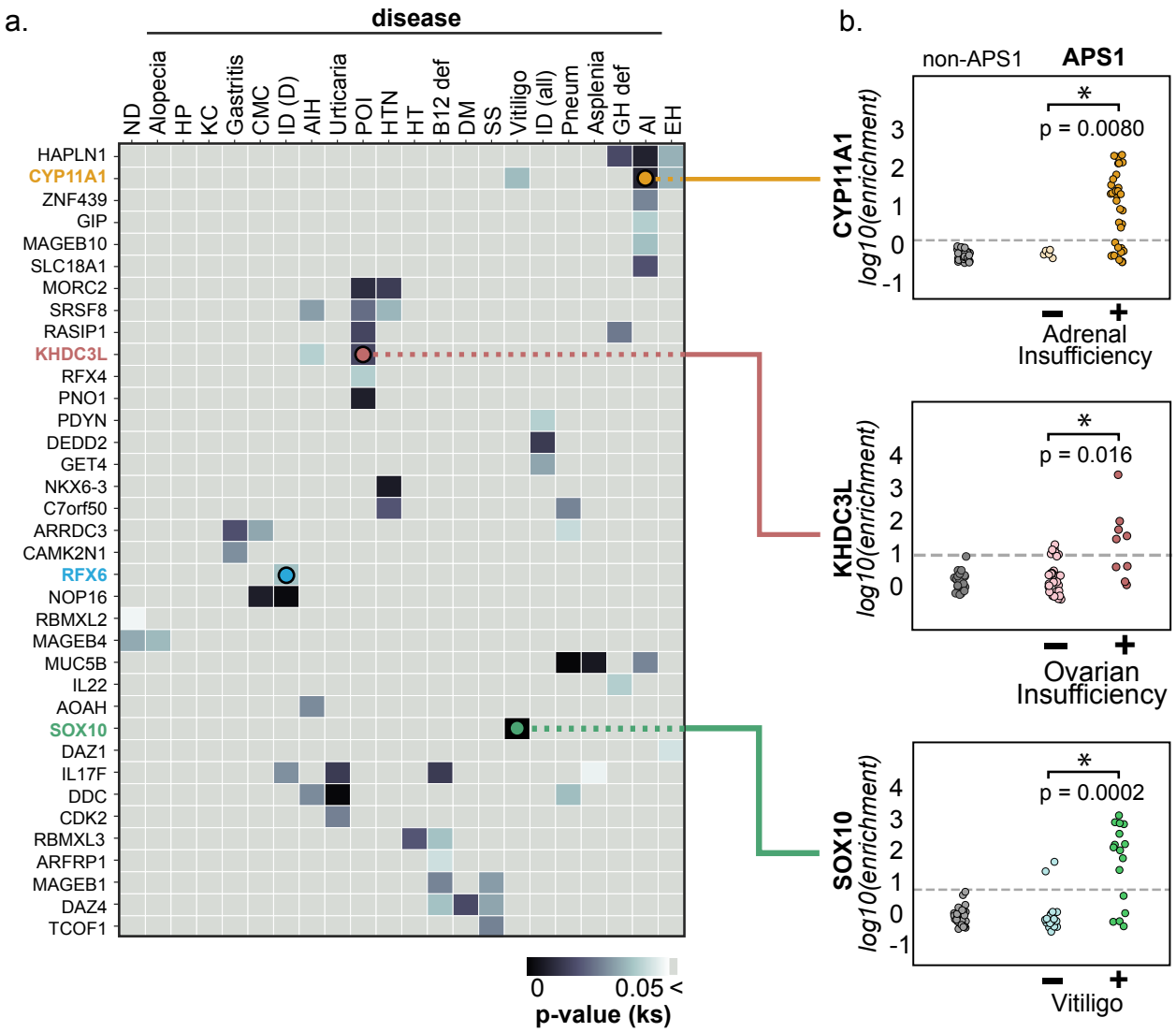

Figure 1.4. PhIP-Seq reproduces known clinical associations. A. Heatmap of p-values (Kolmogorov-Smirnov testing) for differences in gene enrichments for individuals with versus without each clinical phenotype. Significant p-values in the negative direction (where mean PhIP-Seq enrichment is higher in individuals without disease) are masked (colored >0.05). See also Figure 4: Figure Supplement 1. **B.** Anti-CYP11A1 PhIP-Seq enrichments are significantly different between APS1 patients with and without adrenal insufficiency (top panel; Kolmogorov-Smirnov test). Anti-SOX10 PhIP-Seq enrichments are significantly different between APS1 patients with and without Vitiligo (bottom panel). Anti-KHDC3L PhIP-Seq enrichments are significantly different between APS1 patients with and without ovarian insufficiency (middle panel). See also Figure 4: Figure Supplement 2.

ND, nail dystrophy. HP, hypoparathyroidism. KC, keratoconjunctivitis. CMC, chronic mucocutaneous candidiasis. ID (D), Intestinal dysfunction (diarrheal-type). AIH, autoimmune hepatitis. POI, primary ovarian insufficiency. HTN, hypertension. HT, hypothyroidism. B12 def, B12 (vitamin) deficiency. DM, diabetes mellitus. SS, Sjogren's-like syndrome. Pneum,

Pneumonitis. GH def, Growth hormone deficiency. AI, Adrenal Insufficiency. EH, (dental) enamel hypoplasia.

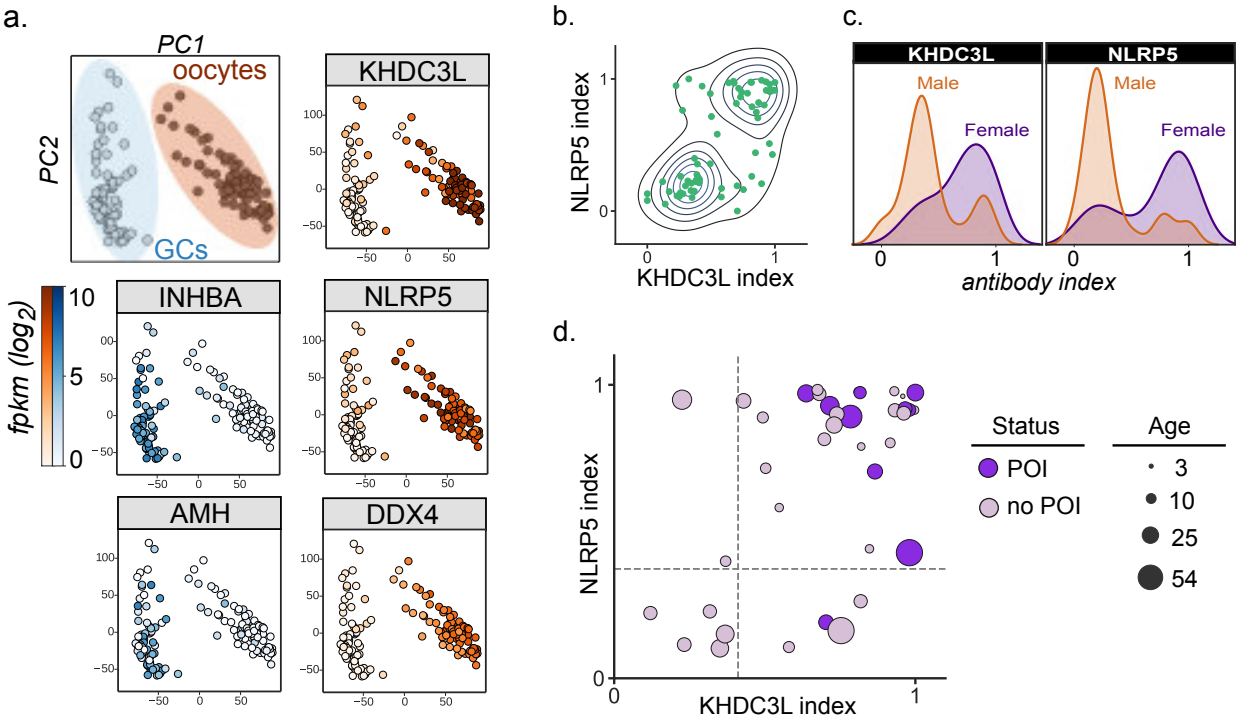

Figure 1.5. Autoantibodies to KHDC3L are associated with ovarian insufficiency. A. Principle component analysis of transcriptome of single human oocytes (red) and granulosa cells (GCs, blue); data from Zhang et al., Mol Cell 2018. KHDC3L is highly expressed in oocytes, along with binding partner NLRP5 and known oocyte marker DDX4. For comparison, known GC markers INHBA and AMH are primarily expressed in the GC population. **B.** APS1 sera that are positive for one of anti-KHDC3L and anti-NLRP5 autoantibodies tend to also be positive for the other. **C.** Antibody indices for both KHDC3L and NLRP5 are increased in females with APS1. **D.** Antibody indices for females with APS1 by age; All 10 patients with primary ovarian insufficiency (POI) are positive for anti-KHDC3L antibodies. Of note, many of the individuals with anti-KHDC3L antibodies but without POI are younger and therefore cannot be fully evaluated for ovarian insufficiency.

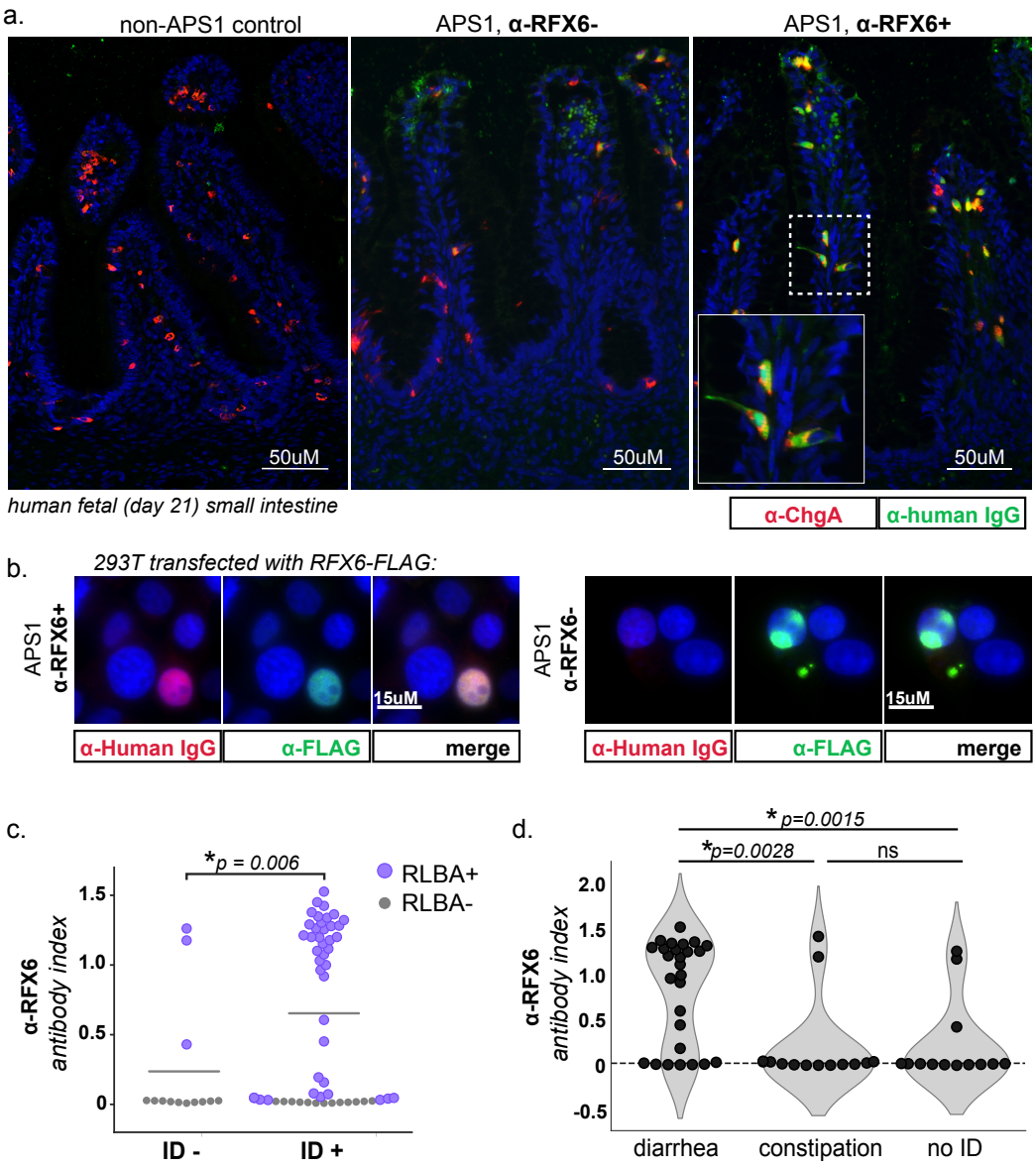

Figure 1.6. APS1 patients with intestinal dysfunction have antibodies to RFX6. A. Anti-RFX6 positive APS1 serum with intestinal dysfunction co-stains Chromogranin-A (ChgA) positive enteroendocrine cells in a nuclear pattern (right panel & inset). In contrast, non-APS1 control sera as well as anti-RFX6 negative APS1 serum do not co-stain ChgA+ enteroendocrine cells (left and center panels). **B.** Anti-RFX6+ serum, but not anti-RFX6- serum, co-stains HEK293T cells transfected with an RFX6-expressing plasmid. See also Figure 6: Figure Supplement 2. **C.** Radioligand binding assay (RLBA) anti-RFX6 antibody index is significantly higher across individuals with intestinal dysfunction (ID; Mann-Whitney U, p = 0.006). Purple color indicates samples that fall above 6 standard deviations of the mean non-APS1 control RLBA antibody index. **D.** Individuals with the diarrheal subtype of ID have a higher frequency of anti-RFX6 antibody positivity as compared to those with constipation-type ID (Mann-Whitney U, p=0.0028) or no ID (p=0.0015). See also Figure 6: Figure Supplement 3.
For associated RFX6 PhIP-Seq & tissue expression data, see Figure 6: Figure Supplement 1.

SUPPLEMENTAL FIGURES

Supplementary Table S1.1. APS1 cohort: Clinical Data.

Patient Code	Gender	Age*	Clinical Phenotypes	Cohort
AIRE.04	F	14	CMC, HP, AI, DM, EH, ND, HTN, SS, Pneumonitis, UE, GH def, ID (D)	**D**
AIRE.05	F	11	CMC, HP, AI, AIH, Gastritis, EH, HTN, Pneumonitis, UE, Vitiligo, ID (B)	**D**
AIRE.09	F	10	HP, AIH, EH, Pneumonitis, UE	**D**
AIRE.13	F	10	CMC, HP, AI, Gastritis, UE, Vitiligo, ID (D)	**D**
AIRE.14	M	7	CMC, AI, AIH, DM, Gastritis, EH, ND, KC, SS, Pneumonitis, UE, Vitiligo, B12 def, ID (C)	**D**
AIRE.18	F	18	CMC, HP, AI, POI, ND, SS	**D**
AIRE.19	M	12	CMC, HP, AI, AIH, Gastritis, EH, Pneumonitis, UE, GH def, Asplenia, ID (B)	**D**
AIRE.20	F	25	CMC, AI, Gastritis, EH, KC, SS, ID (D)	**D**
AIRE.21	M	65	CMC, HP, AI, HT, DM, EH, HTN, SS, Vitiligo, B12 def, ID (B)	**D**
AIRE.23	M	38	CMC, HP, AI, Gastritis, TIN, EH, ND, KC, HTN, Vitiligo, Alopecia, B12 def, Asplenia, ID (D)	**D**
AIRE.24	F	15	CMC, HP, AI, AIH, Gastritis, EH, KC, ID (C)	**D**
AIRE.27	M	18	CMC, AI, AIH, DM, Gastritis, EH, KC, SS, Pneumonitis, UE, Vitiligo, B12 def, ID (B)	**D**
AIRE.08	M	11	CMC, HP, AI, EH, UE	**D**
AIRE.07	M	12	CMC, HP, AI, HT, ND, KC, Alopecia, ID (C)	**D**
AIRE.28	M	15	CMC, HP, AI, Gastritis, EH, KC, Vitiligo, ID (C)	**D**
AIRE.22	F	7	CMC, HP, AIH, Gastritis, EH, ND, SS, Pneumonitis, UE, Alopecia, GH def, ID (D)	**D**
AIRE.29	M	9	AI, AIH, EH, ND, UE, Vitiligo, Alopecia, ID (B)	**D**
AIRE.30	M	17	CMC, HP, AIH, EH, UE, Vitiligo, Alopecia, B12 def, ID (C)	**D**
AIRE.23c	F	41	CMC, HP, AI, HT, POI, EH, SS	**D**
AIRE.31	F	18	CMC, HP, AI, AIH, DM, EH, ND, KC, SS, UE, Vitiligo, ID (D)	**D**
AIRE.33	F	14	HP, AI, AIH, POI, EH, UE, ID (D)	**D**
AIRE.34	F	54	CMC, HP, AI, HT, POI, Gastritis, EH, HTN, SS, Pneumonitis, B12 def, ID (D)	**D**
AIRE.35	F	23	CMC, HP, AI, AIH, HT, POI, Gastritis, EH, SS, Pneumonitis, UE, B12 def, Asplenia, ID (D)	**D**
AIRE.11	M	19	CMC, HP, AI, AIH, TF, Gastritis, EH, SS, UE, Vitiligo, GH def, ID (B)	**D**
AIRE.36	M	15	HP, AI, EH, Alopecia	**D**

Patient Code	Gender	Age*	Clinical Phenotypes	Cohort
AIRE.37	F	28	CMC, HP, AI, POI, EH, SS, UE, ID (D)	**D**
AIRE.38	F	7	HP, AI, EH, ND, UE, Alopecia, ID (C)	**D**
AIRE.17	F	6	CMC, HP, EH, KC, UE, ID (D)	**D**
AIRE.39	F	18	CMC, HP, AI, AIH, HT, EH, ND, KC, Pneumonitis, UE, ID (B)	**D**
AIRE.40	F	16	CMC, HP, AI, AIH, POI, EH, Pneumonitis, UE, Alopecia, Asplenia, ID (D)	**D**
AIRE.41	M	20	CMC, AI, HT, TF, EH, HTN, Vitiligo, Alopecia, ID (D)	**D**
AIRE.44	F	24	CMC, HP, AI, POI, Gastritis, EH, ND, KC, HTN, SS, UE, Alopecia, B12 def, ID (D)	**D**
AIRE.46	F	22	CMC, HP, AI, EH, KC, SS, B12 def, GH def, ID (B)	**D**
AIRE.12	F	7	CMC, HP, AI, Gastritis, EH, KC, SS, Pneumonitis, UE, Vitiligo, B12 def, ID (D)	**D**
AIRE.06	F	16	CMC, HP, AI, AIH, HT, Gastritis, EH, HTN, SS, Vitiligo, ID (D)	**D**
AIRE.50	F	26	CMC, AI, Gastritis, HTN, SS, Pneumonitis, UE, B12 def, ID (B)	**D**
AIRE.02	M	51	CMC, HP, AI, TF, Gastritis, EH, HTN, SS, Hpit, Pneumonitis, Vitiligo, B12 def, ID (D)	**D**
AIRE.03	F	19	HP, AI, POI, TIN, EH, HTN, Pneumonitis, UE	**D**
AIRE.52	F	9	HP, HT, EH, UE, Vitiligo, ID (D)	**D**
AIRE.53	F	8	CMC, HP, AI, HT, EH, HTN, UE, ID (D)	**V**
AIRE.58	M	16	CMC, HP, AI, TF, Gastritis, EH, ND, KC, Alopecia, B12 def, ID (D)	**V**
AIRE.59	M	7	CMC, HP, AI, EH, ND, Alopecia, ID (D)	**V**
AIRE.60	M	19	CMC, ND, EH, Alopecia, ID (C)	**V**
AIRE.61	F	54	CMC, HP, AI, EH, SS, Pneumonitis, ID (C)	**V**
AIRE.62	F	15	AI, AIH, HT, Gastritis, Pneumonitis, UE, ID (C)	**V**
AIRE.55	M	19	CMC, HP, AI, Gastritis, EH, UE, Alopecia	**V**
AIRE.69	M	18	CMC, AI, AIH, ID (B)	**V**
AIRE.56	M	2	AIH, EH, UE, ID (D)	**V**
AIRE.54	F	7	CMC, HP, AI, EH, Pneumonitis, UE	**V**
AIRE.63	F	15	CMC, HP, AI, EH, B12 def, ID (B)	**V**
AIRE.71	F	30	CMC, HP, Gastritis, EH, Pneumonitis, Vitiligo, ID (D)	**V**
AIRE.71B	M	15	CMC, AI, HT, Gastritis, ND, Pneumonitis, Alopecia	**V**
AIRE.74	F	11	CMC, HP, AI, HT, Gastritis, TIN, EH, SS, Pneumonitis, UE, Alopecia, ID (C)	**V**

Patient Code	Gender	Age*	Clinical Phenotypes	Cohort
AIRE.68	F	15	CMC, AI, Gastritis, EH, SS, Pneumonitis, B12 def, ID (C)	**V**
AIRE.70	F	16	CMC, SS, UE, B12 def, ID (C)	**V**
AIRE.66	M	13	CMC, HP, AI, DM, EH, UE, Alopecia	**V**
AIRE.67	M	20	CMC, HP, AI, Pneumonitis, UE, Vitiligo, ID (D)	**V**
AIRE.87	F	15	CMC, HP, AI, AIH, HT, EH, Pneumonitis, Vitiligo, B12 def, ID (B)	**V**
AIRE.65C	M	2	CMC, HP, AI, UE, ID (C)	**V**
AIRE.65B	M	6	CMC, HP, AI, EH	**V**
AIRE.65	F	11	CMC, HP, AI, EH, UE, Vitiligo, GH def, ID (D)	**V**
AIRE.73	F	13	CMC, HP, AIH, HT, POI, EH, ID (B)	**V**
AIRE.76	M	10	CMC, HP, UE, Vitiligo, ID (D)	**V**
AIRE.86	F	3	HP, UE, ID (C)	**V**
AIRE.77	M	10	HP, AIH, HT, SS, Pneumonitis, Vitiligo, Alopecia, ID (D)	**V**
AIRE.78	M	2	HP	**V**
AIRE.79	M	10	CMC, HP, AI, AIH, EH, UE, GH def, Asplenia	**V**

ND, nail dystrophy. HP, hypoparathyroidism. KC, keratoconjunctivitis. CMC, chronic mucocutaneous candidiasis. ID (D, C, B), Intestinal dysfunction (diarrheal-type, constipation-type, both). AIH, autoimmune hepatitis. POI, primary ovarian insufficiency. HTN, hypertension. HT, hypothyroidism. B12 def, B12 (vitamin) deficiency. DM, diabetes mellitus. SS, Sjogren's-like syndrome. GH def, Growth hormone deficiency. AI, Adrenal Insufficiency. EH, (dental) enamel hypoplasia. TF, testicular failure. TIN, Tubulointerstitial Nephritis. Hpit, Hypopituitarism. UE, Urticarial eruption.
D, Discovery cohort; V, Validation cohort.
*Age at most recent evaluation

Supplementary Table S1.2. Tissue-restricted expression patterns of APS1 antigens.

Gene (Human/mouse)	Protein Atlas: RNA specificity category (Tissue)[14]	Selected literature annotations
RFX6/Rfx6	Tissue enhanced	Pancreas Islets (Piccand et al., 2014; S. B. Smith et al., 2010) Intestine Enteroendocrine cells (Gehart et al., 2019; Piccand et al., 2019; S. B. Smith et al., 2010)
KHDC3L/Khdc3	Group enriched	Ovary Oocytes (Y. Zhang et al., 2018; K. Zhu et al., 2015)
ACP4/Acp4	Tissue enhanced	Testes (Yousef et al., 2001) Dental enamel (Green et al., 2019; Seymen et al., 2016; C. E. Smith et al., 2017)
ASMT/Asmt	Tissue enhanced	Brain Pineal Gland (Rath et al., 2016)
GIP/Gip	Tissue enriched	Intestine Enteroendocrine cells (Moody et al., 1984)
NKX6-3 / Nkx6-3	Group enriched	Pancreas PP-cells (Schaum et al., 2018) Intestine (Alanentalo et al., 2006)
PDX1 / Pdx1	Group enriched	Pancreas Islets (Holland et al., 2002; Stoffers et al., 1997)

Supplementary Table S1.3. Antibody information by application.

antibody	Application (IF: immunofluorescence; RLBA: radioligand binding assay; CBA: cell-based assay)	dilution
Anti-NLRP5 (Santa Cruz, Dallas, TX; #sc-50630)	NLRP5 RLBA	1:50
Anti-SOX10 (Abcam, Cambridge, MA, #ab181466)	SOX10 RLBA	1:25
Anti-RFX6 (R&D Systems, Minneapolis, MN; #AF7780)	RFX6 RLBA	1:50
Anti-KHDC3L (Abcam, #ab170298)	KHDC3L RLBA	1:25
Anti-CYP11A1 (Abcam, #ab175408)	CYP11A1 RLBA	1:50
Anti-NKX6-3 (Biorbyt, Cambridge, Cambridgeshire, UK; #orb127108)	NKX6-3 RLBA	1:50
Anti-GIP (Abcam, #ab30679)	GIP RLBA	1:50
Anti-PDX1 (Invitrogen, Carlsbad, CA, #PA5-78024)	PDX1 RLBA	1:50
Anti-ASMT (Invitrogen, #PA5-24721)	ASMT RLBA	1:25
Anti-CHGA (Abcam, Cambridge, MA, USA, # ab15160)	Tissue IF	1:5000
Human serum	Tissue IF CBA IF RLBA	1:4000 (Tissue) 1:500 (CBA) 1:25 (RLBA)
Secondary abs: 488 goat anti-human IgG (Life Technologies, Waltham, MA, USA: #A11013) 546 goat anti-rabbit IgG (Life Technologies, A11010)	Tissue IF	1:400
Secondary abs: 647 goat anti-human IgG (Thermo Fisher, #A-21445) 488 goat anti-rabbit IgG (Thermo Fisher, #A-11034)	CBA IF	1:1000
Anti-DYKDDDDK (D6W5B) (Cell Signaling Technologies, Danvers, MA; #14793)	CBA IF; ACP4 RLBA	1:2000 (CBA IF) 1:125 (RLBA)
Nuclear staining: Hoechst dye (Invitrogen, #33342) DAPI (Thermo Fisher, #D1306)	 Tissue IF CBA IF	

literature-reported antigens

Supplementary Figure S1.1: Literature-reported autoantigens. Hierarchically clustered (Pearson) Z-scored heatmap of literature reported autoantigens that did not meet the cutoff of 10-fold or greater signal over mock-IP in at least 2/39 APS1 sera and in 0/28 non-APS1 control sera.

a.

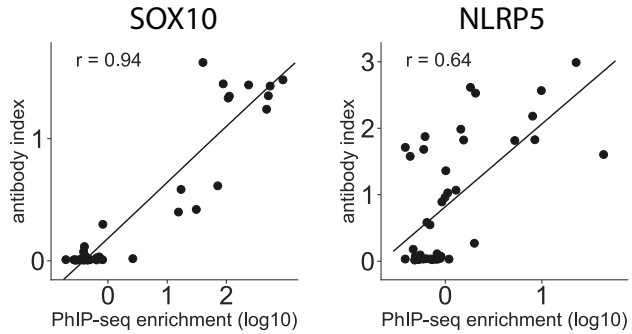

b.

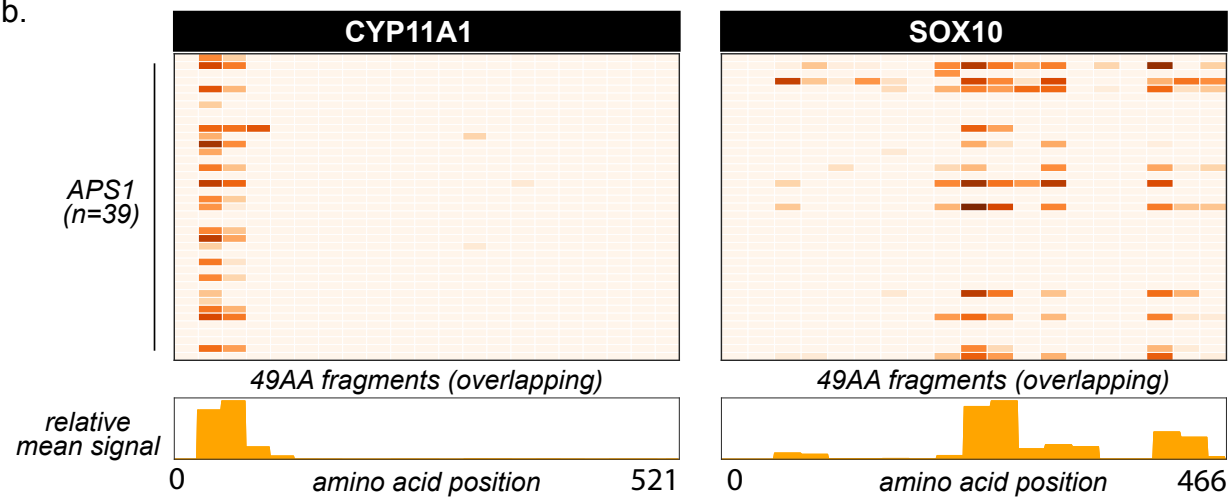

Supplementary Figure S1.2: PhIP-Seq data on NLRP5, SOX10 and CYP11A1. **A.** Scatterplot of individual PhIP-Seq enrichment values (log10) over mock-IP as compared to radioligand binding assay antibody index values (1 = commercial antibody signal) for known antigens SOX10 and NLRP5, with Pearson correlation coefficient r. **B.** PhIP-Seq enables 49 amino acid resolution of antibody signal from APS1 sera to literature-reported antigens CYP11A1 and SOX10. Top panels: PhIP-Seq signal (fold-change of each peptide as compared to signal from mock-IP, log10-scaled) for fragments 1-21 for CYP11A1 and fragments 1-19 for SOX10. Bottom panels: Trace of normalized signal for CYP11A1 and SOX10 fragments across the mean of all 39 APS1 sera.

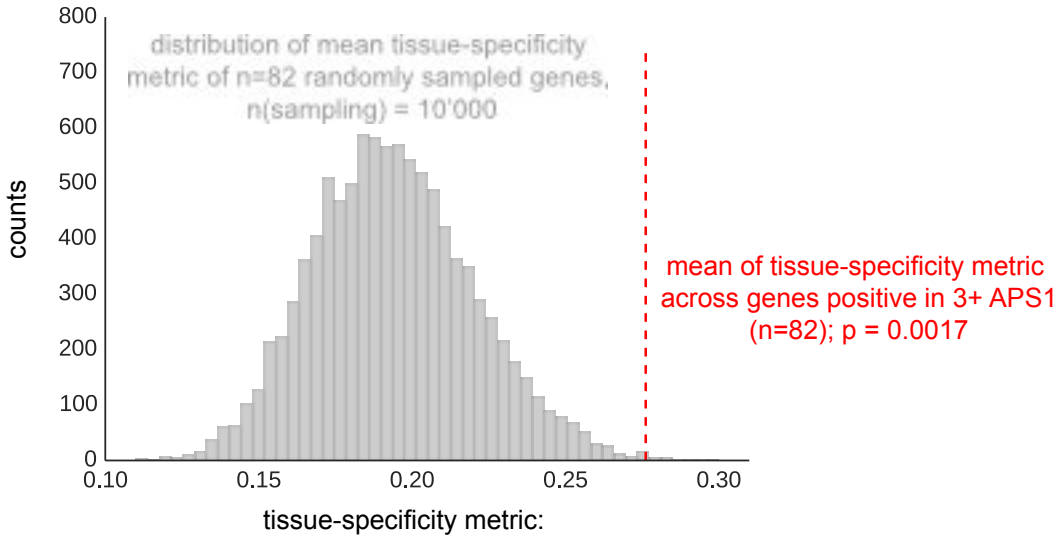

Supplementary Figure S1.3: Tissue-specificity ratio of 82 PhIP-Seq antigens**.** The mean of tissue-specificity ratio of 82 PhIP-Seq antigens (Figure 2) is increased as compared to the tissue-specificity ratio of n=82 randomly sampled genes (n-sampling = 10'000). Data from Protein Atlas, HPA/Gtex/Fantom5 RNA consensus dataset (Uhlen et al., 2015).

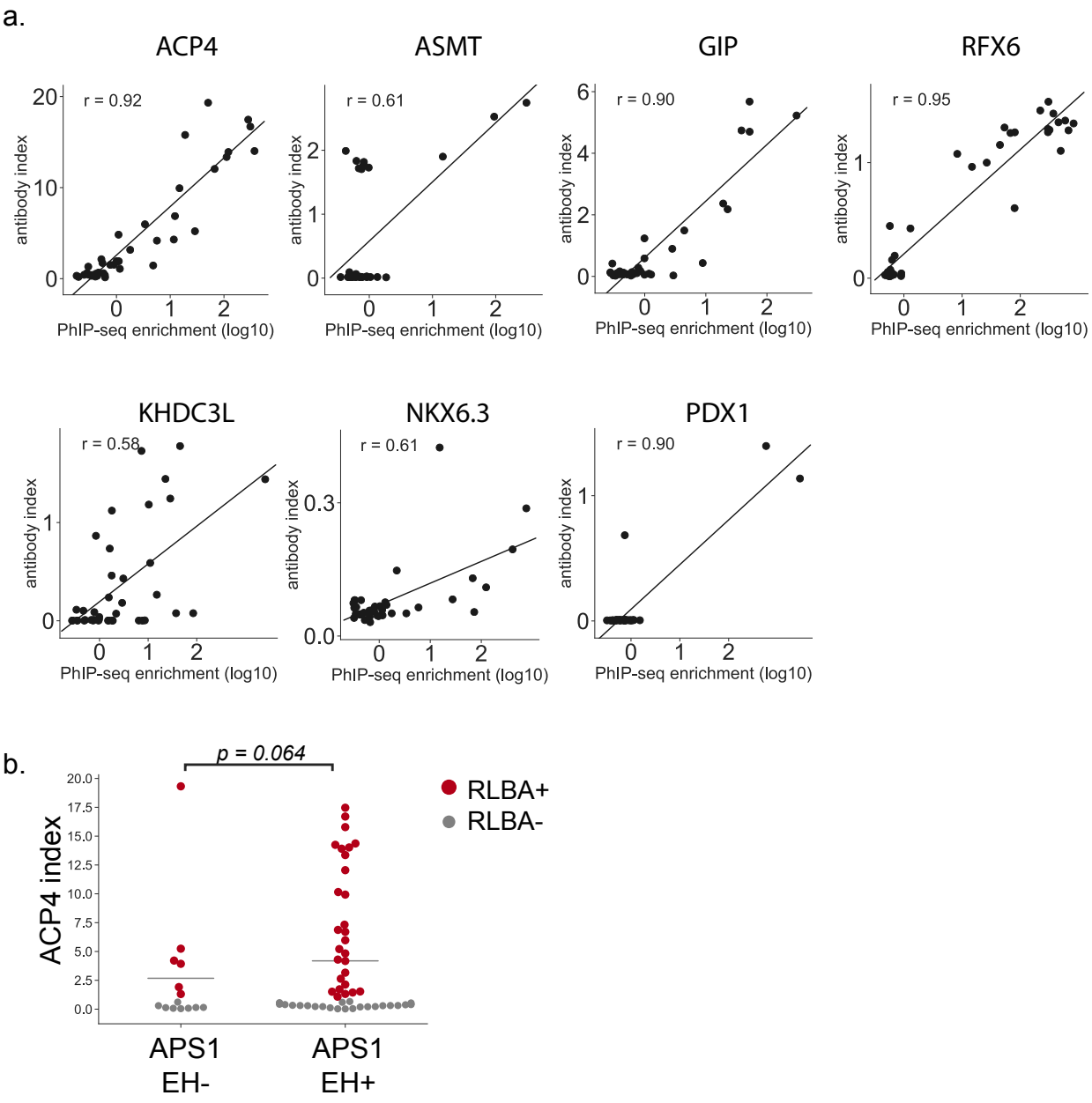

Supplementary Figure S1.4: Comparison of PhIP-Seq and RLBA results**. A**. Scatterplot of individual PhIP-Seq enrichment values (log10) over mock-IP as compared to radioligand binding assay antibody index values (1 = commercial antibody signal) for novel antigens ACP4, ASMT, GIP, RFX6, KHDC3L, NKX6.3, and PDX1, with Pearson correlation coefficient r (Note that for PDX1, there are insufficient positive data points for the correlation to be meaningful). **B**. ACP4 RLBA autoantibody index, broken down by enamel hypoplasia (EH) status.

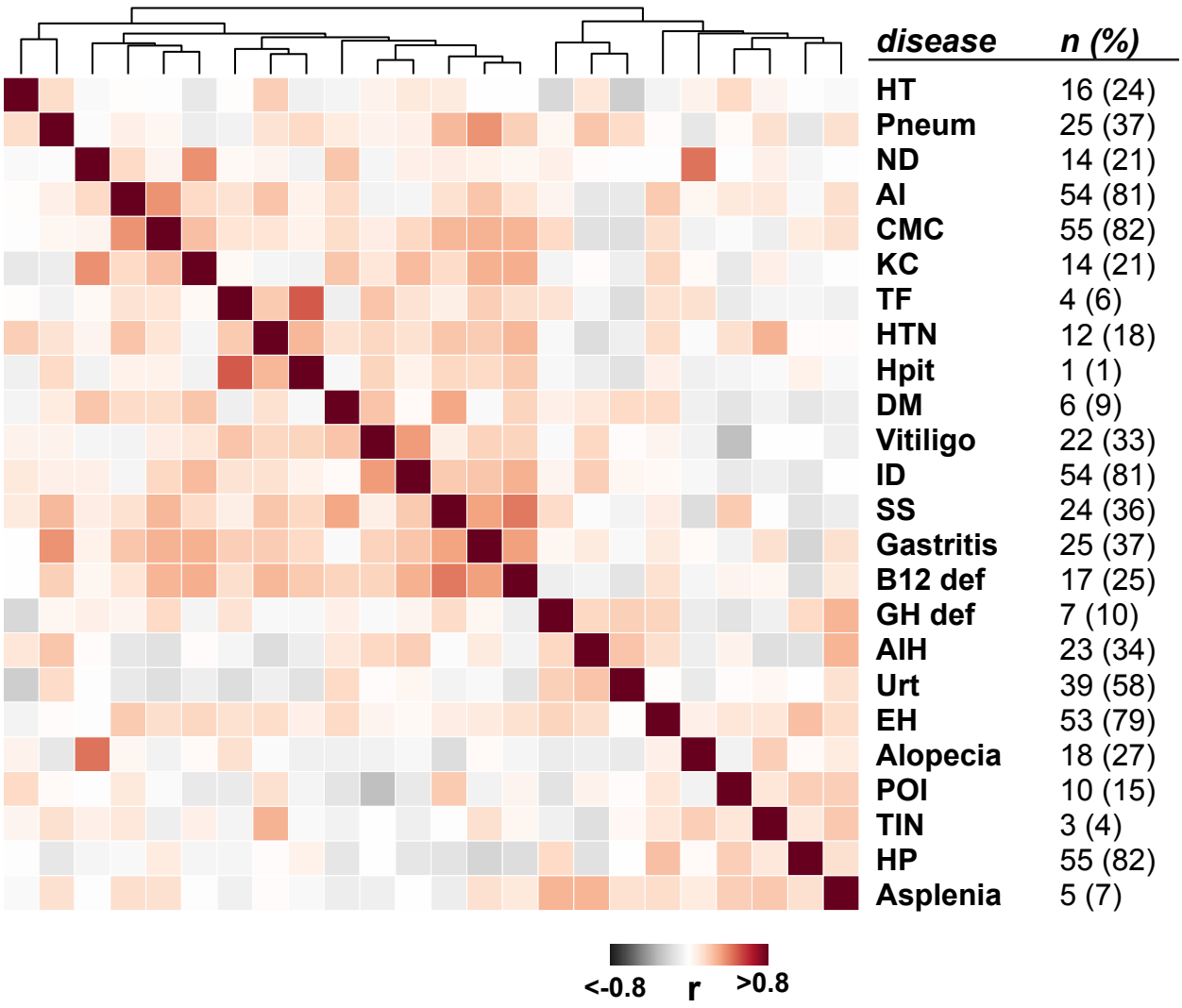

Supplementary Figure S1.5: Clustered disease correlations in the APS1 cohort. Clustered disease correlations in the APS1 cohort (Spearman's rank correlation; n = 67).

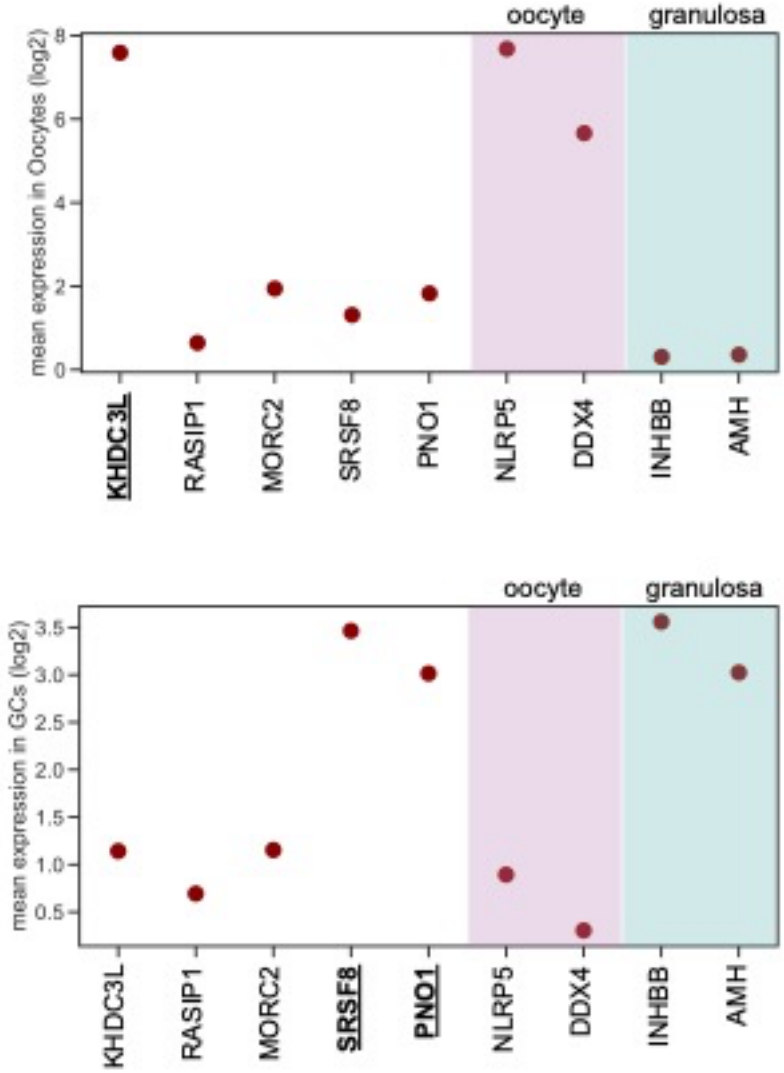

Supplementary Figure S1.6: Granulocyte and oocyte expression tables**.** KHDC3L is highly expressed in oocytes (top), but not in granulosa cells (bottom). In contrast, SRSF8 and PNO1 are highly expressed in granulosa cells, but not in oocytes. Data from (Y. Zhang et al., 2018)

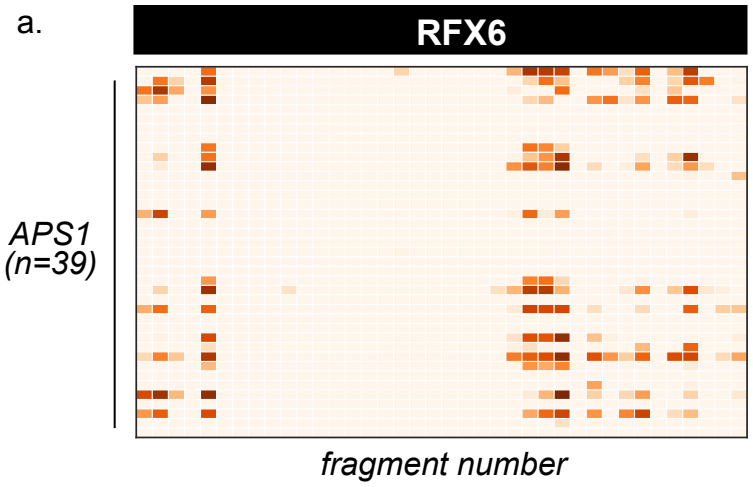

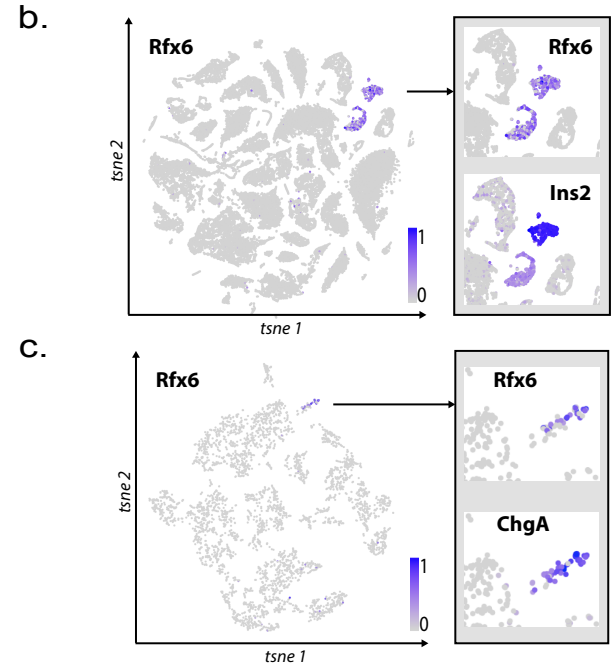

Supplementary Figure S1.7: Supplemental PhIP-Seq and expression data for RFX6. **A.** PhIP-Seq enables 49 amino acid resolution of antibody signal from novel autoantigen RFX6. PhIP-Seq signal (fold-change of each peptide as compared to signal from mock-IP, log10-scaled) for fragments 1-38 for RFX6 from APS1 sera (n=39). **B.** Single cell RNA expression of Rfx6. Left: normalized RNA expression of Rfx6 in single cells from 20 different organs. Right inset: Rfx6 shares an expression pattern with pancreatic beta-cell marker Ins2 (Schaum et al., 2018). **C.** Single cell RNA expression of Rfx6. Left: normalized RNA expression of Rfx6 in single cells from the intestine. Right inset: Rfx6 shares an expression pattern with intestinal enteroendocrine cell marker ChgA (Schaum et al., 2018).

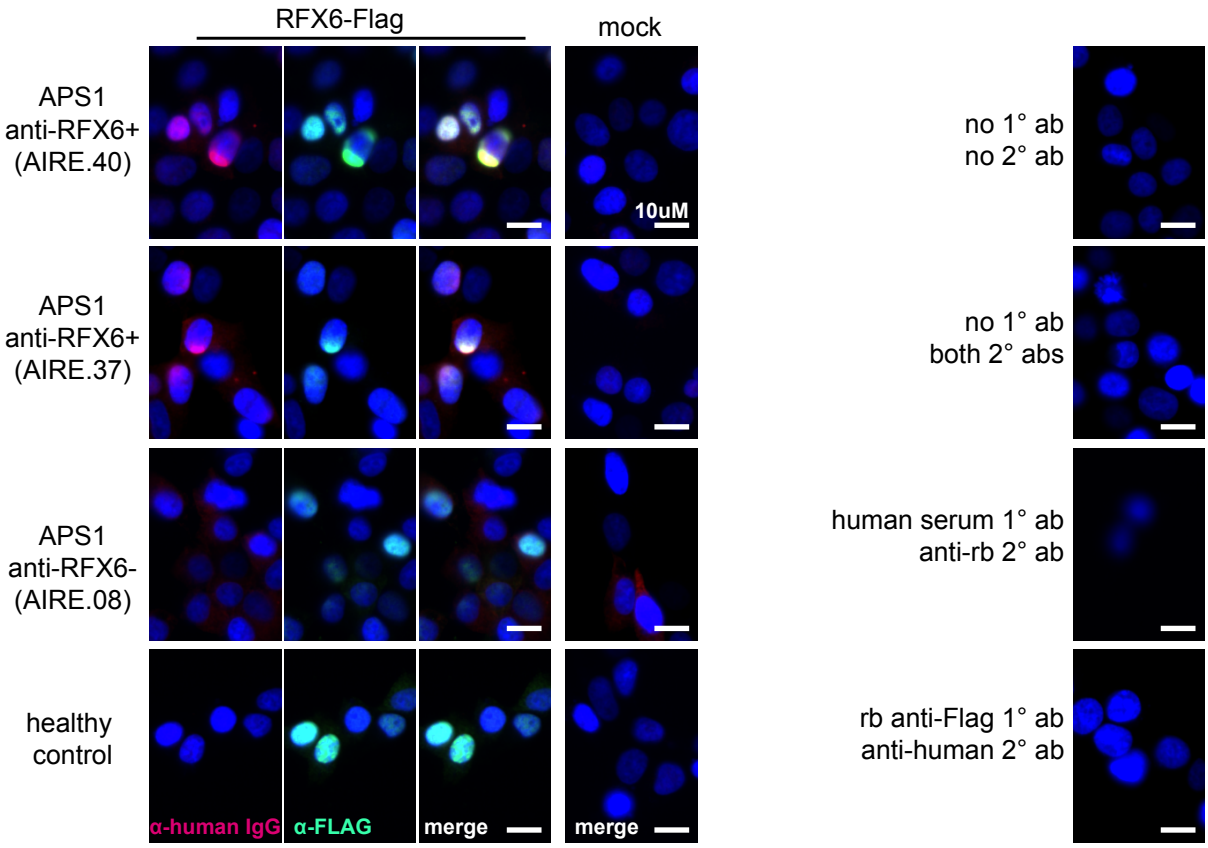

Supplementary Figure S1.8: Control antibody staining panel. Anti-RFX6+ sera (top two panels), but not anti-RFX6- serum or non-APS1 control serum (bottom two panels), co-stain HEK293T cells transfected with an RFX6-expressing plasmid. None of the sera tested stain 293T cells transfected with empty vector ('mock'). No cross-reactivity of secondary antibodies was observed (right panel).

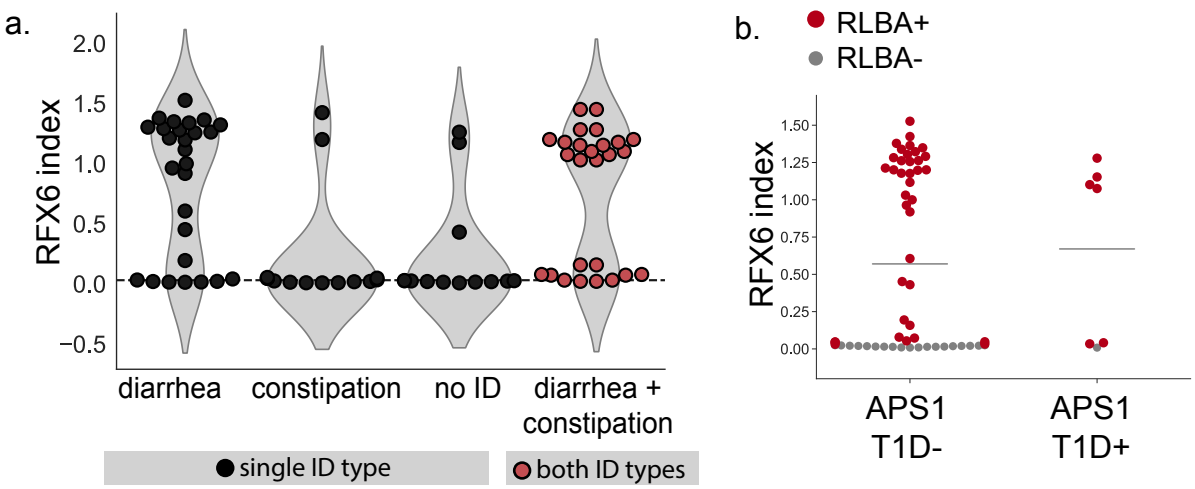

Supplementary Figure S1.9: Additional RFX6 antibody index data by phenotype**. A. APS1** patients with the diarrheal subtype, as well as those with both subtypes of ID (red), have increased anti-RFX6 antibody signal by RLBA as compared to those with constipation-type ID or no ID. B. 6/7 (6 diagnosed prior to serum draw, 1 diagnosed post serum draw) APS1 patients with type 1 diabetes have positive anti-RFX6 signal by RLBA.

ACKNOWLEDGEMENTS

Thanks to Joseph M. Replogle, Jeffrey A. Hussmann, Madhura Raghavan, Hanna Retallack, Brian D. O'Donovan, and members of the DeRisi, Anderson, Lionakis, and German labs for helpful discussions. Thanks to Kari Herrington and the UCSF Nikon Imaging Center for imaging support, as well as Sabrina Mann, Wint Lwin, and the UCSF Center for Advanced Technology for technical support. Thanks to the New York Blood Bank for providing the de-identified human non-inflammatory control plasma samples used in this study.

REFERENCES

Aaltonen, J., Björses, P., Perheentupa, J., Horelli–Kuitunen, N., Palotie, A., Peltonen, L., Lee, Y., Francis, F., Henning, S., Thiel, C., Leharach, H., & Yaspo, M. (1997). An autoimmune disease, APECED, caused by mutations in a novel gene featuring two PHD-type zinc-finger domains. *Nature Genetics*, *17*(4), 399–403. https://doi.org/10.1038/ng1297-399

Ackermann, K., Bux, R., Rüb, U., Korf, H.-W., Kauert, G., & Stehle, J. H. (2006). Characterization of Human Melatonin Synthesis Using Autoptic Pineal Tissue. *Endocrinology*, *147*(7), 3235–3242. https://doi.org/10.1210/en.2006-0043

Adriaenssens, A. E., Biggs, E. K., Darwish, T., Tadross, J., Sukthankar, T., Girish, M., Polex-Wolf, J., Lam, B. Y., Zvetkova, I., Pan, W., Chiarugi, D., Yeo, G., Blouet, C., Gribble, F. M., & Reimann, F. (2019). Glucose-Dependent Insulinotropic Polypeptide Receptor-Expressing Cells in the Hypothalamus Regulate Food Intake. *Cell Metabolism*. https://doi.org/10.1016/j.cmet.2019.07.013

Ahonen, P., Myllärniemi, S., Sipilä, I., & Perheentupa, J. (1990). Clinical Variation of Autoimmune Polyendocrinopathy–Candidiasis–Ectodermal Dystrophy (APECED) in a Series of 68 Patients. *The New England Journal of Medicine*, *322*(26), 1829–1836. https://doi.org/10.1056/nejm199006283222601

Akoury, E., Zhang, L., Ao, A., & Slim, R. (2015). NLRP7 and KHDC3L, the two maternal-effect proteins responsible for recurrent hydatidiform moles, co-localize to the oocyte cytoskeleton. *Human Reproduction (Oxford, England)*, *30*(1), 159 169. https://doi.org/10.1093/humrep/deu291

Alanentalo, T., Chatonnet, F., Karlen, M., Sulniute, R., Ericson, J., Andersson, E., & Ahlgren, U. (2006). Cloning and analysis of Nkx6.3 during CNS and gastrointestinal development. *Gene Expression Patterns*, *6*(2), 162–170. https://doi.org/10.1016/j.modgep.2005.06.012

Alimohammadi, M., Björklund, P., Hallgren, A., Pöntynen, N., Szinnai, G., Shikama, N., Keller, M. P., Ekwall, O., Kinkel, S. A., Husebye, E. S., Gustafsson, J., Rorsman, F., Peltonen, L., Betterle, C., Perheentupa, J., Akerström, G., Westin, G., Scott, H. S., Holländer, G. A., & Kämpe, O. (2008). Autoimmune polyendocrine syndrome type 1 and NALP5, a parathyroid autoantigen. *The New England Journal of Medicine*, *358*(10), 1018 1028. https://doi.org/10.1056/nejmoa0706487

Alimohammadi, M., Dubois, N., Sköldberg, F., Hallgren, Å., Tardivel, I., Hedstrand, H., Haavik, J., Husebye, E. S., Gustafsson, J., Rorsman, F., Meloni, A., Janson, C., Vialettes, B., Kajosaari, M., Egner, W., Sargur, R., Pontén, F., Amoura, Z., Grimfeld, A., … Carel, J.-C. (2009). Pulmonary autoimmunity as a feature of autoimmune polyendocrine syndrome type 1 and identification of KCNRG as a bronchial autoantigen. *Proceedings of the National Academy of Sciences*, *106*(11), 4396–4401. https://doi.org/10.1073/pnas.0809986106

Anderson. (2002). Projection of an Immunological Self Shadow Within the Thymus by the Aire Protein. *Science*, *298*(5597), 1395 1401. https://doi.org/10.1126/science.1075958

Baekkeskov, S., Aanstoot, H., Christgau, S., Reetz, A., limena, Cascalho, M., Folli, F., Richter-Olesen, H., Camilli, D. P., & Camilli, P. (1990). Identification of the 64K autoantigen in insulin-dependent diabetes as the GABA-synthesizing enzyme glutamic acid decarboxylase. *Nature*, *347*(6289), 151 156. https://doi.org/10.1038/347151a0

Bebbere, D., Masala, L., Albertini, D., & Ledda, S. (2016). The subcortical maternal complex: multiple functions for one biological structure? *Journal of Assisted Reproduction and Genetics*, *33*(11), 1 8. https://doi.org/10.1007/s10815-016-0788-z

Berger, M., Scheel, D. W., Macias, H., Miyatsuka, T., Kim, H., Hoang, P., Ku, G. M., Honig, G., Liou, A., Tang, Y., Regard, J. B., Sharifnia, P., Yu, L., Wang, J., Coughlin, S. R., Conklin, B. R., Deneris, E. S., Tecott, L. H., & German, M. S. (2015). Gαi/o-coupled receptor signaling restricts pancreatic β-cell expansion. *Proceedings of the National Academy of Sciences*, *112*(9), 2888–2893. https://doi.org/10.1073/pnas.1319378112

Berson, S. A., Yalow, R. S., Bauman, A., Rothschild, M. A., & Newerly, K. (1956). INSULIN-I131 METABOLISM IN HUMAN SUBJECTS: DEMONSTRATION OF INSULIN BINDING GLOBULIN IN THE CIRCULATION OF INSULIN TREATED SUBJECTS 1. *Journal of Clinical Investigation*, *35*(2), 170–190. https://doi.org/10.1172/jci103262

Betterle, C., Pra, C., Mantero, F., & Zanchetta, R. (2002). Autoimmune Adrenal Insufficiency and Autoimmune Polyendocrine Syndromes: Autoantibodies, Autoantigens, and Their Applicability in Diagnosis and Disease Prediction. *Endocrine Reviews*, *23*(3), 327–364. https://doi.org/10.1210/edrv.23.3.0466

Björk, E., Velloso, L. A., Kämpe, O., & Karlsson, A. F. (1994). GAD Autoantibodies in IDDM, Stiff-Man Syndrome, and Autoimmune Polyendocrine Syndrome Type I Recognize Different Epitopes. *Diabetes*, *43*(1), 161–165. https://doi.org/10.2337/diab.43.1.161

Brozzetti, A., Alimohammadi, M., Morelli, S., Minarelli, V., Hallgren, A., Giordano, R., Bellis, A., Perniola, R., Kämpe, O., & Falorni, A. (2015). Autoantibody Response Against NALP5/MATER

in Primary Ovarian Insufficiency and in Autoimmune Addison's Disease. *The Journal of Clinical Endocrinology & Metabolism*, *100*(5), 1941 1948. https://doi.org/10.1210/jc.2014-3571

Bruserud, Ø., Oftedal, B. E., Landegren, N., Erichsen, M. M., Bratland, E., Lima, K., Jørgensen, A. P., Myhre, A. G., Svartberg, J., Fougner, K. J., Bakke, Åsne, Nedrebø, B. G., Mella, B., Breivik, L., Viken, M. K., Knappskog, P. M., Marthinussen, M. C., Løvås, K., Kämpe, O., … Husebye, E. S. (2016). A Longitudinal Follow-up of Autoimmune Polyendocrine Syndrome Type 1. *The Journal of Clinical Endocrinology & Metabolism*, *101*(8), 2975–2983. https://doi.org/10.1210/jc.2016-1821

Cheng, M., & Anderson, M. S. (2018). Thymic tolerance as a key brake on autoimmunity. *Nature Immunology*, *19*(7), 659–664. https://doi.org/10.1038/s41590-018-0128-9

Choi, H., Kim, T.-H., Yun, C.-Y., Kim, J.-W., & Cho, E.-S. (2016). Testicular acid phosphatase induces odontoblast differentiation and mineralization. *Cell and Tissue Research*, *364*(1), 95–103. https://doi.org/10.1007/s00441-015-2310-9

Clemente, M., Obermayer-Straub, P., Meloni, A., Strassburg, C. P., Arangino, V., Tukey, R. H., Virgiliis, S., & Manns, M. P. (1997). Cytochrome P450 1A2 Is a Hepatic Autoantigen in Autoimmune Polyglandular Syndrome Type 1 1. *The Journal of Clinical Endocrinology & Metabolism*, *82*(5), 1353–1361. https://doi.org/10.1210/jcem.82.5.3913

Conteduca, G., Indiveri, F., Filaci, G., & Negrini, S. (2018). Beyond APECED: An update on the role of the AutoImmune regulator gene (AIRE) in physiology and disease. *Autoimmunity Reviews*, *17*(Immunity 44 2016), 1 17. https://doi.org/10.1016/j.autrev.2017.10.017

DeVoss, J., Shum, A., Johannes, K., Lu, W., Krawisz, A., Wang, P., Yang, T., LeClair, N., Austin, C., Strauss, E., & Anderson. (2008). Effector Mechanisms of the Autoimmune Syndrome in the Murine Model of Autoimmune Polyglandular Syndrome Type 1. *The Journal of Immunology*, *181*(6), 4072 4079. https://doi.org/10.4049/jimmunol.181.6.4072

Du, Y. T., Rayner, C. K., Jones, K. L., Talley, N. J., & Horowitz, M. (2018). Gastrointestinal Symptoms in Diabetes: Prevalence, Assessment, Pathogenesis, and Management. *Diabetes Care*, *41*(3), 627–637. https://doi.org/10.2337/dc17-1536

Ekwall, O., Hedstrand, H., Grimelius, L., Haavik, J., Perheentupa, J., Gustafsson, J., Husebye, E., Kämpe, O., & Rorsman, F. (1998). Identification of tryptophan hydroxylase as an intestinal autoantigen. *The Lancet*, *352*(9124), 279–283. https://doi.org/10.1016/s0140-6736(97)11050-9

Ferré, E. M., Break, T. J., Burbelo, P. D., Allgäuer, M., Kleiner, D. E., Jin, D., Xu, Z., Folio, L. R., Mollura, D. J., Swamydas, M., Gu, W., Hunsberger, S., Lee, C.-C. R., Bondici, A., Hoffman, K. W., Lim, J. K., Dobbs, K., Niemela, J. E., Fleisher, T. A., … Lionakis, M. S. (2019). Lymphocyte-driven regional immunopathology in pneumonitis caused by impaired central immune tolerance. *Science Translational Medicine*, *11*(495), eaav5597. https://doi.org/10.1126/scitranslmed.aav5597

Ferré, E. M., Rose, S. R., Rosenzweig, S. D., Burbelo, P. D., Romito, K. R., Niemela, J. E., Rosen, L. B., Break, T. J., Gu, W., Hunsberger, S., Browne, S. K., Hsu, A. P., Rampertaap, S., Swamydas, M., Collar, A. L., Kong, H. H., Lee, C.-C., Chascsa, D., Simcox, T., … Lionakis, M. S. (2016). Redefined clinical features and diagnostic criteria in autoimmune polyendocrinopathy-candidiasis-ectodermal dystrophy. *JCI Insight*, *1*(13), 1343 19. https://doi.org/10.1172/jci.insight.88782

Fishman, D., Kisand, K., Hertel, C., Rothe, M., Remm, A., Pihlap, M., Adler, P., Vilo, J., Peet, A., Meloni, A., Podkrajsek, K., Battelino, T., Bruserud, Ø., Wolff, A. S., Husebye, E. S., Kluger, N., Krohn, K., Ranki, A., Peterson, H., … Peterson, P. (2017). Autoantibody Repertoire in APECED Patients Targets Two Distinct Subgroups of Proteins. *Frontiers in Immunology*, *8*, 681 15. https://doi.org/10.3389/fimmu.2017.00976

Gavanescu, I., Benoist, C., & Mathis, D. (2008). B cells are required for Aire-deficient mice to develop multi-organ autoinflammation: A therapeutic approach for APECED patients. *Proceedings of the National Academy of Sciences*, *105*(35), 13009–13014. https://doi.org/10.1073/pnas.0806874105

Gehart, H., van Es, J. H., Hamer, K., Beumer, J., Kretzschmar, K., Dekkers, J. F., Rios, A., & Clevers, H. (2019). Identification of Enteroendocrine Regulators by Real-Time Single-Cell Differentiation Mapping. *Cell*, *176*(Dev. Dyn. 194 1992), 1158-1173.e16. https://doi.org/10.1016/j.cell.2018.12.029

Goldspink, D. A., Reimann, F., & Gribble, F. M. (2018). Models and Tools for Studying Enteroendocrine Cells. *Endocrinology*, *159*(12), 3874–3884. https://doi.org/10.1210/en.2018-00672

Hedstrand, H., Ekwall, O., Olsson, M. J., Landgren, E., Kemp, H. E., Weetman, A. P., Perheentupa, J., Husebye, E., Gustafsson, J., Betterle, C., Kämpe, O., & Rorsman, F. (2001). The Transcription Factors SOX9 and SOX10 Are Vitiligo Autoantigens in Autoimmune Polyendocrine Syndrome Type I. *Journal of Biological Chemistry*, *276*(38), 35390 35395. https://doi.org/10.1074/jbc.m102391200

Högenauer, C., Meyer, R. L., Netto, G. J., Bell, D., Little, K. H., Ferries, L., Ana, C. A., Porter, J. L., & Fordtran, J. S. (2001). Malabsorption Due to Cholecystokinin Deficiency in a Patient with Autoimmune Polyglandular Syndrome Type I. *The New England Journal of Medicine*, *344*(4), 270–274. https://doi.org/10.1056/nejm200101253440405

Holland, A. M., Hale, M. A., Kagami, H., Hammer, R. E., & MacDonald, R. J. (2002). Experimental control of pancreatic development and maintenance. *Proceedings of the National Academy of Sciences*, *99*(19), 12236–12241. https://doi.org/10.1073/pnas.192255099

Huhtaniemi, I., Hovatta, O., Marca, A., Livera, G., Monniaux, D., Persani, L., Heddar, A., Jarzabek, K., Laisk-Podar, T., Salumets, A., Tapanainen, J. S., Veitia, R. A., Visser, J. A., Wieacker, P., Wolczynski, S., & Misrahi, M. (2018). Advances in the Molecular Pathophysiology, Genetics, and Treatment of Primary Ovarian Insufficiency. *Trends in Endocrinology & Metabolism*, *29*(6), 400 419. https://doi.org/10.1016/j.tem.2018.03.010

Husebye, E. S., Anderson, M. S., & Kämpe, O. (2018). Autoimmune Polyendocrine Syndromes. *The New England Journal of Medicine*, *378*(12), 1132–1141. https://doi.org/10.1056/nejmra1713301

Husebye, E. S., Gebre-Medhin, G., Tuomi, T., Perheentupa, J., Landin-Olsson, M., Gustafsson, J., Rorsman, F., & Kämpe, O. (1997). Autoantibodies against Aromatic l -Amino Acid Decarboxylase in Autoimmune Polyendocrine Syndrome Type I 1. *The Journal of Clinical Endocrinology & Metabolism*, *82*(1), 147–150. https://doi.org/10.1210/jcem.82.1.3647

Jasti, S., Warren, B. D., McGinnis, L. K., Kinsey, W. H., Petroff, B. K., & Petroff, M. G. (2012).

The Autoimmune Regulator Prevents Premature Reproductive Senescence in Female Mice1. *Biology of Reproduction*, *86*(4), 163 9. https://doi.org/10.1095/biolreprod.111.097501

Jeong, J., Jiang, L., Albino, E., Marrero, J., Rho, H., Hu, J., Hu, S., Vera, C., Bayron-Poueymiroy, D., Rivera-Pacheco, Z., Ramos, L., Torres-Castro, C., Qian, J., Bonaventura, J., Boeke, J. D., Yap, W. Y., Pino, I., Eichinger, D. J., Zhu, H., & Blackshaw, S. (2012). Rapid Identification of Monospecific Monoclonal Antibodies Using a Human Proteome Microarray. *Molecular & Cellular Proteomics*, *11*(6), O111.016253. https://doi.org/10.1074/mcp.o111.016253

Kluger, N., Jokinen, M., Lintulahti, A., Krohn, K., & Ranki, A. (2015). Gastrointestinal immunity against tryptophan hydroxylase-1, aromatic L-amino-acid decarboxylase, AIE-75, villin and Paneth cells in APECED. *Clinical Immunology*, *158*(2), 212–220. https://doi.org/10.1016/j.clim.2015.03.012

Kuroda, N., Mitani, T., Takeda, N., Ishimaru, N., Arakaki, R., Hayashi, Y., Bando, Y., Izumi, K., Takahashi, T., Nomura, T., Sakaguchi, S., Ueno, T., Takahama, Y., Uchida, D., Sun, S., Kajiura, F., Mouri, Y., Han, H., Matsushima, A., … Matsumoto, M. (2005). Development of Autoimmunity against Transcriptionally Unrepressed Target Antigen in the Thymus of Aire-Deficient Mice. *The Journal of Immunology*, *174*(4), 1862–1870. https://doi.org/10.4049/jimmunol.174.4.1862

Landegren, N., Sharon, D., Freyhult, E., Hallgren, A., Eriksson, D., Edqvist, P.-H., Bensing, S., Wahlberg, J., Nelson, L. M., Gustafsson, J., Husebye, E. S., Anderson, M. S., Snyder, M., & Kämpe, O. (2016). Proteome-wide survey of the autoimmune target repertoire in autoimmune polyendocrine syndrome type 1. *Nature Publishing Group*, *6*(1), 1 11. https://doi.org/10.1038/srep20104

Landegren, N., Sharon, D., Shum, A. K., Khan, I. S., Fasano, K. J., Hallgren, Å., Kampf, C., Freyhult, E., Ardesjö-Lundgren, B., Alimohammadi, M., Rathsman, S., Ludvigsson, J. F., Lundh, D., Motrich, R., Rivero, V., Fong, L., Giwercman, A., Gustafsson, J., Perheentupa, J., … Kämpe, O. (2015). Transglutaminase 4 as a prostate autoantigen in male subfertility. *Science Translational Medicine*, *7*(292), 292ra101-292ra101. https://doi.org/10.1126/scitranslmed.aaa9186

Lanzavecchia, A. (1985). Antigen-specific interaction between T and B cells. *Nature*, *314*(6011), 537–539. https://doi.org/10.1038/314537a0

Larman, B. H., Zhao, Z., Laserson, U., Li, M. Z., Ciccia, A., Gakidis, A. M., Church, G. M., Kesari, S., LeProust, E. M., Solimini, N. L., & Elledge, S. J. (2011). Autoantigen discovery with a synthetic human peptidome. *Nature Biotechnology*, *29*(6), 535 541. https://doi.org/10.1038/nbt.1856

Leonard, J. D., Gilmore, D. C., Dileepan, T., Nawrocka, W. I., Chao, J. L., Schoenbach, M. H., Jenkins, M. K., Adams, E. J., & Savage, P. A. (2017). Identification of Natural Regulatory T Cell Epitopes Reveals Convergence on a Dominant Autoantigen. *Immunity*, *47*(1), 107-117.e8. https://doi.org/10.1016/j.immuni.2017.06.015

Li, L., Baibakov, B., & Dean, J. (2008). A Subcortical Maternal Complex Essential for Preimplantation Mouse Embryogenesis. *Developmental Cell*, *15*(3), 416 425. https://doi.org/10.1016/j.devcel.2008.07.010

Liu, C., Li, M., Li, T., Zhao, H., Huang, J., Wang, Y., Gao, Q., Yu, Y., & Shi, Q. (2016). ECAT1 is essential for human oocyte maturation and pre-implantation development of the resulting

embryos. *Scientific Reports*, *6*(1), 38192. https://doi.org/10.1038/srep38192

Maclaren, N., Chen, Q., Kukreja, A., Marker, J., Zhang, C., & Sun, Z. (2001). Autoimmune hypogonadism as part of an autoimmune polyglandular syndrome. *Journal of the Society for Gynecologic Investigation*, *8*(1), S52–S54. https://doi.org/10.1016/s1071-5576(00)00109-x

Malchow, S., Leventhal, D. S., Lee, V., Nishi, S., Socci, N. D., & Savage, P. A. (2016). Aire Enforces Immune Tolerance by Directing Autoreactive T Cells into the Regulatory T Cell Lineage. *Immunity*, *44*(5), 1102 1113. https://doi.org/10.1016/j.immuni.2016.02.009

Mandel-Brehm, C., Dubey, D., Kryzer, T. J., O'Donovan, B. D., Tran, B., Vazquez, S. E., Sample, H. A., Zorn, K. C., Khan, L. M., Bledsoe, I. O., McKeon, A., Pleasure, S. J., Lennon, V. A., DeRisi, J. L., Wilson, M. R., & Pittock, S. J. (2019). Kelch-like Protein 11 Antibodies in Seminoma-Associated Paraneoplastic Encephalitis. *New England Journal of Medicine*, *381*(1), 47–54. https://doi.org/10.1056/nejmoa1816721

Meager, A., Visvalingam, K., Peterson, P., Möll, K., Murumägi, A., Krohn, K., Eskelin, P., Perheentupa, J., Husebye, E., Kadota, Y., & Willcox, N. (2006). Anti-Interferon Autoantibodies in Autoimmune Polyendocrinopathy Syndrome Type 1. *PLoS Medicine*, *3*(7), e289. https://doi.org/10.1371/journal.pmed.0030289

Meyer, S., Woodward, M., Hertel, C., Vlaicu, P., Haque, Y., Kärner, J., Macagno, A., Onuoha, S. C., Fishman, D., Peterson, H., Metsküla, K., Uibo, R., Jäntti, K., Hokynar, K., Wolff, A. S., patient collaborative, A., Meloni, A., Kluger, N., Husebye, E. S., … Hayday, A. (2016). AIRE-Deficient Patients Harbor Unique High-Affinity Disease-Ameliorating Autoantibodies. *Cell*, *166*(3), 582 595. https://doi.org/10.1016/j.cell.2016.06.024

Mitchell, J., Punthakee, Z., Lo, B., Bernard, C., Chong, K., Newman, C., Cartier, L., Desilets, V., Cutz, E., Hansen, I., Riley, P., & Polychronakos, C. (2004). Neonatal diabetes, with hypoplastic pancreas, intestinal atresia and gall bladder hypoplasia: search for the aetiology of a new autosomal recessive syndrome. *Diabetologia*, *47*(12), 2160 2167. https://doi.org/10.1007/s00125-004-1576-3

Moody, A. J., Thim, L., & Valverde, I. (1984). The isolation and sequencing of human gastric inhibitory peptide (GIP). *FEBS Letters*, *172*(2), 142–148. https://doi.org/10.1016/0014-5793(84)81114-x

Nagamine, K., Peterson, P., Scott, H. S., Kudoh, J., Minoshima, S., Heino, M., Krohn, K. J., Lalioti, M. D., Mullis, P. E., Antonarakis, S. E., Kawasaki, K., Asakawa, S., Ito, F., & Shimizu, N. (1997). Positional cloning of the APECED gene. *Nature Genetics*, *17*(4), 393–398. https://doi.org/10.1038/ng1297-393

Nelson, L. M. (2009). Clinical practice. Primary ovarian insufficiency. *The New England Journal of Medicine*, *360*(6), 606 614. https://doi.org/10.1056/nejmcp0808697

Obermayer-Straub, P., Strassburg, C., & Manns, M. (2000). Target Proteins in Human Autoimmunity: Cytochromes P450 and Udp-Glycoronosyltransferases. *Canadian Journal of Gastroenterology and Hepatology*, *14*(5), 429–439. https://doi.org/10.1155/2000/910107

O'Connor, D. T., Burton, D., & Deftos, L. J. (1983). Chromogranin A: Immunohistology reveals its universal occurrence in normal polypeptide hormone producing endocrine glands. *Life Sciences*, *33*(17), 1657–1663. https://doi.org/10.1016/0024-3205(83)90721-x

O'Donovan, B., Mandel - Brehm, C., E. Vazquez, S., Liu, J., Paren, A. V., Anderson, M. S., Kassimatis, T., Zekeridou, A., Hauser, S. L., Pittock, S. J., Chow, E., Wilson, M. R., & DeRisi, J. L. (2018). Exploration of Anti - Yo and Anti - Hu paraneoplastic neurological disorders by PhIP - Seq reveals a highly restricted pattern of antibody epitopes. *Biorxiv.Org*. https://doi.org/10.1101/502187

Oftedal, B. E., Hellesen, A., Erichsen, M. M., Bratland, E., Vardi, A., Perheentupa, J., Kemp, H. E., Fiskerstrand, T., Viken, M. K., Weetman, A. P., Fleishman, S. J., Banka, S., Newman, W. G., Sewell, W. A. C., Sozaeva, L. S., Zayats, T., Haugarvoll, K., Orlova, E. M., Haavik, J., … Husebye, E. S. (2015). Dominant Mutations in the Autoimmune Regulator AIRE Are Associated with Common Organ-Specific Autoimmune Diseases. *Immunity*, *42*(6), 1185–1196. https://doi.org/10.1016/j.immuni.2015.04.021

Ohsie, S., Gerney, G., Gui, D., Kahana, D., Martín, M. G., & Cortina, G. (2009). A paucity of colonic enteroendocrine and/or enterochromaffin cells characterizes a subset of patients with chronic unexplained diarrhea/malabsorption. *Human Pathology*, *40*(7), 1006–1014. https://doi.org/10.1016/j.humpath.2008.12.016

Oliva-Hemker, M., Berkenblit, G., Anhalt, G., & Yardley, J. (2006). Pernicious Anemia and Widespread Absence of Gastrointestinal Endocrine Cells in a Patient with Autoimmune Polyglandular Syndrome Type I and Malabsorption. *The Journal of Clinical Endocrinology & Metabolism*, *91*(8), 2833–2838. https://doi.org/10.1210/jc.2005-2506

Otsuka, N., Tong, Z.-B., Vanevski, K., Tu, W., Cheng, M. H., & Nelson, L. M. (2011). Autoimmune Oophoritis with Multiple Molecular Targets Mitigated by Transgenic Expression of

Mater. *Endocrinology*, *152*(6), 2465 2473. https://doi.org/10.1210/en.2011-0022

Patel, K. A., Kettunen, J., Laakso, M., Stančáková, A., Laver, T. W., Colclough, K., Johnson, M. B., Abramowicz, M., Groop, L., Miettinen, P. J., Shepherd, M. H., Flanagan, S. E., Ellard, S., Inagaki, N., Hattersley, A. T., Tuomi, T., Cnop, M., & Weedon, M. N. (2017). Heterozygous RFX6 protein truncating variants are associated with MODY with reduced penetrance. *Nature Communications*, *8*(1), 1 8. https://doi.org/10.1038/s41467-017-00895-9

Pederson, R. A., & McIntosh, C. H. (2016). Discovery of gastric inhibitory polypeptide and its subsequent fate: Personal reflections. *Journal of Diabetes Investigation*, *7*(S1), 4–7. https://doi.org/10.1111/jdi.12480

Piccand, J., Vagne, C., Blot, F., Meunier, A., Beucher, A., Strasser, P., Lund, M. L., Ghimire, S., Nivlet, L., Lapp, C., Petersen, N., Engelstoft, M. S., Thibault-Carpentier, C., Keime, C., Correa, S., Schreiber, V., Molina, N., Schwartz, T. W., Arcangelis, A., & Gradwohl, G. (2019). Rfx6 promotes the differentiation of peptide-secreting enteroendocrine cells while repressing genetic programs controlling serotonin production. *Molecular Metabolism*, *29*, 24–39. https://doi.org/10.1016/j.molmet.2019.08.007

Pöntynen, N., Miettinen, A., Arstila, P. T., Kämpe, O., Alimohammadi, M., Vaarala, O., Peltonen, L., & Ulmanen, I. (2006). Aire deficient mice do not develop the same profile of tissue-specific autoantibodies as APECED patients. *Journal of Autoimmunity*, *27*(2), 96–104. https://doi.org/10.1016/j.jaut.2006.06.001

Popler, J., Alimohammadi, M., Kämpe, O., Dalin, F., Dishop, M. K., Barker, J. M., Moriarty-Kelsey, M., Soep, J. B., & Deterding, R. R. (2012). Autoimmune polyendocrine syndrome type

1: Utility of KCNRG autoantibodies as a marker of active pulmonary disease and successful treatment with rituximab. *Pediatric Pulmonology*, *47*(1), 84–87. https://doi.org/10.1002/ppul.21520

Posovszky, C., Lahr, G., von Schnurbein, J., Buderus, S., Findeisen, A., Schröder, C., Schütz, C., Schulz, A., batin, K., Wabitsch, M., & Barth, T. (2012). Loss of Enteroendocrine Cells in Autoimmune-Polyendocrine-Candidiasis-Ectodermal-Dystrophy (APECED) Syndrome with Gastrointestinal Dysfunction. *The Journal of Clinical Endocrinology & Metabolism*, *97*(2), E292 E300. https://doi.org/10.1210/jc.2011-2044

Puel, A., Döffinger, R., Natividad, A., Chrabieh, M., Barcenas-Morales, G., Picard, C., Cobat, A., Ouachée-Chardin, M., Toulon, A., Bustamante, J., Al-Muhsen, S., Al-Owain, M., Arkwright, P. D., Costigan, C., McConnell, V., Cant, A. J., Abinun, M., Polak, M., Bougnères, P.-F., … Casanova, J.-L. (2010). Autoantibodies against IL-17A, IL-17F, and IL-22 in patients with chronic mucocutaneous candidiasis and autoimmune polyendocrine syndrome type I. *The Journal of Experimental Medicine*, *207*(2), 291–297. https://doi.org/10.1084/jem.20091983

Rath, M. F., Coon, S. L., Amaral, F. G., Weller, J. L., Møller, M., & Klein, D. C. (2016). Melatonin Synthesis: Acetylserotonin O-Methyltransferase (ASMT) Is Strongly Expressed in a Subpopulation of Pinealocytes in the Male Rat Pineal Gland. *Endocrinology*, *157*(5), 2028–2040. https://doi.org/10.1210/en.2015-1888

Reddy, R., Akoury, E., Nguyen, N., Abdul-Rahman, O. A., Dery, C., Gupta, N., Daley, W. P., Ao, A., Landolsi, H., Fisher, R., Touitou, I., & Slim, R. (2012). Report of four new patients with protein-truncating mutations in C6orf221/KHDC3L and colocalization with NLRP7. *European Journal of Human Genetics*, *21*(9), 957 964. https://doi.org/10.1038/ejhg.2012.274

Rezaei, M., Nguyen, N., Foroughinia, L., Dash, P., Ahmadpour, F., Verma, I., Slim, R., & Fardaei, M. (2016). Two novel mutations in the KHDC3L gene in Asian patients with recurrent hydatidiform mole. *Human Genome Variation*, *3*(1), 16027 5. https://doi.org/10.1038/hgv.2016.27

Rosen, A., & Casciola-Rosen, L. (2014). Autoantigens as Partners in Initiation and Propagation of Autoimmune Rheumatic Diseases. *Annual Review of Immunology*, *34*(1), 1–26. https://doi.org/10.1146/annurev-immunol-032414-112205

Sansom, S. N., Shikama-Dorn, N., Zhanybekova, S., Nusspaumer, G., Macaulay, I. C., Deadman, M. E., Heger, A., Ponting, C. P., & Holländer, G. A. (2014). Population and single-cell genomics reveal the Aire dependency, relief from Polycomb silencing, and distribution of self-antigen expression in thymic epithelia. *Genome Research*, *24*(12), 1918–1931. https://doi.org/10.1101/gr.171645.113

Schaum, N., Karkanias, J., Neff, N. F., May, A. P., Quake, S. R., Wyss-Coray, T., Darmanis, S., Batson, J., Botvinnik, O., Chen, M. B., Chen, S., Green, F., Jones, R. C., Maynard, A., Penland, L., Pisco, A., Sit, R. V., anley, G., Webber, J. T., … Wyss-Coray, T. (2018). Single-cell transcriptomics of 20 mouse organs creates a Tabula Muris. *Nature*, *562*(7727), 1 25. https://doi.org/10.1038/s41586-018-0590-4

Seymen, F., Kim, Y., Lee, Y., Kang, J., Kim, T.-H., Choi, H., Koruyucu, M., Kasimoglu, Y., Tuna, E., Gencay, K., Shin, T., Hyun, H.-K., Kim, Y.-J., Lee, S.-H., Lee, Z., Zhang, H., Hu, J., Simmer, J. P., Cho, E.-S., & Kim, J.-W. (2016). Recessive Mutations in ACPT, Encoding Testicular Acid Phosphatase, Cause Hypoplastic Amelogenesis Imperfecta. *The American Journal of Human*

Genetics, *99*(5), 1199–1205. https://doi.org/10.1016/j.ajhg.2016.09.018

Sharon, D., & Snyder, M. (2014). Serum Profiling Using Protein Microarrays to Identify Disease Related Antigens. *Methods in Molecular Biology (Clifton, N.J.)*, *1176*, 169–178. https://doi.org/10.1007/978-1-4939-0992-6_14

Shum, A. K., Alimohammadi, M., Tan, C. L., Cheng, M. H., Metzger, T. C., Law, C. S., Lwin, W., Perheentupa, J., Bour-Jordan, H., Carel, J., Husebye, E. S., Luca, F., Janson, C., Sargur, R., Dubois, N., Kajosaari, M., Wolters, P. J., Chapman, H. A., Kämpe, O., & Anderson, M. S. (2013). BPIFB1 is a lung-specific autoantigen associated with interstitial lung disease. *Science Translational Medicine*, *5*(206), 206ra139 206ra139. https://doi.org/10.1126/scitranslmed.3006998

Shum, A. K., DeVoss, J., Tan, C. L., Hou, Y., Johannes, K., O'Gorman, C. S., Jones, K. D., Sochett, E. B., Fong, L., & Anderson, M. S. (2009). Identification of an autoantigen demonstrates a link between interstitial lung disease and a defect in central tolerance. *Science Translational Medicine*, *1*(9), 9ra20 9ra20. https://doi.org/10.1126/scitranslmed.3000284

Sifuentes-Dominguez, L. F., Li, H., Llano, E., Liu, Z., Singla, A., Patel, A. S., Kathania, M., Khoury, A., Norris, N., Rios, J. J., Starokadomskyy, P., Park, J. Y., Gopal, P., Liu, Q., Tan, S., Chan, L., Ross, T., Harrison, S., Venuprasad, K., … Burstein, E. (2019). SCGN deficiency results in colitis susceptibility. *ELife*, *8*, e49910. https://doi.org/10.7554/elife.49910

Silva, C., Yamakami, L., Aikawa, N., aujo, D., Carvalho, J., & Bonfá, E. (2014). Autoimmune primary ovarian insufficiency. *Autoimmunity Reviews*, *13*(4–5), 427 430. https://doi.org/10.1016/j.autrev.2014.01.003

Smith, C. E., Whitehouse, L. L., Poulter, J. A., Brookes, S. J., Day, P. F., Soldani, F., Kirkham, J., Inglehearn, C. F., & Mighell, A. J. (2017). Defects in the acid phosphatase ACPT cause recessive hypoplastic amelogenesis imperfecta. *European Journal of Human Genetics*, *25*(8), 1015. https://doi.org/10.1038/ejhg.2017.79

Smith, S. B., Qu, H.-Q., Taleb, N., Kishimoto, N. Y., Scheel, D. W., Lu, Y., Patch, A.-M., Grabs, R., Wang, J., Lynn, F. C., Miyatsuka, T., Mitchell, J., Seerke, R., Désir, J., Eijnden, S., Abramowicz, M., Kacet, N., Weill, J., Renard, M.-È., … German, M. S. (2010). Rfx6 directs islet formation and insulin production in mice and humans. *Nature*, *463*(7282), 775 780. https://doi.org/10.1038/nature08748

Sng, J., Ayoglu, B., Chen, J. W., Schickel, J.-N., Ferré, E. M., Glauzy, S., Romberg, N., Hoenig, M., Cunningham-Rundles, C., Utz, P. J., Lionakis, M. S., & Meffre, E. (2019). AIRE expression controls the peripheral selection of autoreactive B cells. *Science Immunology*, *4*(34), eaav6778. https://doi.org/10.1126/sciimmunol.aav6778

Söderbergh, A., Myhre, A., Ekwall, O., Gebre-Medhin, G., Hedstrand, H., Landgren, E., Miettinen, A., Eskelin, P., Halonen, M., Tuomi, T., Gustafsson, J., Husebye, E. S., Perheentupa, J., Gylling, M., Manns, M. P., Rorsman, F., Kämpe, O., & Nilsson, T. (2004). Prevalence and Clinical Associations of 10 Defined Autoantibodies in Autoimmune Polyendocrine Syndrome Type I. *The Journal of Clinical Endocrinology & Metabolism*, *89*(2), 557–562. https://doi.org/10.1210/jc.2003-030279

Stoffers, D. A., Zinkin, N. T., Stanojevic, V., Clarke, W. L., & Habener, J. F. (1997). Pancreatic agenesis attributable to a single nucleotide deletion in the human IPF1 gene coding sequence.

Nature Genetics, *15*(1), 106–110. https://doi.org/10.1038/ng0197-106

Taplin, C. E., & Barker, J. M. (2009). Autoantibodies in type 1 diabetes. *Autoimmunity*, *41*(1), 11 18. https://doi.org/10.1080/08916930701619169

Uhlen, M., Fagerberg, L., Hallstrom, B., Lindskog, C., Oksvold, P., Mardinoglu, A., Sivertsson, A., Kampf, C., Sjostedt, E., Asplund, A., Olsson, I., Edlund, K., Lundberg, E., Navani, S., Szigyarto, C., Odeberg, J., Djureinovic, D., Takanen, J., Hober, S., … Ponten, F. (2015). Tissue-based map of the human proteome. *Science*, *347*(6220), 1260419 1260419. https://doi.org/10.1126/science.1260419

Virant-Klun, I., Leicht, S., Hughes, C., & Krijgsveld, J. (2016). Identification of Maturation-Specific Proteins by Single-Cell Proteomics of Human Oocytes. *Molecular & Cellular Proteomics : MCP*, *15*(8), 2616 2627. https://doi.org/10.1074/mcp.m115.056887

Wang, J., Cortina, G., Wu, V. S., Tran, R., Cho, J.-H., Tsai, M.-J., Bailey, T. J., Jamrich, M., Ament, M. E., Treem, W. R., Hill, I. D., Vargas, J. H., Gershman, G., Farmer, D. G., Reyen, L., & Martín, M. G. (2006). Mutant Neurogenin-3 in Congenital Malabsorptive Diarrhea. *The New England Journal of Medicine*, *355*(3), 270–280. https://doi.org/10.1056/nejmoa054288

Wang, X., Song, D., Mykytenko, D., Kuang, Y., Lv, Q., Li, B., Chen, B., Mao, X., Xu, Y., Zukin, V., Mazur, P., Mu, J., Yan, Z., Zhou, Z., Li, Q., Liu, S., Jin, L., He, L., Sang, Q., … Wang, L. (2018). Novel mutations in genes encoding subcortical maternal complex proteins may cause human embryonic developmental arrest. *Reproductive BioMedicine Online*, *36*(6), 698–704. https://doi.org/10.1016/j.rbmo.2018.03.009

Welt, C. K. (2008). Autoimmune Oophoritis in the Adolescent. *Annals of the New York Academy of Sciences*, *1135*(1), 118–122. https://doi.org/10.1196/annals.1429.006

Winqvist, O., Gustafsson, J., Rorsman, F., Karlsson, F., & Kämpe, O. (1993). Two different cytochrome P450 enzymes are the adrenal antigens in autoimmune polyendocrine syndrome type I and Addison's disease. *Journal of Clinical Investigation*, *92*(5), 2377–2385. https://doi.org/10.1172/jci116843

Wolff, A., Sarkadi, A., Maródi, L., Kärner, J., Orlova, E., Oftedal, B., Kisand, K., Oláh, É., Meloni, A., Myhre, A., Husebye, E., Motaghedi, R., Perheentupa, J., Peterson, P., Willcox, N., & Meager, A. (2013). Anti-Cytokine Autoantibodies Preceding Onset of Autoimmune Polyendocrine Syndrome Type I Features in Early Childhood. *Journal of Clinical Immunology*, *33*(8), 1341–1348. https://doi.org/10.1007/s10875-013-9938-6

Zhang, W., Chen, Z., Zhang, D., Zhao, B., Liu, L., Xie, Z., Yao, Y., & Zheng, P. (2019). KHDC3L mutation causes recurrent pregnancy loss by inducing genomic instability of human early embryonic cells. *PLOS Biology*, *17*(10), e3000468. https://doi.org/10.1371/journal.pbio.3000468

Zhang, Y., Yan, Z., Qin, Q., Nisenblat, V., Chang, H.-M., Yu, Y., Wang, T., Lu, C., Yang, M., Yang, S., Yao, Y., Zhu, X., Xia, X., Dang, Y., Ren, Y., Yuan, P., Li, R., Liu, P., Guo, H., … Yan, L. (2018). Transcriptome Landscape of Human Folliculogenesis Reveals Oocyte and Granulosa Cell Interactions. *Molecular Cell*, *72*(6), 1 19. https://doi.org/10.1016/j.molcel.2018.10.029

Zhu, H., Bilgin, M., Bangham, R., Hall, D., Casamayor, A., Bertone, P., Lan, N., Jansen, R., Bidlingmaier, S., Houfek, T., Mitchell, T., Miller, P., Dean, R. A., Gerstein, M., & Snyder, M. (2001). Global Analysis of Protein Activities Using Proteome Chips. *Science*, *293*(5537), 2101–

2105. https://doi.org/10.1126/science.1062191

Zhu, K., Yan, L., Zhang, X., Lu, X., Wang, T., Yan, J., Liu, X., Qiao, J., & Li, L. (2015). Identification of a human subcortical maternal complex. *Molecular Human Reproduction*, *21*(4), 320 329. https://doi.org/10.1093/molehr/gau116

Ziegler, B., Schlosser, M., Lühder, F., Strebelow, M., Augstein, P., Northemann, W., Powers, A., & Ziegler, M. (1996). Murine monoclonal glutamic acid decarboxylase (GAD)65 antibodies recognize autoimmune-associated GAD epitope regions targeted in patients with type 1 diabetes mellitus and Stiff-man syndrome. *Acta Diabetologica*, *33*(3), 225–231. https://doi.org/10.1007/bf02048548

CHAPTER 2

BACKGROUND

Autoantibodies provide critical insight into autoimmunity by informing specific protein targets of an aberrant immune response and serving as predictors of disease. Historically, a majority of disease-associated autoantigens were discovered through candidate-based approaches by assuming that likely antigens would be specifically expressed in the tissue(s) of interest. By contrast, the development of proteome-wide screening approaches has enabled the systematic and unbiased discovery of autoantigens.

Two complementary approaches to proteome-wide autoantibody discovery include printed protein arrays and Phage-Immunoprecipitation Sequencing (PhIP-seq) (Jeong et al., 2012; Larman et al., 2011; Sharon and Snyder, 2014; Zhu et al., 2001). While powerful, printed protein arrays can be cost- and volume-prohibitive and are not flexible to adapting or generating new antigen libraries. On the other hand, PhIP-seq, originally developed by Larman *et al*., uses the throughput of arrayed oligonucleotide synthesis to enable very large libraries at comparatively low cost (Larman et al., 2011). However, phage-based techniques remain hindered by labor-intensive protocols that prevent broader accessibility and scaling.

Recently, we and others have adapted and applied Phage Immunoprecipitation-Sequencing (PhIP-Seq) to detect novel, disease associated autoantibodies targeting autoantigens across a variety of autoimmune contexts (Larman et al., 2013; Mandel-Brehm et al., 2019; O'Donovan et al., 2018; Vazquez et al., 2020). However, as with most high-throughput experiments, both technical and biological limitations exist. From a technical standpoint, PhIP-Seq libraries express programmed sets of linear peptides, and thus this technique is inherently less sensitive for conformational antigens (Vazquez et al., 2020; Wang et al., 2021). Nonetheless, the technique allows hundreds of thousands to millions of discreet peptide entities to be represented in a deterministic manner, including the multiplicity of protein isoforms and variants that are known to exist in actual cells. In this sense, PhIP-seq is complementary to mass

spectrometry and other techniques that leverage fully native proteins. Given that many forms of autoimmunity, such as APS1, exhibit significant phenotypic heterogeneity, the true number of patients with a shared disease-associated autoantibodies may be low (Ferre et al., 2016). Therefore, the screening of large cohorts is an essential step for identifying shared antigens and would benefit from a scaled PhIP-seq approach for high throughput testing.

Beyond the benefits of detecting low-frequency or low-sensitivity antigens, a scaled approach to PhIP-Seq would also facilitate increased size of healthy control cohorts. Recently, PhIP-Seq has been deployed to explore emerging forms of autoimmune and autoinflammatory disease, including COVID19-associated Multisystem Inflammatory Syndrome in Children (MIS-C) (Gruber et al., 2020). However, these studies suffer from a relative paucity and variety of control samples, resulting in low confidence of the disease-specificity of the suggested autoantigens. These questions of disease-specificity, rare antigens, and antigen overlap can only be addressed in larger, scaled experiments. However, to our knowledge, a published, widely accessible, and robustly tested protocol allowing for hundreds of samples to be run in parallel does not currently exist.

Here, we develop a high-throughput PhIP-Seq protocol. We demonstrate the power of this protocol by validating our previously reported APS1 antigens in an expanded, multi-cohort study, and implement machine learning approaches that enable robust prediction of APS1 disease status. We further explore novel disease-antigen relationships across IPEX and RAG1/2 deficiency with autoimmune features, cohorts of Kawasaki disease, and emerging COVID19 phenotypes with possible autoimmune underpinnings. In the future, scaled PhIP-Seq cohort studies could be used across additional syndromic and sporadic autoimmune diseases to develop an atlas of linear B cell autoantigens.

RESULTS

Design and Implementation of a scaled PhIP-Seq protocol

The ability to process large numbers of patient samples for PhIP-Seq in a highly uniform manner has several important benefits, including reduction of batch effects between samples from the same cohorts as well as between disease and controls cohorts, detection of lower-frequency autoantigens, and the ability to simultaneously include large numbers of control samples.

In creating a scaled protocol, we searched for a method that would allow 600-800 samples to be run fully in parallel to reduce any batch or plate-to-plate variability. Thus, each wash or transfer step needed to be performed in rapid succession for all plates. We also prioritized reduction of any well-to-well contamination, particularly given that small, early contamination can amplify across subsequent rounds of immunoprecipitation. Finally, we required our protocol to minimize consumable waste and maximize benchtop accessibility without robotics or other specialized equipment.

A benchtop vacuum-based protocol (rapid, consistent wash times) in deep-well 96-well filter plates with single-use foil seals (no well-to-well contamination) was best suited (Figure 2.1A). The data for APS1 samples on our moderate-throughput manual multichannel protocols were closely correlated with vacuum-based output, including identification of previously validated antigens within each sample (Figure 2.1B). Additional protocol improvements included: 3-D printing template for vacuum plate adaptors (for easy centrifugation and incubation steps); direct addition of protein A/G beads to E. coli lysis without a preceding elution step; shortened lysis step by using square-well plates with semi-permeable membrane for aeration; and options for smaller volume and decreased reagent library preparation in both 96-well and 384-well formats. A detailed protocol, including custom part designs, for both high-throughput vacuum-based and moderate throughput multichannel-based protocols is available at protocols.io.

Large control cohorts are critical for identifying disease-specific autoantibodies

Some assays for autoantigen discovery, such as protein arrays, are often used as a quantitative measure of how autoreactive an individual serum sample may be. In contrast, PhIP-Seq is an enrichment-based assay in which binders are serially enriched and amplified. A practical limitation of this technique is that non-specific phage may be also be amplified, in addition to a natural diversity of autoreactive, but non-disease related peptides. We tested whether we could detect global differences between case and control cohorts as a measure of autoreactivity. As each APS1 patient is known to have multiple, high-affinity antibodies to self-proteins (Fishman et al., 2017; Landegren et al., 2016; Meyer et al., 2016; Vazquez et al., 2020), we reasoned that this would be an ideal cohort to determine whether a global autoreactive state was discernible. As expected, each individual sample exhibits a spectrum of enriched genes, regardless of disease status (Figure 2.2A), indicating that measures of simple enrichment are inadequate for discrimination of cases from controls.

We and others have shown that PhIP-Seq can robustly detect disease-associated antigens by comparing antigen-specific signal between disease and control cohorts (Larman et al., 2011; Mandel-Brehm et al., 2019; O'Donovan et al., 2018; Vazquez et al., 2020). In this dataset, we further evaluated the importance of control cohort size. We iteratively down-sampled the number of healthy control samples in our dataset to 5, 10, 25, 50, 100, or 150 (out of n=186 total control samples). The number of apparent hits was determined in each condition, where a gene-level hit was called when the following criteria were met: 1) at least 10% of APS1 samples and less than 2 control samples with a Z-score > 10, 2) no control sample exhibiting higher signal than the highest patient signal, and 3) a minimum of one strong positive patient sample (50-fold enrichment over mock-IP). Using these conservative criteria, a control set of 10 resulted in (on average) 404 apparent hits, while increasing the control set to 50 removed an additional 388 non-specific (by definition) hits (Figure 2.2B). Further increasing the number of control samples to 150 samples had diminishing returns, although 4-5 more candidates were removed as being non-

specific, reducing the chance of false positives, and ultimately leaving only ~1% of the original candidate list for further investigation. In sum, in order to improve downstream analysis aimed at detecting disease-associated hits, PhIP-Seq experimental design should include a large and matched number – likely 50 or more even for small cohorts – of non-disease controls.

Scaled PhIP-Seq replicates and expands autoantigen repertoires across multiple independent cohorts of APS1

We previously identified and validated PhIP-Seq hits based on shared positivity of a given hit between 3 (out of 39) or more patients with APS1 (Vazquez et al., 2020). While this enabled us to robustly detect frequently shared antigens within a small disease cohort, antigens with lower frequencies – or with low detection sensitivity – would likely fall below this conservative detection threshold.

To improve both sensitivity and specificity, we utilized scaled PhIP-Seq to explore expanded cohorts of disease, including a much larger (n=128) APS1 cohort spanning 2 North American cohorts and 1 Swedish cohort. All hits present in at least 10% of APS1 patients also spanned all 3 cohorts, thus further validating broad prevalence of antigens that were previously been described by us (RFX6, ACPT, TRIM50, CROCC2, GIP, NKX6-3, KHDC3L) and others (SOX10, LCN1) (Figure 2.2C) (Fishman et al., 2017; Hedstrand et al., 2001; Vazquez et al., 2020). At the gene level, we detected 39 candidate hits that were present in ≥6/128 (>4%) of APS1 and in 2 or fewer controls (≤2/186, ≤1%) (Figure 2.3A & 2.3B). As expected, the larger cohort yielded new candidate antigens that had not been detected previously. For example, prodynorphin (PDYN) is a secreted opioid peptide thought to be involved in regulation of addiction-related behaviors (*reviewed in* (Fricker et al., 2020)). PDYN was enriched by 6/133 (4.5%) of patient samples and subsequently was validated by Radioligand Binding Assay (RLBA) (Figure 2.3C).

Indeed, this validated antigen was present in our previous investigations (Vazquez et al., 2020), however, it was enriched in too few samples to qualify for follow up.

Other notable hits with relevant tissue-restricted expression were also observed. For example, SPAG17 is closely related to the known APS1 autoantigen SPAG16 and is expressed primarily in male germ cells and in the lung, with murine genetic mutations resulting in ciliary dyskinesis with pulmonary phenotypes (Fishman et al., 2017; Teves et al., 2013). Also potentially related to ciliary and/or pulmonary autoimmunity is CROCC2/Rootletin, a protein expressed in ciliated cells, which we previously observed, and now recognize at a high frequency across multiple cohorts (Uhlen et al., 2015; Yang et al., 2002). Similarly, GAS2L2 is a ciliary protein expressed in the airway, with genetic loss of function in mice resulting in impaired mucociliary clearance, and clustered closely with CROCC2 (Bustamante-Marin et al., 2019; Uhlen et al., 2015) in this dataset. These novel putative antigens together hint at potential mucociliary airway autoreactivity. CT45A10 and GPR64 are both proteins with expression restricted primarily to male gonadal tissues (Uhlen et al., 2015). GABRR1 is a GABA receptor expressed primarily in the central nervous system as well as on platelets (Ge et al., 2006; Zhu et al., 2019); and TRIM2 is implicated in genetic disorders of demyelination within the peripheral nervous system, and therefore may be of interest to the chronic inflammatory demyelinating polyneuropathy (CIDP) phenotype that can be seen in some patients with APS1 (Li et al., 2020; Valenzise et al., 2017). In addition to our previously described intestinally expressed autoantigens RFX6, NKX6-3, and GIP, we also identify CDHR5, a transmembrane cadherin-family protein expressed on the enterocyte cell surface, as a putative autoantigen in APS1 (Crawley et al., 2014; Uhlen et al., 2015).

APS1 disease prediction by machine learning

APS1 is a clinically heterogeneous disease, and it is also heterogeneous with respect to autoantibodies (Ferre et al., 2016; Fishman et al., 2017; Landegren et al., 2016; Meyer et al.,

2016; Vazquez et al., 2020). Because a PhIP-seq simultaneously interrogates autoreactivity to hundreds of thousands of peptides, we hypothesized that unsupervised machine learning techniques could be used to create a classifier that would distinguish APS1 cases from healthy controls. We applied a simple logistic regression classifier to our full gene-level APS1 (n=128) and control (n=186) datasets, resulting in excellent prediction of disease status (AUC = 0.95, Figure 2.4A). Moreover, we found that the classification model was driven strongly by many of the previously identified autoantigens, including RFX6, KHDC3L, and others (Figure 2.4B), in addition to some targets that have not been previously examined (Vazquez et al., 2020). These results demonstrate that the data-rich nature of PhIP-seq autoreactive antigen enrichment provides fertile ground for machine learning techniques, and further suggest that such data could be used to derive diagnostic signatures with strong clinical predictive value.

IPEX syndrome, a syndromic counterpart to APS1

IPEX syndrome, characterized by defective peripheral immune tolerance secondary to impaired T regulatory cell (Treg) function, is a syndromic counterpart to APS1. In IPEX, peripheral tolerance rather than central tolerance is impaired, resulting in a phenotypic constellation of autoimmunity that partially overlaps with APS1 (Bacchetta et al., 2006; Powell et al., 1982). Notably, the majority of IPEX patients exhibit severe enteropathy, with early-onset severe diarrhea and failure to thrive, with many of these children harboring anti-enterocyte antibodies detected by indirect immunofluorescence (Bacchetta et al., 2006; Gambineri et al., 2018; Powell et al., 1982). We hypothesized that the same PhIP-seq approach that was successful for APS1 would also yield informative hits for IPEX. A total of 27 patient samples were analyzed using scaled PhIP-seq and the data processed in the same manner as for APS1.

A handful of IPEX autoantigens targeting intestinally expressed antigens have been described, including harmonin (USH1A) and ANKS5B (Eriksson et al., 2019; Kobayashi et al.,

2011). In our data, enrichment of USH1A was observed in 2 IPEX patients, and this signal was fully correlated with anti-ANKS5B as previously described (Supp.Fig. 2.1A) (Eriksson et al., 2019).

Several novel putative autoantigens were observed to be shared between 3 or more IPEX patients (Figure 2.5A). Among these were several with expression restricted to the intestine, including BEST4, a protein expressed by a specific subset of enterocytes, BTNL8, a butyrophilin-like molecule highly expressed in the gut epithelium, ST6GALNAC1, and ITGA4 (Figure 5A) (Mayassi et al., 2019; Schaum et al., 2018; Uhlen et al., 2015). BEST4 and BTNL8 were selected for validation by whole protein immunoprecipitation. A total of 4/26 (15%) of IPEX patients were positive for anti-BEST4 autoantibodies (Figure 2.5B). In the case of BTLN8, orthogonal validation identified 11/26 (42%) of IPEX patients who were positive for anti-BTNL8 antibodies (Figure 2.5B). While the majority of patients in the cohort had clinical enteropathy, it is nonetheless interesting that all patients with anti-BTNL8 and/or BEST4 antibodies also had clinical evidence of enteropathy (Supplementary Table S2.1). Taken together, these results suggest that anti-BEST4 and anti-BTNL8 are associated with IPEX enteropathy, however additional investigation will be required to understand whether this association is indirect or directly related to pathology.

Overlap of intestinal autoantigen BEST4 in the setting of hypomorphic Rag1/2 mutations

Hypomorphic Rag1/2 mutations represent an additional and notoriously phenotypically heterogeneous form of monogenic immune dysregulation. Absent Rag complex activity leads to absent peripheral T and B cells, therefore causing severe combined immunodeficiency (SCID). However, many patients have hypomorphic mutations to Rag1/2, and therefore rather than presenting with SCID can present with Omenn Syndrome (OS), Atypical SCID (AS), and Combined Immune Deficiency with Granulomas and Autoimmunity (CID-G/AI) (Delmonte et al., 2018, 2020). The autoimmune phenotypes are most frequently autoimmune cytopenias, but also include other autoimmunities including cutaneous and intestinal manifestations. While anti-

cytokine antibodies have been described, other disease-associated autoantibody targets remain to be identified (Delmonte et al., 2020).

62 patients with hypomorphic RAG1/2 mutations were screened by PhIP-seq to ascertain overlap with APS1 and IPEX antigens, as well as for novel autoantigen specificities. Minimal overlap was observed between RAG1/2 and APS1 and IPEX. However, two samples from Rag1/2 patients indicated the presence of anti-BEST4 antibodies (Figure 2.5C), which were confirmed through orthogonal validation using whole protein (Figure 2.5D). Both positive patients had CID-G/AI, indicating the presence of autoimmune features. Remarkably – given that enteropathy in the setting of hypomorphic Rag1/2 deficiency is rare – one of the two individuals harboring anti-BEST4 antibodies also had very early onset inflammatory bowel disease (VEO-IBD).

Several other putative antigens amongst the larger Rag1/2 deficiency cohort were revealed. Nearly half of the cohort sera enriched for peptides derived from ZNF365 (Suppl. Fig. S2.1B). ZNF365 is a protein associated with multiple autoimmune diseases, as evidenced by GWAS studies showing that variants in ZNF365 are associated with Crohn's disease and autoimmune uveitis (Haritunians et al., 2011; Hou et al., 2020). Many patients also had evidence of autoantibodies targeting RELL2, a TNF receptor binding partner, and CEACAM3, a phagocyte receptor that recognizes human specific pathogens and is important for opsonin-independent phagocytosis of bacteria (Bonsignore et al., 2020; Moua et al., 2017). Autoantibodies targeting these antigens could potentially play a role in the auto-inflammation seen in certain cases of hypomorphic Rag1/2 and/or increased susceptibility to particular infections, and will require additional future follow-up.

PhIP-seq rare shared candidate autoantigens in MIS-C

MIS-C leads to critical illness in ~70% of affected children, and is thought to exist on a spectrum with Kawasaki Disease (KD), the most common cause of acquired pediatric heart disease in the US. Despite hints for a role of abnormal adaptive immunity and autoantibodies in

the pathogenesis of KD and MIS-C, the etiologies of both diseases remain enigmatic (Feldstein et al., 2020; Newburger et al., 2016). Recently, PhIP-Seq has been deployed to explore COVID19-associated MIS-C (Gruber et al., 2020). However, this study included only 4 healthy controls and 9 MIS-C patients and as our results have shown, removal of false-positive PhIP-seq hits requires the use of substantial numbers of unaffected controls (Figure 2.2C). Furthermore, these previously published hits lacked orthogonal validation. Therefore, we sought to examine an MIS-C cohort in light of these results, as well as to explore for possible autoantibody overlap between Kawasaki disease and MIS-C.

First, 20 MIS-C, 20 pediatric febrile controls, and 20 COVID-19 controls were examined by PhIP-seq, each of which were compared to a cohort of adult healthy controls (n=87). No evidence for specific enrichment was observed for any of the previously reported candidate antigens that overlapped with our PhIP-Seq library (Figure 2.6A). Methodologic and sample differences could, in part, account for differences in our results, however, these results suggest that PhIP-seq hits should be subjected to external replication and/or validation.

Analysis of our MIS-C cohort for shared candidate hits yielded only 3 candidate hits, each in 2/20 patient sera. These were CD34, RPS6KB1, and CAPZB (Figure 2.6B). While these targets may be of interest, disease-association remains uncertain. These results suggest that a much larger MIS-C cohort, controlled by an equally large set of healthy controls, will be required to detect rare shared antigens with confidence.

PhIP-Seq screen of a cohort of Kawasaki Disease patients

To address the question of possible autoantibody overlap between KD and MIS-C, as well as to screen for possible KD-specific autoantibodies, we analyzed a large cohort of KD by PhIP-Seq. Using the same hit selection criteria as previously, we detected 25 shared hits among 3 or more of the 70 KD samples, which were specific to KD relative to adult healthy controls (Figure 2.6C). Of these 25 shared KD hits, 17 were absent from additional control groups including the

febrile pediatric patients. Each of these hits was present in only a small subset of KD samples, suggesting significant heterogeneity among samples.

Some of the candidate antigens have possible connections to the systemic inflammation seen in KD, including SPATA2 (6/70, 8.6%) samples, and ALOX5B (X/70, X%). SPATA2 is a protein known to regulate the TNF receptor response, with murine knockout of SPATA2 resulting in increased activation of NFkB and MAPK (Schlicher and Maurer, 2016). Similarly, ALOX15 family of lipoxygenases is known to be responsive to Th2-induced anti-inflammatory cytokine IL-4 and IL-13 in human macrophages and thereby likely plays a role in suppressing inflammatory responses, and polymorphisms have been linked the development of coronary artery disease (Snodgrass and Brüne, 2019; Wuest et al., 2014).

Other KD candidate autoantigens exhibited tissue expression patterns relationships that suggest possible relationships to sub-phenotypes seen in KD. For example, it is well described that a subset of KD patients develop pancreatitis (Prokic et al., 2010). We found that 7/70 of the KD patients (10%) have increased signal for autoantibodies targeting FBXL19, a protein which was recently shown to have increased serum levels which correlated with the severity of disease in patients with acute pancreatitis (Ma et al., 2020); and 10/70 for pancreas-expressed protein RESP18 (Zhang et al., 2007). Taken together, our data suggest that autoantibody presence in KD and MIS-C may be more heterogenous than within classical monogenic autoimmunities including IPEX and APS1.

Autoantigen overlap between KD and MIS-C

Given the possible overlap of KD with MIS-C, we also searched for these shared KD hits within MIS-C, and found that 6 of these 17 KD hits were present in one or more MIS-C samples. Of these, CGNL1 was of particular interest given the very high enrichment values in patients and absence of signal from all controls, as well as the pattern of expression. CGNL1 is an endothelial junction protein and is highly expressed in the cardiac endothelium (Chrifi et al., 2017; Schaum

et al., 2018). We confirmed anti-CGNL1 autoantibodies using a radioligand binding assay with whole CGNL1 protein (Figure 2.6D). We also identified an additional positive KD patient that had not been detected by PhIP-Seq. These data suggest that anti-CGNL1 antibodies, while rare, may be associated with KD and/or MIS-C, however additional investigation and validation will be required.

Application of scaled PhIP-Seq to severe COVID-19

Recently, it was reported that over 10% of severe COVID-19 pneumonia is characterized by the presence of anti-type 1 Interferon autoantibodies, a specificity that overlaps with APS1 (Bastard et al., 2020, 2021a; Meager et al., 2006; Meyer et al., 2016; Wijst et al., 2021). We therefore looked for possible overlap of additional antigens between APS1 and COVID19. As expected, we had low sensitivity for the known anti-type I Interferon autoantibodies by PhIP-Seq, likely due to the conformational nature of these antigens. We did not detect substantial overlap of any of the other antigens that were found in 5% or more of APS1 samples, suggesting that autoantibody commonalities between APS1 and severe COVID may be limited (Figure 2.7A).
PhIP-seq was then used to investigate patients with severe COVID19 pneumonia (n=100) relative to patients with mild to moderate COVID19 (n=55) and non-COVID healthy controls (n=125) (Figure 2.7B). A small number of putative antigens were identified in 4 or more of the severe COVID group (>4%), but not within our control group, including MCAM, CHRM5, and EEA1. Of these, only EEA1, an early endosomal protein, had a frequency of >10% (Mu et al., 1995). Notably, the set of anti-EEA1 positive patients was almost fully distinct from the anti-Type I interferon positive group, with only 1 patient shared between the groups (Figure 2.7B). Given the importance of the finding of autoantibodies to Type 1 IFNs in 10-20% of severe to critical COVID19 pneumonia, our data suggest that EEA1 may also have predictive potential worth further investigation.

DISCUSSION

PhIP-Seq is a powerful tool for antigen discovery due to its throughput and scalability. Continually declining costs in sequencing paired with scaled protocols such as the ones presented here result in a low per-sample cost and experimental time, and declining costs of custom oligonucleotide based-libraries further support versatile adaptations to the existing libraries (Román-Meléndez et al., 2021; Vogl et al., 2021). Yet, as the technology is relatively new, increased discussion around best practices in experimental design, methodology, and data interpretation is needed. In this work, we contribute to these efforts by presenting an accessible, carefully documented (protocols.io) scaled lab protocol. We anticipate that scaling and low cost will facilitate cross-platform comparisons of autoimmune sera, enabling a more systematic understanding of each platform's abilities and shortcomings, as well as best ways to combine platforms for comprehensive autoantibody profiling. Indeed, recent work compared sensitivities for a subset of secreted antigens across fixed protein arrays, yeast display (REAP), and PhIP-Seq (Wang et al., 2021). This principle can in the future be applied to other groups of proteins and antigens to better understand specific strengths and weaknesses of high-throughput antigen discovery, especially when datasets contain overlapping patient-specific sera.

Our scaled data also reinforces the importance of best practices, including large control cohorts to improve specificity and orthogonal validations for evaluation of sensitivity. First, in regard to specificity, we find that the absence of appropriately sized control cohorts can result in false-positive associations between enriched protein sequences and disease. Thus, these results caution against overinterpretation of reported disease-specific autoantigens in PhIP-Seq or other expanded antigen screening technologies such as near-proteome wide fixed protein arrays which utilize smaller control cohorts, often without orthogonal validation experiments. Second, in regard to sensitivity, PhIP-seq is optimized for linear antigens and thus is inherently less robust for detection of confirmational or modified epitopes. For example, our previous work highlights that

known anti-IFN and anti-GAD65 antibodies can be detected only in a handful of APS1 samples by PhIP-Seq, while orthogonal assays using whole conformation protein demonstrate increased sensitivity (Vazquez et al., 2020). Similarly, the increased sensitivity of whole protein validation relative to PhIP-Seq for BTNL8 autoantibodies highlights the need for rapid and sensitive secondary assays to confirm or even increase the importance of a given candidate antigen. We anticipate that these principles of specificity and validation will also prove informative across other, related PhIP-Seq modalities (Mina et al., 2019; Román-Meléndez et al., 2021; Vogl et al., 2021).

As in our previous work, we were able to identify a number of novel APS1 antigens. These were revealed in addition to our previously described antigens by leveraging scaling to detect lower-frequency hits such as PDYN. PDYN is a secreted opioid precursor of the central nervous system, and while PDYN-knockout mice are largely phenotypically normal, they do experience hyperalgesia and altered anxiety-related behaviors relative to wildtype mice (McLaughlin et al., 2003; Sharifi et al., 2001; Wang et al., 2001). Future studies on whether anti-PDYN antibodies may themselves be able to mediate these phenotypes will be of great interest. In addition to uncovering lower frequency autoantigens, we were also interested to study any antigen overlap between APS1 and other syndromic autoimmune diseases. Interestingly, we saw only limited signal for common APS1 antigens across the other disease contexts, suggesting that common antigens such as RFX6, KHDC3L and others may not be shared across other multiorgan autoimmune syndromes including IPEX and Rag deficiency.

In contrast, we were able to detect antigen overlap between IPEX and Rag-deficient patients in the form of anti-BEST4 antibodies. BEST4 is a well-characterized, cell-surface intestinal ion channel (Qu and Hartzell, 2008). Recently BEST4 has become a standard and specific marker for a subset of enterocytes in the duodenum and colon, including CFTR+ enterocytes, which are involved in fluid homeostasis (Busslinger et al., 2021; Elmentaite et al., 2021; Smillie et al., 2019). The findings of anti-BEST4 autoantibodies across both IPEX and CID-G/AI illustrate our ability to gain important novel insights into monogenic forms of immune

dysregulation using PhIP-Seq. The presence of an IPEX antigen BEST4 within CID-G/AI suggests a possible etiologic link between the two diseases, possibly relating to Treg dysfunction. Furthermore, given that BEST4 autoantibodies are found across 2 distinct etiologies of IBD, as well as that BEST4 is intestinally expressed, we believe future experiments specifically searching for the presence of anti-BEST4 antibodies in IBD and other forms of autoimmune enteropathy are warranted.

Our second novel IPEX antigen, BTNL8, is also of particular interest given its high frequency in IPEX (11/26) as well as its biological functions. BTN and BTNL-family members belong to the family of B7 co-stimulatory receptors known to modulate T-cell responses, with structural similarity to CD80 and PD-L1 (Chapoval et al., 2013; Rhodes et al., 2015). Broadly, BTNL-family members are thought to participate primarily in regulation of gamma-delta T cells, with BTNL8/BTNL3 implicated in gut epithelial immune homeostasis (Barros et al., 2016; Chapoval et al., 2013). Given the cell-surface expression pattern of BTNL8, it is conceivable that antibodies to these proteins could play a functional role in immune checkpoints, rather than only the bystander role implicated for most autoantibodies to intracellular antigens. Interestingly, recent studies in patients with celiac disease have demonstrated a reduction in BTNL3/BTNL8 expression following acute episodes of inflammation, with an associated loss of the physiological normal gamma/delta T-cell subset of gut intraepithelial lymphocytes (Mayassi et al., 2019).

While some of our datasets reveal strong, common antigens such as BTLN8 and BEST4. others suggest that PhIP-Seq screens may more often result in heterogenous datasets than in the fortuitous discovery of single, common autoantigens. This may be true in particular in the setting of complex or multiorgan phenotypes, including MIS-C and KD. In this way, our results indicating only rare, shared putative antigens in these 2 diseases were not entirely unexpected, especially given that the etiologies of both diseases have remained elusive. Nonetheless, a number of observations point to a possible role for abnormal adaptive immunity and autoantibodies (reviewed in (Sakurai, 2019)). Both diseases improve markedly following

intravenous immunoglobulin (IVIG) therapy, and genetic studies show that children with mutations to genes involving B-cell and antibody function are more likely to develop KD (reviewed in (Onouchi, 2018)). Autoantibodies targeting clinically relevant tissue such as the heart or endothelium have also been shown to exist in KD, though the specific antigen targets have yet to be determined (Cunningham et al., 1999; FUJIEDA et al., 1997; GRUNEBAUM et al., 2002). We therefore felt that an autoantibody screen in both diseases could substantially contribute to our understanding of these diseases. Although found only at low frequency, it is possible that anti-CGNL1 antibodies may describe a subset of specificities within anti-endothelial cell antibodies, given the endothelial expression of CGNL1 as well as its implications in cardiovascular disease (Chrifi et al., 2017). Particularly in the setting of MIS-C, expanded cohorts both for validation for CGNL1 as well as for as-of-yet undescribed antigen specificities may add additional information for otherwise poorly understood diseases.

There is increasing evidence for a role for autoantibodies in other acquired disease states that have not been classified *per se* as autoimmune diseases, including severe COVID-19 pneumonia (Bastard et al., 2020, 2021b; Wijst et al., 2021). We found PhIP-Seq signal to EEA1 in 11% of patients with severe COVID19 pneumonia, while signal in patients with mild COVID19 was absent. Interestingly, similarly to anti-IFN antibodies, anti-EEA1 antibodies have also previously been reported in the setting of systemic lupus erythematosus (SLE) (Selak et al., 2000; Stinton et al., 2004; Waite et al., 1998). While intriguing, future studies will be needed to determine whether the specificity of EEA1 autoantibodies to severe-critical COVID-19 can be replicated in independent cohorts, as well as in orthogonal assays.

Beyond presenting novel candidate autoantigens, this work also provides the first evidence for predictive or diagnostic value from bulk PhIP-Seq data input using a linear regression model in the disease APS1. While we were able to successfully implement a machine learning algorithm to differentiate between APS1 and healthy control samples (Figure 4A), limitations in number of MIS-C and pediatric control samples precluded us from performing these same

analyses on MIS-C and KD. However, we believe that with a larger discovery cohort and matched pediatric controls a diagnostic machine learning algorithm may be possible, in part because in our preliminary cohorts presented here, patients appear to exhibit a particular and distinct autoantibody signature (Figure 6C). Thus, scaled PhIP-Seq represents an avenue to not only discover and compare novel autoantigens within and across cohorts of autoimmune disease, but also suggests an exciting possibility of diagnostic or prognostic value in an even wider variety of immune dysregulatory contexts. Investigation of optimal data input, additional machine learning algorithms, and application to expanded disease cohorts should be explored in future studies.

Finally, we emphasize that in order to broadly understand autoantibody profiles, full PhIP-Seq data availability is critical for enabling expanded analysis and comparison across datasets, cohorts, and research groups. Importantly, groups with expertise in specific disease areas may add value by re-analyzing and evaluating candidate hits using additional metrics for hit prioritization, including increased weighting of orthogonal expression and/or genetic data. Full PhIP-Seq data for all cohorts presented here are linked to this publication and are available for download at Dryad.

MATERIALS & METHODS

PhIP-Seq data alignment and normalization

Fastq files were aligned at the level of amino acids using RAPSearch2 (PMID: 22039206). For gene level analysis, all peptide counts mapping to the same gene were summed. 0.5 reads were added to all genes, and raw reads were normalized by converting to percentage of total reads per sample. Fold change over mock-IP (FC) was calculated on a gene-by-gene basis by dividing sample read percentage by mean read percentage in corresponding AG bead-only samples. Z-scores were calculated using FC values; for each disease sample by using all corresponding healthy controls, and for each healthy control samples by using all other healthy controls. The positive threshold used for detection of shared candidate antigens was a Z-score >=10. Shared hits were then determined by positive rate in the specified percentage of patient samples and under a specified percentage (<2% unless otherwise specified) in controls. In addition, at least one positive sample was required to have a minimum FC of 50 or above. Finally, no candidate antigens were allowed where any positive control samples signal fell above the highest patient sample.

Radioligand Binding Assay

Radioligand binding assay was performed as described in (Vazquez et al. 2020, Elife) for each gene of interest (GOI). Briefly, GOI-myc-flag constructs was used to *in vitro* transcribe and translate [35S]-methionine labeled protein, which was subsequently column purified, immunoprecipitated with patient serum on Sephadex protein A/G beads, and counts per million (cpm) were read out on a 96-well liquid scintillation reader (MicroBeta Trilux, Perkin Elmer). Constructs: PDYN (Origene, #RC205331), BEST4 (Origene, #RC211033), BTNL8(Origene, #RC215370), CGNL1 (Origene, #RC223121). Anti-MYC (Cell Signaling Technologies, #2272S)

and/or anti-FLAG (Cell Signaling Technologies, #1493S) antibodies were used as positive controls for immunoprecipitations.

Statistics

Statistics for Radioligand binding assay were performed as described in (Vazquez et al. 2020, Elife). Briefly, the antibody index for each sample was calculated as: (sample value – mean blank value) / (positive control antibody value – mean blank value).

We applied a logistic regression classifier on log-transformed PhIP-Seq RPK values from APS1 patients (n = 128) versus healthy controls (n = 186) using the scikit-learn package [citation*] with a liblinear solver and L1 regularization. The model was evaluated with five-fold cross-validation.

ACKNOWLEDGEMENTS

We thank members of the DeRisi and Anderson labs for helpful discussions. We thank the New York Blood Center and CPMC blood center for providing deidentified healthy control plasma.

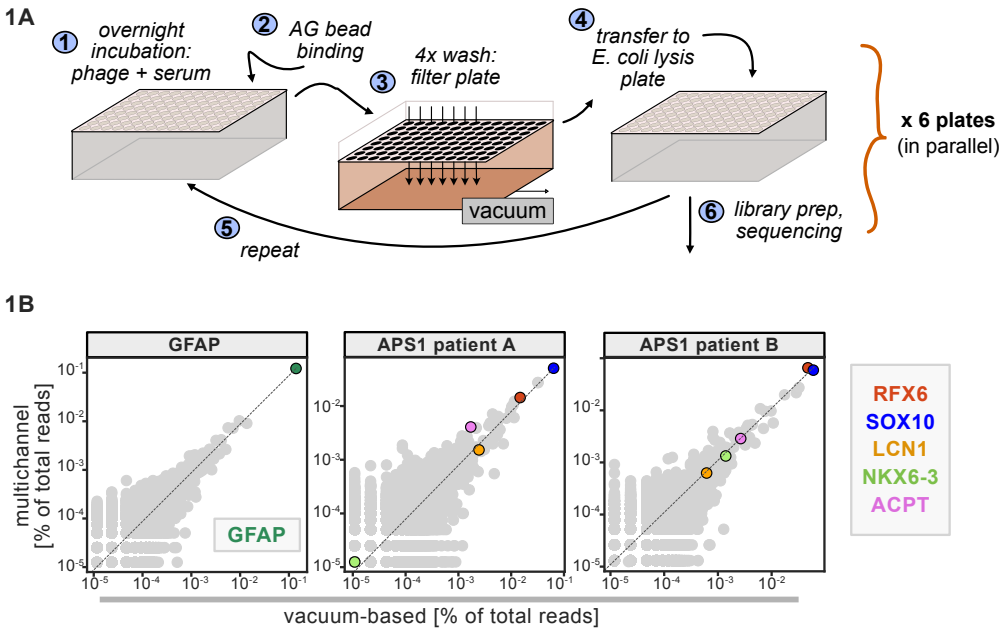

Figure 2.1. Motivation for scaled PhIP-Seq. A) Schematic of vacuum-based scaled PhIP-Seq protocol, allowing for parallelized batches of 400-600 samples. B) Comparison of moderate-throughput multichannel protocol data to high-throughput vacuum-based protocol data, with axes showing normalized read percentages. Controls include a commercial polyclonal anti-GFAP antibody (left), APS1 patient A with known and validated autoantibodies RFX6, SOX10, ACPT and LCN1 (center), and APS1 patient B with the same known and validated autoantibodies as well as NKX6-3.

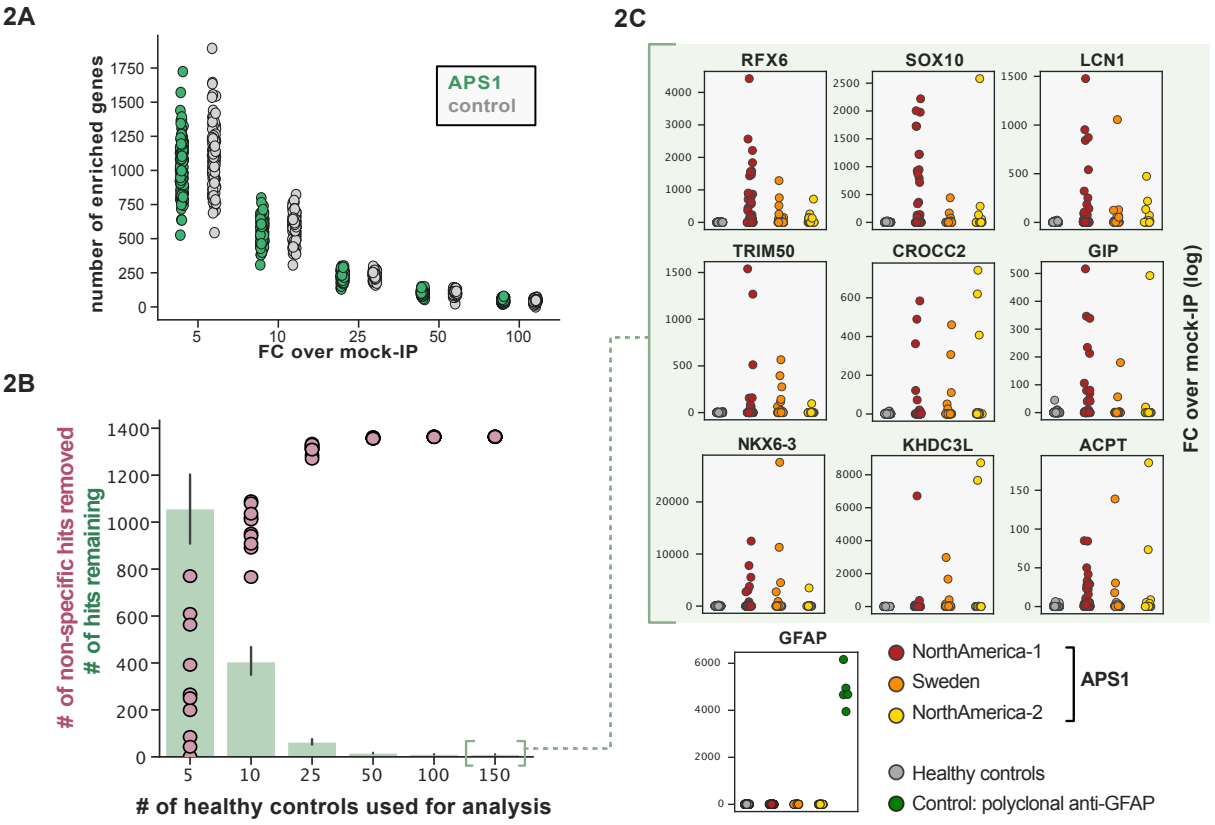

Figure 2.2. Application of scaled PhIP-Seq to expanded APS1 and control cohorts. A) Number of hits per sample reaching 5, 10, 25, 50, and 100-fold enrichment relative to mock-IP samples. Each dot represents a single APS1 patient (green) or non-APS1 control (grey). **B)** When looking for disease-specific hits, increasing the number of healthy controls results in fewer apparent hits and is therefore critical. Shared hits are defined as gene-level signal (>10-fold change over mock-IP) which is shared among 10% of APS1 samples (n=128), present in fewer than 2% of healthy controls, and with at least 1 APS1 sample with a high signal (FC of 50<). Random down-sampling was performed 10 times for each healthy control bin. **C)** 9 gene-level hits are present in 10%< of a combined 3-group APS1 cohort. North-America-1, n = 62; Sweden, n = 40; North-America-2, n = 26. Anti-GFAP control antibody (n=5) indicates that results are consistent across plates and exhibit no well-to-well contamination.

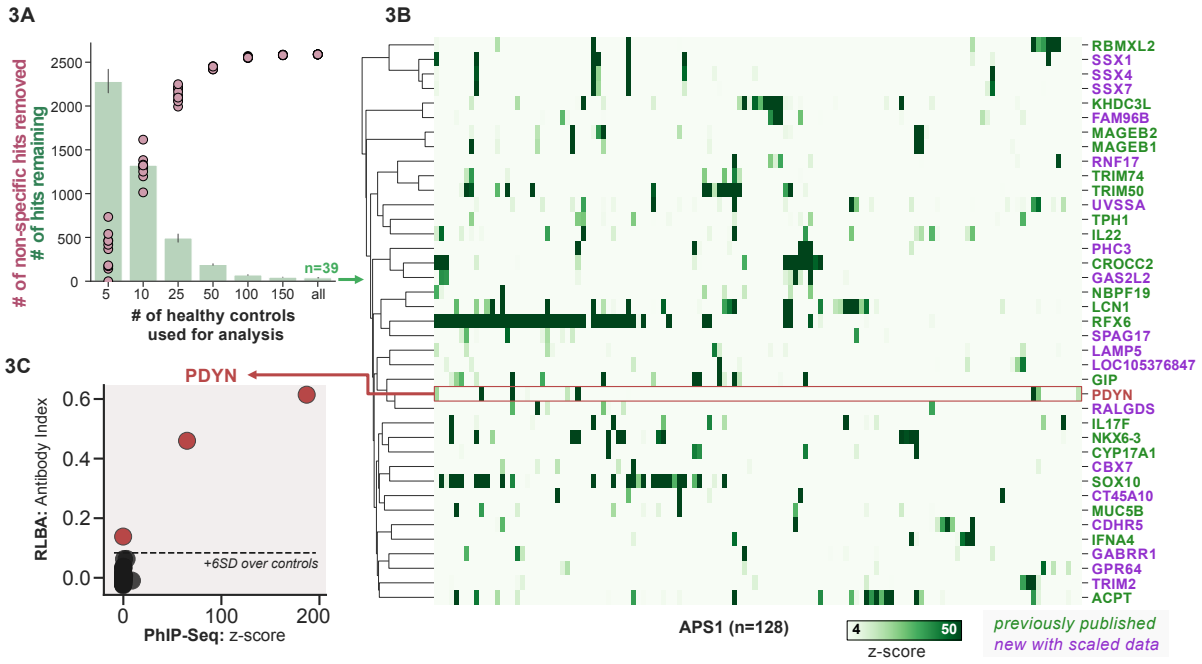

Figure 2.3. Expansion of APS1 autoantigens across multiple cohorts. A) Increasing the number of healthy controls results in fewer apparent hits and is therefore critical. Shared hits are defined as gene-level signal (>10-fold change over mock-IP) which is shared among 4%< of APS1 samples (n=128), present in fewer than 2% of healthy controls, and with at least 1 APS1 sample with a high signal (FC of 50<). Random downsampling was performed 10 times for each healthy control bin. **B)** 39 candidate hits present in 4%< of the APS1 cohort. **C)** Rare, novel anti-PDYN autoantibodies validate at whole-protein level, with PhIP-Seq and whole-protein RLBA data showing good concordance.

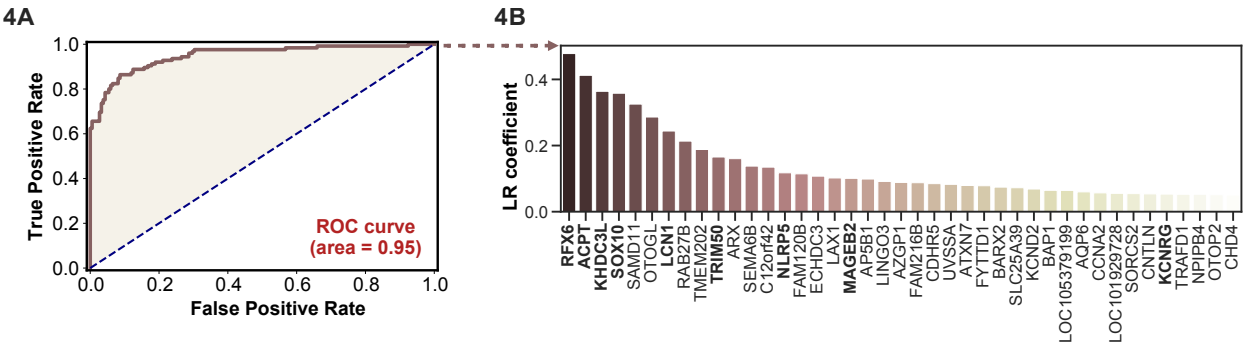

Figure 2.4. Application of machine learning to APS1 PhIP-Seq data. A) ROC curve for prediction of APS1 versus control disease status (left). **B)** The highest logistic regression (LR) coefficients include known antigens RFX6, KHDC3L, and others (right).

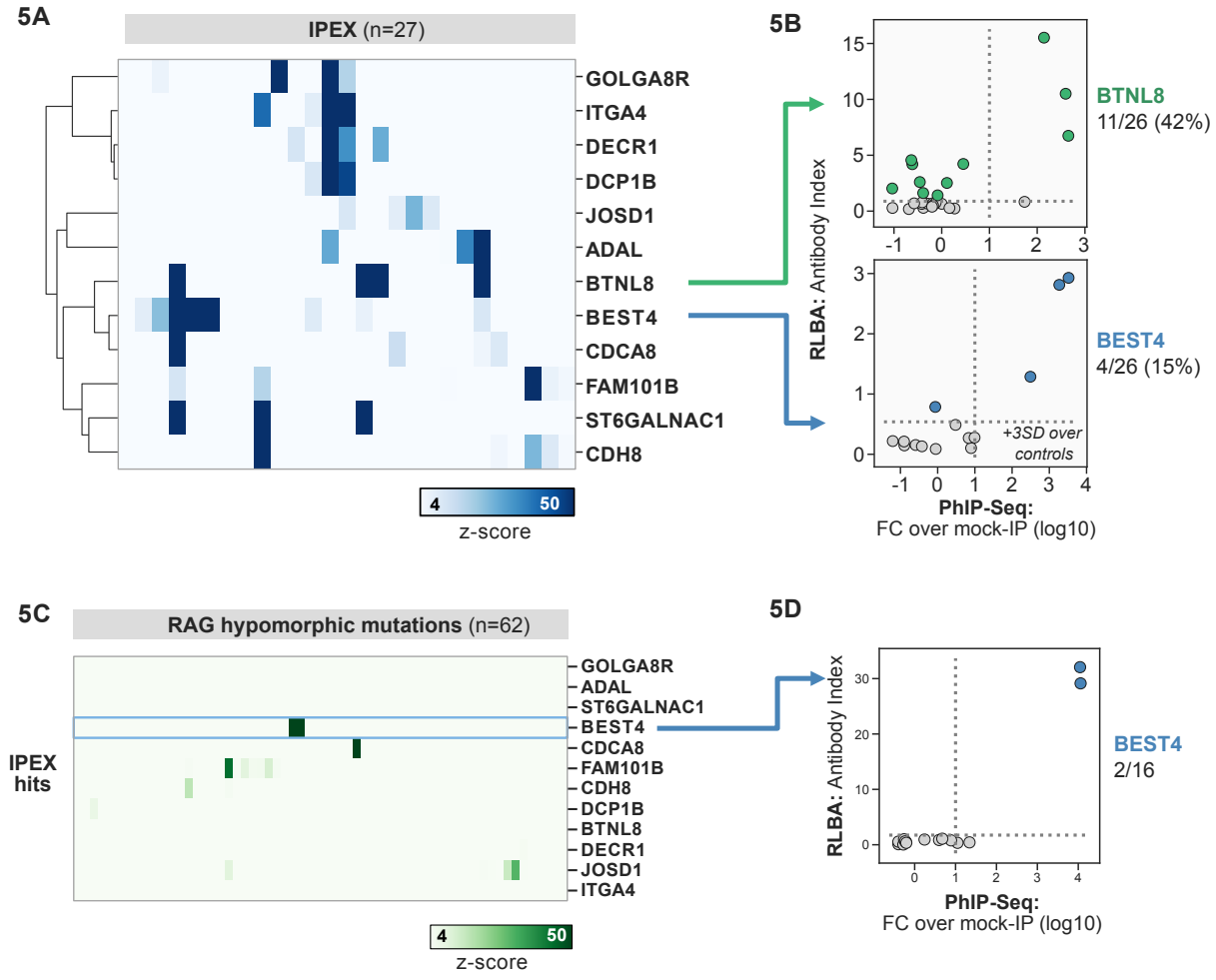

Figure 2.5. PhIP-Seq screening in IPEX and RAG deficiency. A) PhIP-Seq heatmap of most frequent shared antigens among IPEX, with color indicating z-score relative to a cohort of non-IPEX controls. **B)** Radioligand binding assay for BTNL8 reveal additional anti-BTNL8 positive IPEX patients (top). Radioligand binding assay for BEST4 autoantibodies correlates well with PhIP-Seq data (bottom). **C**) PhIP-Seq screen of patients with hypomorphic mutations in Rag1/2 reveals 2 patients with anti-BEST4 signal. **D)** Orthogonal radioligand binding assay validation of anti-BEST4 antibodies in both PhIP-Seq anti-BEST4 positive patients.

Suppl. 2A

Suppl. 2B

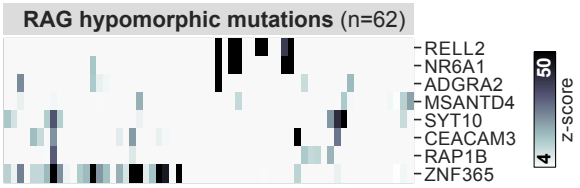

Supplementary Figure S2.1. Supporting data in IPEX and RAG deficiency. A) PhIP-Seq has low detection sensitivity for known antigens USH1C and ANKS4B, but those patients with positive signal exhibit the previously reported coupled signal for both antigens. **B)** Additional, shared putative antigens within the cohort of RAG-deficient patients (n=62).

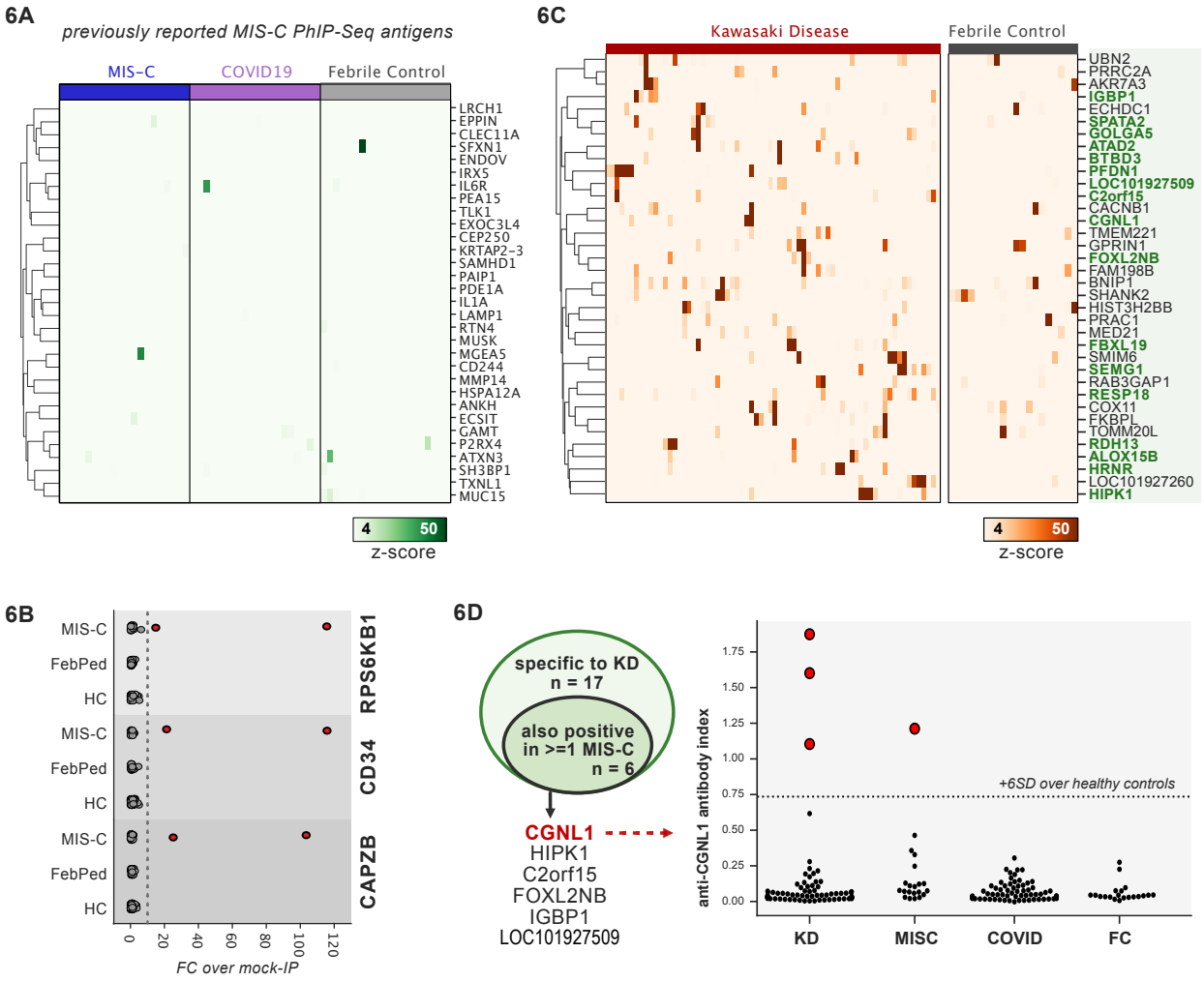

Figure 2.6. Scaled PhIP-Seq in MIS-C and Kawasaki Disease. A) Heatmap of signal for putative hits from *Gruber et al. 2020*, among n=20 of each of MISC, adult COVID19 controls, and pediatric febrile controls. **B)** Only rare, shared PhIP-Seq signal is found among n=20 MISC patients. **C)** Heatmap of putative antigens in a cohort of n = 70 KD patients. Hits that are specific to KD, and are not found among n=20 febrile controls, are highlighted in green. **D)** A small number of rare putative antigens are shared between KD and MISC. Radioligand binding assay confirms antibody reactivity to whole protein form of CGNL1 in 3 KD patients and 1 MISC patient.

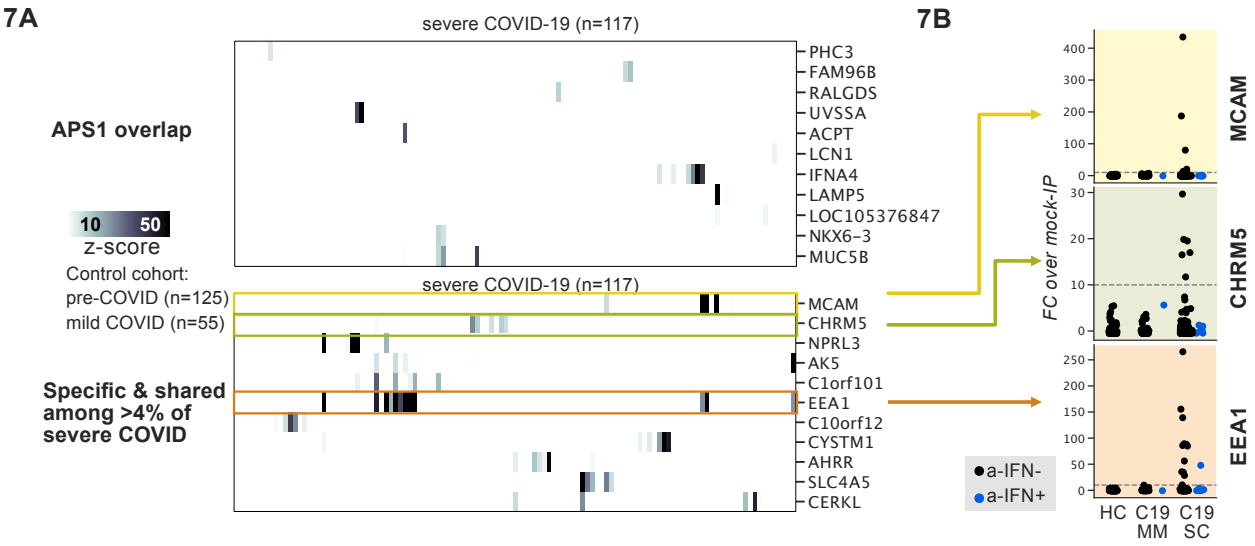

Figure 2.7. PhIP-Seq screening in severe forms of COVID-19. A) Screening of patients with severe COVID19 pneumonia shows little overlap with APS1, but enables discovery of possible novel disease associated autoantigens including EEA1. **B)** Putative novel antigens EEA1, CHRM5, and MCAM are primarily found in anti-IFN-negative patients, suggesting the possibility of other frequent, independent disease-associated antibodies in severe COVID19.

SUPPLEMENTAL TABLES

Supplementary Table S2.1. Clinical data for IPEX cohort

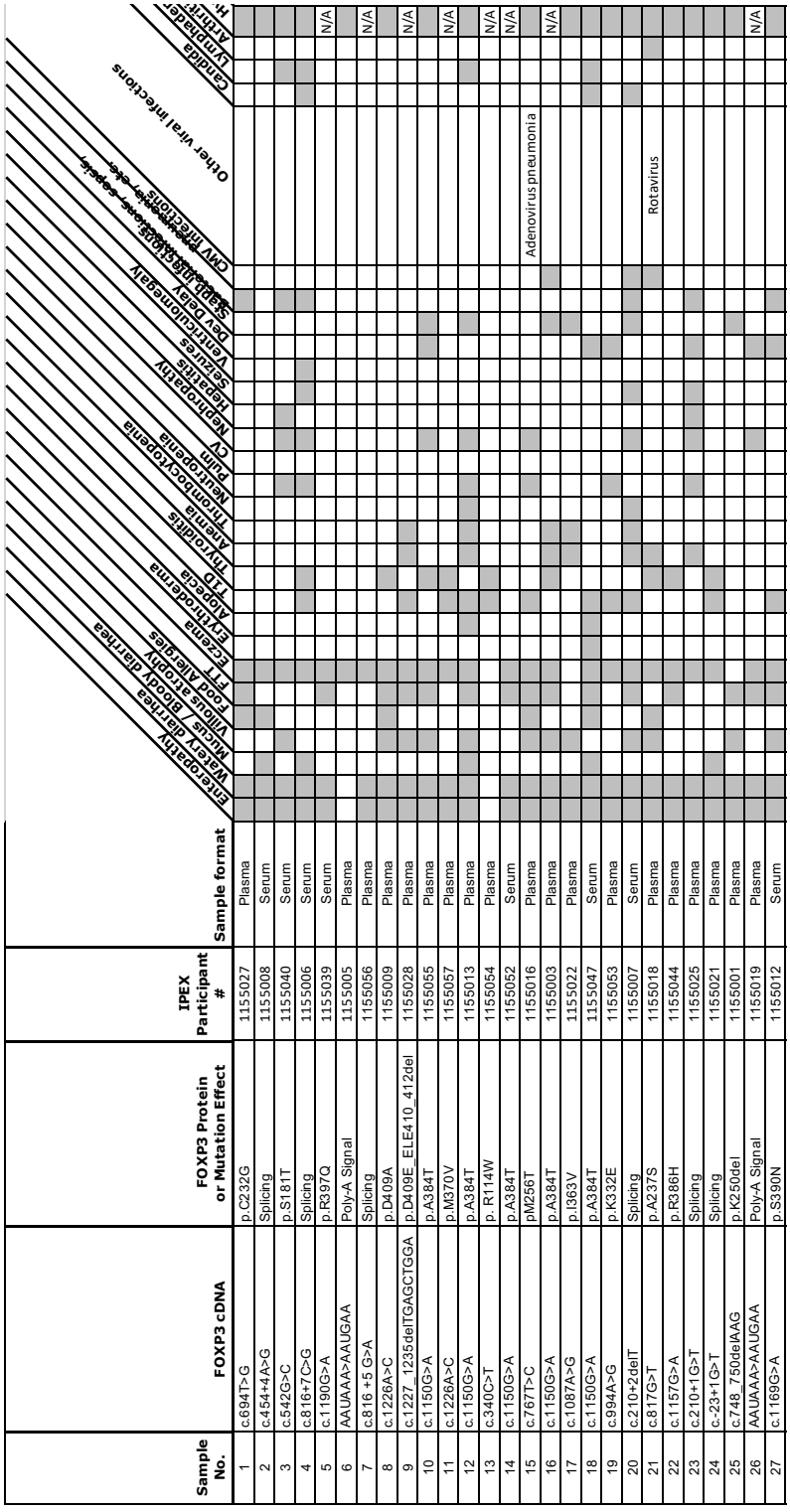

Sample No.	FOXP3 cDNA	FOXP3 Protein or Mutation Effect	IPEX Participant #	Sample format	Enteropathy	Watery diarrhea	Mucus	Villous / Blood diarrhea	Food Allergies	FPT	Eczema	EXFTH	Alopecia	T1D	Thyroiditis	Anemia	Thrombocytopenia	Neutropenia	Pulm	CD	Nephropathy	Hepatitis	Seizures	Ventriculomegaly	Dev Delay	Sepsis	CMV Infections	Other viral infections	Candida	Lymphadenopathy	Arthritis	Hx
1	c.694T>G	p.C232G	1155027	Plasma																												
2	c.454+4A>G	Splicing	1155008	Serum																												
3	c.542G>C	p.S181T	1155040	Serum																												
4	c.816+7C>G	Splicing	1155006	Serum																												
5	c.1190G>A	p.R397Q	1155039	Serum																											N/A	
6	AAUAAA>AAUGAA	Poly-A Signal	1155005	Plasma																												
7	c.816 +5 G>A	Splicing	1155056	Plasma																											N/A	
8	c.1226A>C	p.D409A	1155009	Plasma																												
9	c.1227_1235delTGAGCTGGA	p.D409E_ELE410_412del	1155028	Plasma																											N/A	
10	c.1150G>A	p.A384T	1155055	Plasma																												
11	c.1226A>C	p.M370V	1155057	Plasma																											N/A	
12	c.1150G>A	p.A384T	1155013	Plasma																												
13	c.340C>T	p. R114W	1155054	Plasma																											N/A	
14	c.1150G>A	p.A384T	1155052	Serum																											N/A	
15	c.767T>C	pM256T	1155016	Plasma																								Adenovirus pneumonia				
16	c.1150G>A	p.A384T	1155003	Plasma																											N/A	
17	c.1087A>G	p.I363V	1155022	Plasma																												
18	c.1150G>A	p.A384T	1155047	Serum																												
19	c.994A>G	p.K332E	1155053	Plasma																												
20	c.210+2delT	Splicing	1155007	Serum																												
21	c.817G>T	p.A237S	1155018	Plasma																								Rotavirus				
22	c.1157G>A	p.R386H	1155044	Plasma																												
23	c.210+1G>T	Splicing	1155025	Plasma																												
24	c.-23+1G>T	Splicing	1155021	Plasma																												
25	c.748_750delAAG	p.K250del	1155001	Plasma																												
26	AAUAAA>AAUGAA	Poly-A Signal	1155019	Plasma																											N/A	
27	c.1169G>A	p.S390N	1155012	Serum																												

REFERENCES

Alimohammadi, M., Björklund, P., Hallgren, A., Pöntynen, N., Szinnai, G., Shikama, N., Keller, M.P., Ekwall, O., Kinkel, S.A., Husebye, E.S., et al. (2008). Autoimmune polyendocrine syndrome type 1 and NALP5, a parathyroid autoantigen. New Engl J Medicine *358*, 1018 1028.

Bacchetta, R., Passerini, L., Gambineri, E., Dai, M., Allan, S.E., Perroni, L., Dagna-Bricarelli, F., Sartirana, C., Matthes-Martin, S., Lawitschka, A., et al. (2006). Defective regulatory and effector T cell functions in patients with FOXP3 mutations. J Clin Invest *116*, 1713–1722.

Barros, R.D.M., Roberts, N.A., Dart, R.J., Vantourout, P., Jandke, A., Nussbaumer, O., Deban, L., Cipolat, S., Hart, R., Iannitto, M.L., et al. (2016). Epithelia Use Butyrophilin-like Molecules to Shape Organ-Specific γδ T Cell Compartments. Cell *167*, 203-218.e17.

Bastard, P., Rosen, L.B., Zhang, Q., Michailidis, E., Hoffmann, H.-H., Zhang, Y., Dorgham, K., Philippot, Q., Rosain, J., Béziat, V., et al. (2020). Autoantibodies against type I IFNs in patients with life-threatening COVID-19. Science *370*, eabd4585.

Bastard, P., Orlova, E., Sozaeva, L., Lévy, R., James, A., Schmitt, M.M., Ochoa, S., Kareva, M., Rodina, Y., Gervais, A., et al. (2021a). Preexisting autoantibodies to type I IFNs underlie critical COVID-19 pneumonia in patients with APS-1. J Exp Med *218*, e20210554.

Bastard, P., Michailidis, E., Hoffmann, H.-H., Chbihi, M., Voyer, T.L., Rosain, J., Philippot, Q., Seeleuthner, Y., Gervais, A., Materna, M., et al. (2021b). Auto-antibodies to type I IFNs can underlie adverse reactions to yellow fever live attenuated vaccine. J Exp Med *218*.

Bonsignore, P., Kuiper, J.W.P., Adrian, J., Goob, G., and Hauck, C.R. (2020). CEACAM3—A Prim(at)e Invention for Opsonin-Independent Phagocytosis of Bacteria. Front Immunol *10*, 3160.

Busslinger, G.A., Weusten, B.L.A., Bogte, A., Begthel, H., Brosens, L.A.A., and Clevers, H. (2021). Human gastrointestinal epithelia of the esophagus, stomach, and duodenum resolved at single-cell resolution. Cell Reports *34*, 108819.

Bustamante-Marin, X.M., Yin, W.-N., Sears, P.R., Werner, M.E., Brotslaw, E.J., Mitchell, B.J., Jania, C.M., Zeman, K.L., Rogers, T.D., Herring, L.E., et al. (2019). Lack of GAS2L2 Causes PCD by Impairing Cilia Orientation and Mucociliary Clearance. Am J Hum Genetics *104*, 229–245.

Chapoval, A.I., Smithson, G., Brunick, L., Mesri, M., Boldog, F.L., Andrew, D., Khramtsov, N.V., Feshchenko, E.A., Starling, G.C., and Mezes, P.S. (2013). BTNL8, a butyrophilin-like molecule that costimulates the primary immune response. Mol Immunol *56*, 819–828.

Chrifi, I., Hermkens, D., Brandt, M.M., Dijk, C.G.M. van, Bürgisser, P.E., Haasdijk, R., Pei, J., Kamp, E.H.M. van de, Zhu, C., Blonden, L., et al. (2017). Cgnl1, an endothelial junction complex protein, regulates GTPase mediated angiogenesis. Cardiovasc Res *113*, 1776–1788.

Crawley, S.W., Shifrin, D.A., Grega-Larson, N.E., McConnell, R.E., Benesh, A.E., Mao, S., Zheng, Y., Zheng, Q.Y., Nam, K.T., Millis, B.A., et al. (2014). Intestinal Brush Border Assembly Driven by Protocadherin-Based Intermicrovillar Adhesion. Cell *157*, 433–446.

Cunningham, M.W., Meissner, H.C., Heuser, J.S., Pietra, B.A., Kurahara, D.K., and Leung, D.Y. (1999). Anti-human cardiac myosin autoantibodies in Kawasaki syndrome. J Immunol Baltim Md 1950 *163*, 1060–1065.

Delmonte, O.M., Schuetz, C., and Notarangelo, L.D. (2018). RAG Deficiency: Two Genes, Many Diseases. J Clin Immunol *38*, 646–655.

Delmonte, O.M., Villa, A., and Notarangelo, L.D. (2020). Immune dysregulation in patients with RAG deficiency and other forms of combined immune deficiency. Blood *135*, 610–619.

Elmentaite, R., Kumasaka, N., Roberts, K., Fleming, A., Dann, E., King, H.W., Kleshchevnikov, V., Dabrowska, M., Pritchard, S., Bolt, L., et al. (2021). Cells of the human intestinal tract mapped across space and time. Nature *597*, 250–255.

Eriksson, D., Bacchetta, R., Gunnarsson, H.I., Chan, A., Barzaghi, F., Ehl, S., Hallgren, Å., Gool, F. van, Sardh, F., Lundqvist, C., et al. (2019). The autoimmune targets in IPEX are dominated by gut epithelial proteins. J Allergy Clin Immun *144*, 327-330.e8.

Feldstein, L.R., Rose, E.B., Horwitz, S.M., Collins, J.P., Newhams, M.M., Son, M.B.F., Newburger, J.W., Kleinman, L.C., Heidemann, S.M., Martin, A.A., et al. (2020). Multisystem Inflammatory Syndrome in U.S. Children and Adolescents. New Engl J Medicine *383*, NEJMoa2021680.

Ferre, E.M.N., Rose, S.R., Rosenzweig, S.D., Burbelo, P.D., Romito, K.R., Niemela, J.E., Rosen, L.B., Break, T.J., Gu, W., Hunsberger, S., et al. (2016). Redefined clinical features and

diagnostic criteria in autoimmune polyendocrinopathy-candidiasis-ectodermal dystrophy. Jci Insight *1*, 1343 19.

Fishman, D., Kisand, K., Hertel, C., Rothe, M., Remm, A., Pihlap, M., Adler, P., Vilo, J., Peet, A., Meloni, A., et al. (2017). Autoantibody Repertoire in APECED Patients Targets Two Distinct Subgroups of Proteins. Front Immunol *8*, 681 15.

Fricker, L.D., Margolis, E., Gomes, I., and Devi, L.A. (2020). Five decades of research on opioid peptides: Current knowledge and unanswered questions. Mol Pharmacol *98*, mol.120.119388.

FUJIEDA, M., OISHI, N., and KURASHIGE, T. (1997). Antibodies to endothelial cells in Kawasaki disease lyse endothelial cells without cytokine pretreatment. Clin Exp Immunol *107*, 120–126.

Gambineri, E., Mannurita, S.C., Hagin, D., Vignoli, M., Anover-Sombke, S., DeBoer, S., Segundo, G.R.S., Allenspach, E.J., Favre, C., Ochs, H.D., et al. (2018). Clinical, Immunological, and Molecular Heterogeneity of 173 Patients With the Phenotype of Immune Dysregulation, Polyendocrinopathy, Enteropathy, X-Linked (IPEX) Syndrome. Front Immunol *9*, 2411.

Ge, S., Goh, E.L.K., Sailor, K.A., Kitabatake, Y., Ming, G., and Song, H. (2006). GABA regulates synaptic integration of newly generated neurons in the adult brain. Nature *439*, 589–593.

Gruber, C.N., Patel, R.S., Trachtman, R., Lepow, L., Amanat, F., Krammer, F., Wilson, K.M., Onel, K., Geanon, D., Tuballes, K., et al. (2020). Mapping Systemic Inflammation and Antibody Responses in Multisystem Inflammatory Syndrome in Children (MIS-C). Cell *183*, 982-995.e14.

GRUNEBAUM, E., BLANK, M., COHEN, S., AFEK, A., KOPOLOVIC, J., MERONI, P.L., YOUINOU, P., and SHOENFELD, Y. (2002). The role of anti-endothelial cell antibodies in Kawasaki disease –in vitro and in vivo studies. Clin Exp Immunol *130*, 233–240.

Haritunians, T., Jones, M.R., McGovern, D.P.B., Shih, D.Q., Barrett, R.J., Derkowski, C., Dubinsky, M.C., Dutridge, D., Fleshner, P.R., Ippoliti, A., et al. (2011). Variants in ZNF365 isoform D are associated with Crohn's disease. Gut *60*, 1060.

Hedstrand, H., Ekwall, O., Olsson, M.J., Landgren, E., Kemp, E.H., Weetman, A.P., Perheentupa, J., Husebye, E., Gustafsson, J., Betterle, C., et al. (2001). The Transcription Factors SOX9 and SOX10 Are Vitiligo Autoantigens in Autoimmune Polyendocrine Syndrome Type I. J Biol Chem *276*, 35390 35395.

Hou, S., Li, N., Liao, X., Kijlstra, A., and Yang, P. (2020). Uveitis genetics. Exp Eye Res *190*, 107853.

Jeong, J.S., Jiang, L., Albino, E., Marrero, J., Rho, H.S., Hu, J., Hu, S., Vera, C., Bayron-Poueymiroy, D., Rivera-Pacheco, Z.A., et al. (2012). Rapid Identification of Monospecific Monoclonal Antibodies Using a Human Proteome Microarray. Mol Cell Proteomics *11*, O111.016253.

Kobayashi, I., Kubota, M., Yamada, M., Tanaka, H., Itoh, S., Sasahara, Y., Whitesell, L., and Ariga, T. (2011). Autoantibodies to villin occur frequently in IPEX, a severe immune dysregulation, syndrome caused by mutation of FOXP3. Clin Immunol *141*, 83–89.

Landegren, N., Sharon, D., Freyhult, E., Hallgren, A., Eriksson, D., Edqvist, P.-H., Bensing, S., Wahlberg, J., Nelson, L.M., Gustafsson, J., et al. (2016). Proteome-wide survey of the autoimmune target repertoire in autoimmune polyendocrine syndrome type 1. Sci Rep-Uk *6*, 1 11.

Larman, H.B., Zhao, Z., Laserson, U., Li, M.Z., Ciccia, A., Gakidis, M.A.M., Church, G.M., Kesari, S., LeProust, E.M., Solimini, N.L., et al. (2011). Autoantigen discovery with a synthetic human peptidome. Nat Biotechnol *29*, 535 541.

Larman, H.B., Laserson, U., Querol, L., Verhaeghen, K., Solimini, N.L., Xu, G.J., Klarenbeek, P.L., Church, G.M., Hafler, D.A., Plenge, R.M., et al. (2013). PhIP-Seq characterization of autoantibodies from patients with multiple sclerosis, type 1 diabetes and rheumatoid arthritis. J Autoimmun *43*, 1 9.

Li, J.J., Sarute, N., Lancaster, E., Otkiran-Clare, G., Fagla, B.M., Ross, S.R., and Scherer, S.S. (2020). A recessive Trim2 mutation causes an axonal neuropathy in mice. Neurobiol Dis *140*, 104845.

Ma, Q., Gan, G.-F., Niu, Y., and Tong, S.-J. (2020). Analysis of associations of FBXL19-AS1 with occurrence, development and prognosis of acute pancreatitis. Eur Rev Med Pharmaco *24*, 12763–12769.

Mandel-Brehm, C., Dubey, D., Kryzer, T.J., O'Donovan, B.D., Tran, B., Vazquez, S.E., Sample, H.A., Zorn, K.C., Khan, L.M., Bledsoe, I.O., et al. (2019). Kelch-like Protein 11 Antibodies in Seminoma-Associated Paraneoplastic Encephalitis. New Engl J Med *381*, 47–54.

Mayassi, T., Ladell, K., Gudjonson, H., McLaren, J.E., Shaw, D.G., Tran, M.T., Rokicka, J.J., Lawrence, I., Grenier, J.-C., Unen, V. van, et al. (2019). Chronic Inflammation Permanently Reshapes Tissue-Resident Immunity in Celiac Disease. Cell *176*, 967-981.e19.

McLaughlin, J.P., Marton-Popovici, M., and Chavkin, C. (2003). κ Opioid Receptor Antagonism and Prodynorphin Gene Disruption Block Stress-Induced Behavioral Responses. J Neurosci *23*, 5674–5683.

Meager, A., Visvalingam, K., Peterson, P., Möll, K., Murumägi, A., Krohn, K., Eskelin, P., Perheentupa, J., Husebye, E., Kadota, Y., et al. (2006). Anti-Interferon Autoantibodies in Autoimmune Polyendocrinopathy Syndrome Type 1. Plos Med *3*, e289.

Meyer, S., Woodward, M., Hertel, C., Vlaicu, P., Haque, Y., Kärner, J., Macagno, A., Onuoha, S.C., Fishman, D., Peterson, H., et al. (2016). AIRE-Deficient Patients Harbor Unique High-Affinity Disease-Ameliorating Autoantibodies. Cell *166*, 582 595.

Mina, M.J., Kula, T., Leng, Y., Li, M., Vries, R.D. de, Knip, M., Siljander, H., Rewers, M., Choy, D.F., Wilson, M.S., et al. (2019). Measles virus infection diminishes preexisting antibodies that offer protection from other pathogens. Science *366*, 599–606.

Moua, P., Checketts, M., Xu, L.-G., Shu, H.-B., Reyland, M.E., and Cusick, J.K. (2017). RELT family members activate p38 and induce apoptosis by a mechanism distinct from TNFR1. Biochem Bioph Res Co *491*, 25–32.

Mu, F.-T., Callaghan, J.M., Steele-Mortimer, O., Stenmark, H., Parton, R.G., Campbell, P.L., McCluskey, J., Yeo, J.-P., Tock, E.P.C., and Toh, B.-H. (1995). EEA1, an Early Endosome-

Associated Protein. EEA1 IS A CONSERVED α-HELICAL PERIPHERAL MEMBRANE PROTEIN FLANKED BY CYSTEINE “FINGERS” AND CONTAINS A CALMODULIN-BINDING IQ MOTIF ∗. J Biol Chem *270*, 13503–13511.

Newburger, J.W., Takahashi, M., and Burns, J.C. (2016). Kawasaki Disease. J Am Coll Cardiol *67*, 1738–1749.

O’Donovan, B., Mandel - Brehm, C., Sara E. Vazquez, Liu, J., Paren, A.V., Anderson, M.S., Kassimatis, T., Zekeridou, A., Hauser, S.L., Pittock, S.J., et al. (2018). Exploration of Anti - Yo and Anti - Hu paraneoplastic neurological disorders by PhIP - Seq reveals a highly restricted pattern of antibody epitopes. Biorxiv.

Onouchi, Y. (2018). The genetics of Kawasaki disease. Int J Rheum Dis *21*, 26–30.

Powell, B.R., Buist, N.R.M., and Stenzel, P. (1982). An X-linked syndrome of diarrhea, polyendocrinopathy, and fatal infection in infancy. J Pediatrics *100*, 731–737.

Prokic, D., Ristic, G., Paunovic, Z., and Pasic, S. (2010). Pancreatitis and atypical Kawasaki disease. Pediatric Rheumatology Online J *8*, 8–8.

Qu, Z., and Hartzell, H.C. (2008). Bestrophin Cl− channels are highly permeable to HCO3−. Am J Physiol-Cell Ph *294*, C1371–C1377.

Rhodes, D.A., Reith, W., and Trowsdale, J. (2015). Regulation of Immunity by Butyrophilins. Annu Rev Immunol *34*, 1–22.

Román-Meléndez, G.D., Monaco, D.R., Montagne, J.M., Quizon, R.S., Konig, M.F., Astatke, M., Darrah, E., and Larman, H.B. (2021). Citrullination of a phage-displayed human peptidome library reveals the fine specificities of rheumatoid arthritis-associated autoantibodies. Ebiomedicine *71*, 103506.

Sakurai, Y. (2019). Autoimmune Aspects of Kawasaki Disease. J Invest Allerg Clin *29*, 251–261.

Schaum, N., Karkanias, J., Neff, N.F., May, A.P., Quake, S.R., Wyss-Coray, T., Darmanis, S., Batson, J., Botvinnik, O., Chen, M.B., et al. (2018). Single-cell transcriptomics of 20 mouse organs creates a Tabula Muris. Nature *562*, 1 25.

Schlicher, L., and Maurer, U. (2016). SPATA2: New insights into the assembly of the TNFR signaling complex. Cell Cycle *16*, 1–2.

Selak, S., Woodman, R.C., and Fritzler, M.J. (2000). Autoantibodies to early endosome antigen (EEA1) produce a staining pattern resembling cytoplasmic anti-neutrophil cytoplasmic antibodies (C-ANCA). Clin Exp Immunol *122*, 493–498.

Sharifi, N., Diehl, N., Yaswen, L., Brennan, M.B., and Hochgeschwender, U. (2001). Generation of dynorphin knockout mice. Mol Brain Res *86*, 70–75.

Sharon, D., and Snyder, M. (2014). Serum Profiling Using Protein Microarrays to Identify Disease Related Antigens. Methods Mol Biology Clifton N J *1176*, 169–178.

Smillie, C.S., Biton, M., Ordovas-Montanes, J., Sullivan, K.M., Burgin, G., Graham, D.B., Herbst, R.H., Rogel, N., Slyper, M., Waldman, J., et al. (2019). Intra- and Inter-cellular Rewiring of the Human Colon during Ulcerative Colitis. Cell *178*, 714-730.e22.

Snodgrass, R.G., and Brüne, B. (2019). Regulation and Functions of 15-Lipoxygenases in Human Macrophages. Front Pharmacol *10*, 719.

Stinton, L.M., Eystathioy, T., Selak, S., Chan, E.K.L., and Fritzler, M.J. (2004). Autoantibodies to protein transport and messenger RNA processing pathways: endosomes, lysosomes, Golgi complex, proteasomes, assemblyosomes, exosomes, and GW bodies. Clin Immunol *110*, 30–44.

Teves, M.E., Zhang, Z., Costanzo, R.M., Henderson, S.C., Corwin, F.D., Zweit, J., Sundaresan, G., Subler, M., Salloum, F.N., Rubin, B.K., et al. (2013). Sperm-Associated Antigen–17 Gene Is Essential for Motile Cilia Function and Neonatal Survival. Am J Resp Cell Mol *48*, 765–772.

Uhlen, M., Fagerberg, L., Hallstrom, B.M., Lindskog, C., Oksvold, P., Mardinoglu, A., Sivertsson, A., Kampf, C., Sjostedt, E., Asplund, A., et al. (2015). Tissue-based map of the human proteome. Science *347*, 1260419 1260419.

Valenzise, M., Aversa, T., Salzano, G., Zirilli, G., Luca, F.D., and Su, M. (2017). Novel insight into Chronic Inflammatory Demyelinating Polineuropathy in APECED syndrome: molecular mechanisms and clinical implications in children. Ital J Pediatr *43*, 11.

Vazquez, S.E., Ferré, E.M., Scheel, D.W., Sunshine, S., Miao, B., Mandel-Brehm, C., Quandt, Z., Chan, A.Y., Cheng, M., German, M., Lionakis, M., DeRisi, J. L. and Anderson, M.S, 2020.

Identification of novel, clinically correlated autoantigens in the monogenic autoimmune syndrome APS1 by proteome-wide PhIP-Seq. Elife, 9, p.e55053.

Vogl, T., Klompus, S., Leviatan, S., Kalka, I.N., Weinberger, A., Wijmenga, C., Fu, J., Zhernakova, A., Weersma, R.K., and Segal, E. (2021). Population-wide diversity and stability of serum antibody epitope repertoires against human microbiota. Nat Med *27*, 1442–1450.

Waite, R.L., Sentry, J.W., Stenmark, H., and Toh, B.-H. (1998). Autoantibodies to a Novel Early Endosome Antigen 1. Clin Immunol Immunop *86*, 81–87.

Wang, E.Y., Dai, Y., Rosen, C.E., Schmitt, M.M., Dong, M.X., Ferré, E.M.N., Liu, F., Yang, Y., Gonzalez-Hernandez, J.A., Meffre, E., et al. (2021). REAP: A platform to identify autoantibodies that target the human exoproteome. Biorxiv 2021.02.11.430703.

Wang, Z., Gardell, L.R., Ossipov, M.H., Vanderah, T.W., Brennan, M.B., Hochgeschwender, U., Hruby, V.J., Malan, T.P., Lai, J., and Porreca, F. (2001). Pronociceptive Actions of Dynorphin Maintain Chronic Neuropathic Pain. J Neurosci *21*, 1779–1786.

Wijst, M.G.P. van der, Vazquez, S.E., Hartoularos, G.C., Bastard, P., Grant, T., Bueno, R., Lee, D.S., Greenland, J.R., Sun, Y., Perez, R., et al. (2021). Type I interferon autoantibodies are associated with systemic immune alterations in patients with COVID-19. Sci Transl Med *13*, eabh2624.

Winqvist, O., Gustafsson, J., Rorsman, F., Karlsson, F.A., and Kämpe, O. (1993). Two different cytochrome P450 enzymes are the adrenal antigens in autoimmune polyendocrine syndrome type I and Addison's disease. J Clin Invest *92*, 2377–2385.

Wuest, S.J.A., Horn, T., Marti-Jaun, J., Kühn, H., and Hersberger, M. (2014). Association of polymorphisms in the ALOX15B gene with coronary artery disease. Clin Biochem *47*, 349–355.

Yang, J., Liu, X., Yue, G., Adamian, M., Bulgakov, O., and Li, T. (2002). Rootletin, a novel coiled-coil protein, is a structural component of the ciliary rootlet. J Cell Biology *159*, 431–440.

Zhang, G., Hirai, H., Cai, T., Miura, J., Yu, P., Huang, H., Schiller, M.R., Swaim, W.D., Leapman, R.D., and Notkins, A.L. (2007). RESP18, a homolog of the luminal domain IA-2, is found in dense core vesicles in pancreatic islet cells and is induced by high glucose. J Endocrinol *195*, 313–321.

Zhu, F., Feng, M., Sinha, R., Murphy, M.P., Luo, F., Kao, K.S., Szade, K., Seita, J., and Weissman, I.L. (2019). The GABA receptor GABRR1 is expressed on and functional in hematopoietic stem cells and megakaryocyte progenitors. Proc National Acad Sci *116*, 18416–18422.

Zhu, H., Bilgin, M., Bangham, R., Hall, D., Casamayor, A., Bertone, P., Lan, N., Jansen, R., Bidlingmaier, S., Houfek, T., et al. (2001). Global Analysis of Protein Activities Using Proteome Chips. Science *293*, 2101–2105.

Publishing Agreement

It is the policy of the University to encourage open access and broad distribution of all theses, dissertations, and manuscripts. The Graduate Division will facilitate the distribution of UCSF theses, dissertations, and manuscripts to the UCSF Library for open access and distribution. UCSF will make such theses, dissertations, and manuscripts accessible to the public and will take reasonable steps to preserve these works in perpetuity.

I hereby grant the non-exclusive, perpetual right to The Regents of the University of California to reproduce, publicly display, distribute, preserve, and publish copies of my thesis, dissertation, or manuscript in any form or media, now existing or later derived, including access online for teaching, research, and public service purposes.

DocuSigned by:
Sara Vazquez
CD13D23DA3A14E0...
Author Signature

12/1/2021
Date